

REPORT

*Final NAPL Investigation Report
Pine Street Canal Superfund Site
Burlington, Vermont*

**Submitted to:
Green Mountain Power**

**Submitted by:
ARCADIS BBL
Hart Crowser, Inc.**

Project 69852, February 1, 2008



REPORT

***Final NAPL Investigation Report
Pine Street Canal Superfund Site
Burlington, Vermont***

**Submitted to:
Green Mountain Power**

February 1, 2008

Respectfully
submitted,

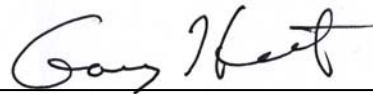
ARCADIS



Barry L. Kellems, P.E.
Associate



Philip A. Spadaro, L.G.
Senior Vice President



Garry E. Horvitz, P.E.
Senior Principal



Table of Contents

Section	Executive Summary	ES-1
Section	1. Introduction	1-1
1.1	Purpose	1-1
1.2	Site Description	1-1
1.3	Report Organization	1-2
Section	2. Exploration and Testing Activities	2-1
2.1	Groundwater and NAPL Monitoring at Existing Monitoring Wells.....	2-1
2.1.1	Groundwater Level and NAPL Thickness Measurements	2-2
2.1.2	NAPL Sampling and Analysis.....	2-2
2.2	Diver Survey and Sampling Activities	2-2
2.2.1	Diver NAPL and Gas Observations.....	2-2
2.2.2	Cap Surface Swabbing and Analysis for NAPL.....	2-3
2.2.3	Water Column Seep Sampling and Analysis for NAPL.....	2-4
2.3	Cap Coring and Chemical Testing to Assess NAPL Migration	2-5
2.3.1	Spring Investigation	2-5
2.3.2	Summer Investigation.....	2-5
2.3.3	Winter Investigation	2-6
2.4	Subsurface TarGOST™ Probing and Confirmation Borings	2-6
2.4.1	Spring Investigation	2-7
2.4.2	Winter Investigation	2-8
2.5	Subsurface CPT Probing and Borings to Assess Geotechnical Conditions	2-9
2.5.1	Subsurface CPT Probing.....	2-9
2.5.2	Geotechnical Confirmation Sampling and Analysis.....	2-9
2.6	Piezometer and Temperature Probe Installation and Monitoring	2-10
2.6.1	Spring 2006 Piezometer Installation.....	2-10
2.6.2	Spring 2006 Piezometer Decommissioning	2-11
2.6.3	Winter 2007 Piezometer Installation.....	2-11
2.7	Cap Settlement Plate Installation and Monitoring	2-11
Section	3. Field and Laboratory Results	3-1
3.1	Soil Physical Characteristics	3-1
3.1.1	Data Quality	3-2
3.1.2	CPT and Boring Results	3-2
3.1.3	Soil Classification Parameters.....	3-2
3.1.3.1	Soil Classification.....	3-2
3.1.3.2	Water Content	3-3
3.1.3.3	Grain Size Analysis.....	3-3
3.1.3.4	Atterberg Limits.....	3-3
3.1.3.5	Bulk Density	3-3
3.1.3.6	Organic Content.....	3-3
3.1.4	Compressibility and Consolidation Parameters.....	3-4
3.1.5	Soil Strength Parameters	3-4
3.1.6	Hydraulic Conductivity	3-5
3.1.7	Cap Settlement Parameters	3-6
3.1.8	Cap Thickness Measurement.....	3-7

3.2	Groundwater Potentiometric and Temperature Data.....	3-7
3.2.1	Data Quality.....	3-7
3.2.2	Depth to Groundwater and Groundwater Elevation Data.....	3-9
3.2.2.1	Monitoring Well Data.....	3-9
3.2.2.2	Piezometer Data.....	3-9
3.2.3	Surface Water Elevations.....	3-10
3.2.4	Groundwater Temperature Data from Spring 2006 Piezometers.....	3-11
3.2.4.1	Groundwater and Surface Water Temperature Comparison from Spring 2006 Piezometers.....	3-11
3.2.5	NAPL Thickness Data.....	3-12
3.3	NAPL Sampling and Analysis.....	3-12
3.3.1	NAPL Sampling Data Quality.....	3-12
3.3.2	NAPL Sampling Analytical Data.....	3-13
3.3.2.1	NAPL Sampling PAH Results.....	3-13
3.3.2.2	NAPL Sampling BTEX Results.....	3-14
3.3.2.3	NAPL Sampling Physical Results.....	3-14
3.4	Diver Survey and Sampling Activities.....	3-14
3.4.1	Data Quality.....	3-15
3.4.1.1	Spring Investigation.....	3-15
3.4.1.2	Summer Investigation.....	3-15
3.4.2	Observations.....	3-15
3.4.2.1	Spring Investigation.....	3-15
3.4.2.2	Summer Investigation.....	3-16
3.4.3	Cap Surface Swab Analytical Data.....	3-16
3.4.3.1	Cap Surface Swab PAH Results.....	3-16
3.4.3.2	Cap Surface Swab TPH Results.....	3-17
3.4.4	Water Column NAPL Seep Analytical Data.....	3-17
3.4.4.1	Water Column NAPL Seep PAH Results.....	3-18
3.4.4.2	Water Column NAPL Seep TPH Results.....	3-18
3.5	Cap Sand Quality Characteristics.....	3-18
3.5.1	Cap Sand Data Quality.....	3-19
3.5.1.1	Spring Investigation.....	3-19
3.5.1.2	Summer Investigation.....	3-19
3.5.1.3	Winter Investigation.....	3-19
3.5.2	Cap Sand TarGOST™ Results.....	3-20
3.5.3	Cap Sand PAH Results.....	3-20
3.5.3.1	Spring Investigation.....	3-20
3.5.3.2	Summer Investigation.....	3-20
3.5.3.3	Winter Investigation.....	3-21
3.5.4	Cap Sand TPH Results.....	3-21
3.5.4.1	Spring Investigation.....	3-21
3.5.4.2	Summer Investigation.....	3-21
3.5.4.3	Winter Investigation.....	3-21
3.5.5	Cap Sand TOC Results.....	3-22
3.6	Subsurface Soil Quality Characteristics.....	3-22
3.6.1	Subsurface Soil Data Quality.....	3-22
3.6.1.1	Spring Investigation.....	3-22
3.6.1.2	Winter Investigation.....	3-22
3.6.2	Subsurface Soil TarGOST™ Results.....	3-23
3.6.2.1	Spring Investigation.....	3-23
3.6.2.2	Winter Investigation.....	3-23
3.6.3	Subsurface Soil Confirmation Borings.....	3-23
3.6.3.1	Subsurface Soil PAH Results.....	3-23
3.6.3.2	Subsurface Soil TPH Results.....	3-24
3.6.3.3	Subsurface Soil TOC Results.....	3-24

Section	4. Evaluation and Discussion of Results	4-1
4.1	Methodology.....	4-1
4.2	Estimated Residual Saturation Criteria for Coal Tar NAPL	4-2
4.2.1	TPH-based NAPL Mobility Criteria	4-2
4.2.2	TarGOST™-based Mobility Criteria	4-3
4.2.3	Results.....	4-4
4.3	Potentially Mobile Subsurface NAPL	4-4
4.3.1	Location of Subsurface NAPL	4-4
4.3.1.1	3-D Modeling Methodology.....	4-5
4.3.1.2	3-D Model Results	4-6
4.3.2	Mass of Subsurface NAPL	4-7
4.3.3	Discussion of Subsurface NAPL.....	4-9
4.4	NAPL within the Sand Cap.....	4-10
4.4.1	NAPL within the Canal Sand Cap	4-10
4.4.1.1	Locations of NAPL within the Canal Sand Cap	4-10
4.4.1.2	Mass of NAPL within the Canal Sand Cap.....	4-11
4.4.1.3	Discussion of NAPL within the Canal Sand Cap	4-13
4.4.2	Thickness of the Canal Sand Cap.....	4-14
4.4.2.1	Distribution of the Sand Cap Thickness.....	4-14
4.4.2.2	Discussion of the Sand Cap Thickness	4-15
4.4.3	NAPL within the West Bank Cap	4-15
4.4.3.1	Locations of NAPL within the West Bank Cap.....	4-15
4.5	NAPL Deposition on Cap Surface.....	4-16
4.5.1	Locations of NAPL Deposition.....	4-16
4.5.2	Mass of NAPL Deposition.....	4-17
4.5.3	Discussion of NAPL Deposition on Cap Surface.....	4-18
4.6	NAPL Seepage into the Canal	4-18
4.6.1	Locations of NAPL Seepage	4-19
4.6.2	Rate of NAPL Seepage	4-19
4.6.3	Discussion of NAPL Seepage into the Canal	4-21
4.7	Hydrogeologic Considerations for NAPL Mobility	4-22
4.7.1	Vertical Hydraulic Gradient Data Calculated Using Spring 2006 Piezometers	4-22
4.7.1.1	Groundwater Fluctuation with Change in Surface Water	
	Elevation Using Spring 2006 Piezometers	4-23
4.7.2	Horizontal Hydraulic Gradients Calculated Using Spring and	
	Winter 2007 Piezometers	4-23
Section	5. Update of Conceptual Site Model	5-1
5.1	NAPL Migration via Hydraulic Gradient	5-1
5.1.1	NAPL Migration via Vertical Hydraulic Gradient.....	5-1
5.1.2	NAPL Migration via Horizontal Hydraulic Gradient	5-3
5.2	NAPL Migration via Localized Bearing-Capacity Failures and Consolidation	
	Settlement	5-5
5.3	NAPL Migration via Preferential Pathways	5-7
5.4	NAPL Migration via Gas Bubble-induced Transport.....	5-8
5.5	Summary of NAPL Migration Mechanisms	5-10
5.6	Combined Evaluation of Location and Migration of NAPL.....	5-10
Section	6. Conclusions	6-1
Section	7. References	7-1

Tables

2-1	Summary of Spring, Summer, and Winter Investigation Sampling Locations
2-2	Monitoring Well Coordinates
2-3	Piezometer Coordinates and Screen Depths
3-1	Sediment Classification Results
3-2	Estimated Fluid Expelled from Cap Surface from 2003 to 2006
3-3	Sediment Hydraulic Conductivity Testing Results
3-4	Hydraulic Parameters from Previous Investigations
3-5	Cap Settlement Plate Results
3-6	Cap Thickness Measurements
3-7	Monitoring Well Gauging Data
3-8	Groundwater Vertical Gradients
3-9	NAPL Chemistry Results
3-10	NAPL Physical Properties
3-11	Surface Water Observation Data from the Spring Investigation
3-12	Surface Water Observation Data from the Summer Investigation
3-13	Cap Swab Details
3-14	Cap Swab Chemistry Results
3-15	Water Column NAPL Seep Chemistry Results
3-16	Cap Core Chemistry Results from the Spring Investigation
3-17	Cap Core Chemistry Results from the Summer Investigation
3-18	Cap Core Chemistry Results from the Winter Investigation
3-19	Confirmation Sample Chemistry Results from the Spring Investigation
3-20	Confirmation Sample Chemistry Results from the Winter Investigation
4-1	NAPL Mass Calculation Results
4-2	West Bank Cap Coring Analysis

Figures

1-1	Vicinity Map
1-2	General Site Plan
1-3	Extent of Canal and West Bank Sand Caps
2-1	Monitoring Well and Piezometer Locations
2-2	Diver Observation and Sampling Locations
2-3	Subaqueous Investigation Locations
3-1	Section A-A' West Bank Profile
3-2	Section B-B' Western Canal Profile
3-3	Section C-C' Center Canal Profile
3-4	Section D-D' Eastern Canal Profile
3-5	Section E-E' East Bank Profile
3-6	Sections F-F' and G-G'
3-7	Section H-H'
3-8	2006 Piezometer Groundwater Elevation Data
3-9	2007 Piezometer Groundwater Elevation Data
3-10	2006 and 2007 Surface Water Elevation Data
3-11	2006 Piezometer Groundwater Temperature Data
4-1	TPH-based and TarGOST™-based NAPL Mobility Criteria
4-2	TarGOST™ Sample Locations: Oblique View from the Southwest

-
- 4-3 TarGOST™ Sample Locations: Oblique View from the Southeast
 - 4-4 3-D Modeling TarGOST™ Distribution in Stratigraphic Units: View from the Southwest
 - 4-5 3-D Modeling TarGOST™ Distribution in Stratigraphic Units: View from the Southeast
 - 4-6 3-D Modeling TarGOST™ Distribution in Stratigraphic Units: Section A-A'
 - 4-7 3-D Modeling TarGOST™ Distribution in Stratigraphic Units: Section B-B'
 - 4-8 3-D Modeling TarGOST™ Distribution in Stratigraphic Units: Section C-C'
 - 4-9 3-D Modeling TarGOST™ Distribution in Stratigraphic Units: Section D-D'
 - 4-10 3-D Modeling TarGOST™ Distribution in Stratigraphic Units: Section E-E'
 - 4-11 3-D Modeling TarGOST™ Distribution in Stratigraphic Units: Section F-F' and G-G'
 - 4-12 3-D Modeling TarGOST™ Distribution in Stratigraphic Units: Section H-H'
 - 4-13 Relative Mass of Mobile NAPL in the Canal Subsurface
 - 4-14 Relative Concentration of NAPL in the Lower Portion of the Cap
 - 4-15 Relative Mass of NAPL in the Surface of the Cap
 - 4-16 Relative Thickness of Sand Cap
 - 4-17 Relative Rate of NAPL Seepage in 2006
 - 4-18 Vertical Hydraulic Gradient Data Plot
 - 4-19 Horizontal Hydraulic Gradient Data Plot
 - 5-1 Historical Conceptual Site Model
 - 5-2 Revised Conceptual Site Model
 - 5-3 Area of Potential NAPL Controls

Appendices

- A Daily Field Reports
- B Photo Log
- C Boring Logs
- D Chemical Data Quality Review and Laboratory Certificate of Analysis
- E TarGOST™ Results
- F CPT Results
- G Geotechnical Testing Report
- H NAPL Physical Testing Report
- I Piezometer Water Level Data
- J Calculation Sheets
- K Historical NAPL Data
- L Response to Comments

Acronyms and Abbreviations

3-D	-	three-dimensional
ASTM	-	American Society for Testing and Materials
bgs	-	below ground surface
bss	-	below the sediment surface
BTEX	-	benzene, toluene, ethylbenzene, and xylenes
CPT	-	cone penetrometer test(ing)
DQI	-	data quality indicator
DQO	-	data quality objective
EPRI	-	Electric Power Research Institute
LDPE	-	low-density polyethylene
MGP	-	manufactured gas plant
MVS	-	Mining Visualization System
NAPL	-	nonaqueous-phase liquid
NAVD88	-	1988 North American Vertical Datum
PAH	-	polycyclic aromatic hydrocarbon
PID	-	photoionization detector
PVC	-	polyvinyl chloride
QA	-	quality assurance
QAPP	-	Quality Assurance Project Plan
RE	-	reference emission
RS	-	residual saturation
TarGOST™	-	tar-specific green optical screening tool
TOC	-	total organic carbon
TPH	-	total petroleum hydrocarbons
USEPA	-	U.S. Environmental Protection Agency
VOC	-	volatile organic compound
VDEC	-	Vermont Department of Environmental Conservation

Units of Measure

C	-	Celsius
cm	-	centimeter
ft ²	-	square feet
ft/day	-	feet per day
ft/ft	-	foot/foot
ft/yr	-	feet per year
g	-	gram
g/ft ²	-	grams per square foot
g/mL	-	grams per milliliter
g/yr	-	grams per year
kg	-	kilogram
kg/L	-	kilograms per liter
KSF	-	kips per square foot
L	-	liter
lb/ft ³	-	pounds per cubic foot

lb/kg	-	pounds per kilogram
µg/droplet	-	micrograms per droplet
µg/g	-	micrograms per gram
µg/kg	-	micrograms per kilogram
µg/m ²	-	micrograms per square meter
µg/second	-	micrograms per second
µg/wipe	-	micrograms per wipe
mg/g	-	milligrams per gram
mg/kg	-	milligrams per kilogram
m ²	-	square meter
m ³	-	cubic meter
ppm	-	parts per million
pcf	-	pounds per cubic foot
psf	-	pounds per square foot
tons/ft ²	-	tons per square foot

Executive Summary

Introduction

This NAPL investigation report was prepared by ARCADIS BBL and Hart Crowser, Inc. in accordance with the Nonaqueous-Phase Liquid (NAPL) Action Plan and the Field Investigation Work Plan for the Pine Street Canal Superfund Site in Burlington, Vermont. The Action Plan proposed a path forward to address NAPL migration at the site. The Work Plan was the first step in implementation of the Action Plan.

The Work Plan identified data gaps and proposed a series of field investigations to fill them. The NAPL field investigation was conducted in three events (spring, summer, and winter). In spring and summer 2006, surface and subsurface investigations of the canal were conducted to assess NAPL migration to the water column. In winter 2007, a subsurface investigation of the canal banks was conducted.

This NAPL investigation report presents the results of the spring, summer, and winter investigations, including field observations, field data, laboratory data, and an evaluation of the data, and updates the conceptual site model with respect to NAPL migration mechanisms. In addition, this report presents conclusions regarding the data gaps identified in the Work Plan.

Sampling and Analysis

Activities carried out during the spring, summer, and winter NAPL investigations are summarized as follows:

- Groundwater level and NAPL thickness measurements were obtained at selected existing monitoring wells (spring, summer and winter).
- Two existing monitoring wells were sampled for NAPL; these samples were analyzed to characterize the NAPL physical properties (viscosity, density, interfacial tension) and concentration of polycyclic aromatic hydrocarbons (PAHs) and benzene, toluene, ethylbenzene, and xylenes (BTEX) (spring)
- Divers made observations of gas bubble and NAPL seepage in the canal at two separate time intervals (spring and summer).
- Divers swabbed the cap surface in grids of 1 square meter and at specific active seep locations to evaluate NAPL deposition on the cap surface; these samples were analyzed for PAHs and total petroleum hydrocarbons (TPH) (spring and summer).
- Water column seep sampling was conducted to quantitatively characterize the nature and extent of NAPL migrating to the surface water of the canal; these samples, which consisted of NAPL droplets captured on a Teflon[®] net, were analyzed for PAHs and TPH (spring and summer).
- The cap sand and subsurface soil were probed using TarGOST[™] (tar-specific green optical screening tool) and cone penetrometer testing (CPT) to assess possible mechanisms of NAPL migration and the areal and vertical extent of mobile NAPL (spring and winter).
- Cap sand and subsurface soil were sampled and analyzed for confirmation chemical (TPH and PAH) characteristics and geotechnical conditions (spring, summer and winter).

-
- Piezometers were installed in the canal and on the canal banks to assess horizontal and vertical hydraulic gradients (spring 2006 through fall 2007).
 - Temperature probes were installed beneath the canal to assess the temperature dependence of gas bubbles rising into the canal (spring through fall 2006).
 - Settlement monitoring of the sand cap was conducted (spring through fall 2006).

Geotechnical tests included soil classification, water content, grain size distribution, Atterberg limits, bulk density, organic content, compressibility and consolidation parameters, soil strength parameters, hydraulic conductivity, cap settlement parameters, and cap thickness measurements. A generalized stratigraphic profile was developed as follows, from the bottom of the water column downward: sand cap material, organic silt/sediment, peat, stratified silt and sand, and silty clay to clayey silt.

Data collected to evaluate site hydrogeology included manual groundwater level measurements, groundwater elevation and temperature data from pressure transducers and temperature probes, NAPL thickness gauging data, and groundwater flow evaluations (from previous investigations). A strong linear relationship between surface water elevation and groundwater elevation was observed in the clayey silt layer, the deep organic silt/sediment layer, and the shallow organic silt/sediment layer, indicating that the organic silt/sediment layer and the clayey silt layer are hydraulically connected to and influenced by variations in surface water elevation.

Data validation was performed in accordance with the Work Plan's Quality Assurance Project Plan. On the basis of that review, the data were deemed usable for the intended purpose.

Evaluation of Analytical Results and Conclusions

The following information provides a basis to evaluate and select NAPL controls at the site and is generally conservative with respect to the extent and mass of NAPL. To evaluate NAPL location and mass with respect to the potential for NAPL seepage into the canal, a grid was projected onto the canal. Each cell in the grid is 25 feet by 25 feet in plan view, which is a reasonable size to create a modular design for NAPL controls. The values depicting location and mass of NAPL are derived using conservative (high-end) assumptions. Since appropriate controls will be designed for any location within a cell that has a high potential for NAPL migration, the NAPL masses are calculated based on the maximum chemistry results within that cell. Therefore, the calculated masses per cell represent a reasonably conservative order-of-magnitude estimate of the maximum NAPL migration that could require controls during the design.

This section discusses relative order-of-magnitude masses of NAPL within different stratigraphic layers at the site. This does not represent a mass balance. Since these masses are order-of-magnitude estimates, the actual NAPL mass or seepage associated with each cell may be lower or higher.

NAPL Seepage into the Canal

In the spring and summer of 2006, NAPL seepage into the canal was observed between Transects T9 and T12, with the majority between Transects T10 and T11. Seepage was mostly associated with gas bubbles and varied in location, timing, and rate. Limited NAPL seeps also occur as globules rising to the canal surface without gas bubbles. We estimate that the rate of NAPL seepage into the canal is on the order of 111,000 grams per year (111 kilograms per year). The estimated maximum rate of NAPL seepage per cell was 32 kg per year, which

was estimated on the western side of the canal near Transect T10+75. Based on observed seepage, the overall area of potential seepage is approximately 14,000 square feet (ft²), or about one-third of an acre.

NAPL Deposition on the Cap Surface

The majority of NAPL deposition, defined as the amount of NAPL that can be quantified using cap swabs, was observed between Transects T10+50 and T11+50 and appears to be correlated with the observed seepage locations. We estimate that the mass of NAPL deposition on the top of the cap is on the order of 2.5 kg in the area of interest. On a cell basis, the estimated maximum mass of NAPL deposition is on the order of 0.5 kg, which was estimated on the western side of the canal near Transects T10+75 and T11. Significant NAPL mass is also present in the upper portion of the sand cap (defined as the top 4 inches), which is discussed below.

NAPL within the Sand Cap

Based on 2006 sampling conducted to characterize the presence of NAPL within the canal sand cap, the area of observed NAPL in the cap is generally similar to and coincident with the area of observed NAPL seepage into the canal. To estimate locations where NAPL is potentially migrating upward through the cap, the mass of NAPL in the upper and lower portions of the sand cap were calculated separately. We estimate that the mass of NAPL in the upper portion (i.e., the top 4 inches) of the sand cap is on the order of 756 kg and the mass of NAPL in the lower portion (i.e., below the top 4 inches) of the sand cap is on the order of 2,400 kg. On a cell basis, the estimated maximum mass of NAPL in the upper portion of the sand cap is on the order of 158 kg (on the western side of the canal near Transect T11+25) and in the lower portion of the sand cap is on the order of 1,450 kg (on the western side of the canal near Transect T11). Approximately 77 percent of the total estimated mass of NAPL within the lower portion of the cap (below the top 4 inches) is found in three 25-ft by 25-ft cells (10.4A, 10.4C, and 11.1A).

Five out of a total of 25 cap coring locations in the canal exhibited increased NAPL concentrations toward the bottom of the cap, indicating that NAPL may be migrating upward through the lower portion of the cap at these locations. Generally, the cap coring locations did not show visible horizontal gradation of NAPL. A visible horizontal gradation of NAPL, indicative of a vertical seepage path, could be observed in the core sample at a few locations. However, based on the volume of NAPL within the pore space of the sand, this mass is interpreted as residual NAPL and is not expected to be mobile.

During the winter investigation an additional nine cap cores (on three transects) were conducted in the west bank cap. The west bank cap coring results indicate that limited, localized, discrete intervals of NAPL are present at the apparent interface between the base of the cap and the underlying soil. However, no continuous pathway of NAPL from the cribbing to the canal was observed.

Thickness of the Sand Cap

Forty-two sand cap thickness measurements were obtained. Of these, 10 measurements were less than 1.5 feet, the cap's minimum design thickness. Most cells with low sand cap thickness also exhibited NAPL seepage and relatively high NAPL concentrations within the cap.

Potentially Mobile Subsurface NAPL

NAPL is potentially mobile in soil and sediment matrices at concentrations above residual saturation. At concentrations at or below residual saturation, NAPL is trapped within soil pores by capillary forces, which are greater than gravity or hydraulic forces, and the NAPL is immobile.

Based on the 2006 subsurface explorations beneath the canal and three-dimensional modeling, the majority of the subsurface NAPL is within the peat layer beneath the canal. The area of interpreted mobile NAPL within the subsurface is larger than the area of observed NAPL seepage. The estimated mass of mobile NAPL in the canal subsurface in the area of interest is on the order of 521,000 kg. Approximately 70 percent of the interpreted mobile NAPL is in the peat layer. On a cell basis, the maximum mass of mobile NAPL in the canal subsurface was 17,200 kg on the western side of the canal near Transect T10+50. The other cells with the highest mass of subsurface mobile NAPL tended to be in the middle of the canal.

Investigation data indicate that there is a significant mass of potentially mobile NAPL present beneath the canal. It generally does not appear to extend into the stratified silt and sand or clayey silt layers underlying the peat. Therefore, the vertical extent of potentially mobile NAPL has been adequately defined at the site.

Although the horizontal extent of potentially mobile NAPL has not been completely defined at the site, the lack of observed NAPL seepage north or south of the spring investigation boundaries indicates that the horizontal extent of potentially mobile NAPL along the canal length has been defined for the purposes of this study.

Based on the winter investigation, the horizontal extent of potentially mobile NAPL along the banks of the canal is less than the extent of mobile NAPL beneath the canal. The calculated mass of potentially mobile NAPL beneath the west and east banks is 11 percent and 6 percent, respectively, of the total mass of potentially mobile NAPL beneath the canal and banks. Furthermore, NAPL concentrations beneath the banks appear to decrease with distance away from the canal. In the vicinity of documented seepage to the canal, the only significant NAPL observed beneath the banks is in the former slip on the east bank, and even here NAPL concentrations are lower than beneath the canal. These results are consistent with historical observation of subsurface NAPL at the site.

Conceptual Site Model

The conceptual site model for NAPL migration, originally presented in the Action Plan, is updated based primarily on four potential NAPL migration mechanisms:

- NAPL migration via vertical hydraulic gradient – Vertical hydraulic gradients in the clayey silt and organic silt/sediment are sufficient for upward NAPL movement toward the base of the sand cap. This mechanism makes it possible for localized pools of NAPL to form at the interface between the organic silt/sediment and the sand cap. Upward NAPL movement through the sand cap via hydraulic gradient is unlikely due to lower hydraulic gradients within the sand cap. Other NAPL migration mechanisms, however, can cause the NAPL to migrate through the sand cap into the canal.
- NAPL migration via horizontal hydraulic gradient – Horizontal hydraulic gradients in both the east and west banks fluctuate seasonally, correlating with surface water levels and groundwater recharge. Gradients capable of mobilizing NAPL towards the canal are likely not present or are only present intermittently.

-
- NAPL migration via localized bearing-capacity failures – Consolidation settlement may have contributed to NAPL migration through the sand cap in the past, but it is anticipated that under current conditions, consolidation settlement will play a decreasing role in NAPL migration to the canal. NAPL migration to the canal, however, may still occur along localized bearing-capacity failures. Implementation of the selected NAPL controls has the potential to create NAPL migration by this preferential pathway under certain conditions of loading from construction equipment, as well as loading from the capping material type(s) and placement approach.
 - NAPL migration via preferential pathways – NAPL wicking along the cribbing and NAPL migration via preferential flow paths (such as hydraulic fractures and high-porosity zones) are potential NAPL migration mechanisms to the canal.
 - NAPL migration via gas bubble-induced transport – Gas bubbles are an observed method of NAPL migration to the canal.

Our overall conclusion is that NAPL may have migrated from the NAPL-rich peat layer to the organic silt/sediment layer and the base of the sand cap in the past as a result of consolidation and is continuing to migrate due to the effect of vertical hydraulic gradients. From the organic silt/sediment layer, gas bubbles carry the NAPL through the cap and into the canal. The effect is most pronounced where the cap is thinnest. This migration pathway appears to be the most significant of the potential ongoing NAPL migration pathways and is the primary pathway that the NAPL controls must address.

For the west bank and the majority of the east bank in the area of seepage (T9 to T12+50), which was the focus of this investigation, there is no indication that there are significant NAPL pools or that NAPL is migrating into the canal from the banks. However, there is potentially mobile NAPL within the former slip along the east bank. The NAPL controls must address the primary and secondary migration mechanisms and the impact of potentially mobile NAPL in the former slip on the cap and its ability to prevent NAPL releases. Two forms of NAPL control are possible at the site:

- Control of NAPL already on the surface of the cap
- Control of NAPL migration into the canal

Based on a multi-faceted analysis, the contiguous area of cap requiring NAPL control is approximately 14,000 ft², or one-third of an acre (Figure 5-3). The exact dimensions of the NAPL controls on the cap, and the need for NAPL controls on the banks, will be determined as part of the evaluation and analysis presented in the NAPL Controls Report.

1. Introduction

1.1 Purpose

This NAPL investigation report was prepared by ARCADIS BBL and Hart Crowser, Inc. in accordance with the Nonaqueous-Phase Liquid (NAPL) Action Plan (BBL and Hart Crowser 2006a) and the Field Investigation Work Plan (Work Plan) (BBL and Hart Crowser 2006b) for the Pine Street Canal Superfund Site in Burlington, Vermont. The Action Plan proposed a path forward to address NAPL migration at the site. The Work Plan was the first step in implementation of the Action Plan.

The Work Plan identified data gaps and proposed a series of field investigations to fill them. The NAPL field investigation was conducted in three events (spring, summer, and winter). In spring and summer 2006, surface and subsurface investigations of the canal were conducted to assess NAPL migration to the water column. In winter 2007, a subsurface investigation of the canal banks was conducted while the banks were frozen, to avoid increased NAPL migration resulting from equipment loading.

This NAPL investigation report presents the results of the spring, summer, and winter investigations, which were conducted from May 1 through May 24, 2006, August 14 through August 17, 2006, and February 1 through February 22, 2007, respectively. The report includes field observations, field data, laboratory data, and an evaluation of the data and updates the conceptual site model with respect to NAPL migration mechanisms.

This task is being performed concurrently with the NAPL Controls Report.

1.2 Site Description

The Pine Street Canal Superfund Site is located in Burlington, Vermont near the shore of Lake Champlain (Figure 1-1). The site is situated in an urban residential/industrial area about 0.5 mile south of downtown Burlington and is surrounded by manufacturing and commercial facilities, as well as by residential neighborhoods with medium to high population density. The Vermont Railroad tracks mark the western boundary of the site. The Burlington recreation path and the shore of Lake Champlain lie immediately west of, and adjacent to, the Vermont Railroad tracks. The site is approximately 70 acres in area and is substantially undeveloped. The primary physical features of the site are an abandoned barge canal and turning basin, which are hydraulically connected to Lake Champlain through a partially restricted inlet/outlet under the Vermont Railroad trestle bridge. The canal and turning basin were constructed during the industrialization of this area, which began in approximately 1868. In addition to the open-water environment (approximately 5 to 6 acres) formed by the canal and turning basin, the site consists of a 21-acre vegetated wetland area and a 45-acre upland area. A site plan showing study subareas and transect locations is presented on Figure 1-2. The work described in this report was performed in subareas 1 and 2.

The Burlington Light & Power Manufactured Gas Plant (MGP) operated from around the turn of the 20th century until 1966. Figure 1-2 shows the location of the former MGP east of the canal on Pine Street. As described in Section 2 of the Action Plan (BBL and Hart Crowser 2006a) and Appendix A of the Work Plan (BBL and Hart Crowser 2006b), analysis suggests that the Burlington Light & Power MGP formed the basis for coal tar releases in and around the canal.

In September of 2004, a Remedial Action Construction Completion Report was prepared by The Johnson Company on behalf of the Performing Defendants. During the course of the studies and remedial action taken at the site, the site was broken up into “study subareas”. Study subareas 1 and 2 comprise “the canal”. In the canal areas, the selected remedy consisted primarily of capping the canal sediments with a sand cap. The areal extent of the canal sand cap is shown on Figure 1-3. This work was primarily done during the winter months when the canal was frozen and accomplished in the dry to take advantage of the increased strength of the exposed sediments.

After the canal cap construction was completed in 2003, NAPL was observed on the west bank of the canal (both outside, i.e., west of, the timber cribbing as well as on the cap itself adjacent to the cribbing). This required development of a “NAPL response strategy” during the fall of 2003 which included the recommendation for additional sand capping over the affected portion of the west bank and removal of NAPL from impacted adjacent areas within the canal. The areal extent of the west bank sand cap is shown on Figure 1-3. This additional work on the west bank cap was completed in the summer of 2004.

Subsequent to the canal and west bank capping, NAPL was encountered on probes of the cap surface, and sheens associated with methane bubbles were noted most predominantly in the areas between Transects T9 and T12. The continued presence of NAPL on the cap prompted the need for the additional studies discussed in this report to determine the source of the NAPL and the mechanism by which the NAPL is migrating to the canal, as well as to identify potential measures for NAPL control.

1.3 Report Organization

This report is organized as follows:

- Section 2 summarizes the exploration and testing activities
- Section 3 summarizes the field and laboratory results
- Section 4 presents our evaluation of the data, including estimation of NAPL masses and loadings
- Section 5 updates the conceptual site model with respect to NAPL migration mechanisms
- Section 6 presents our conclusions based on our evaluation of the data
- Section 7 provides the references cited in the report

The following appendices are presented at the end of the report:

- Appendix A presents the daily field reports prepared during the field investigation
- Appendix B presents a photographic log prepared during the field investigation
- Appendix C presents the boring logs prepared during the field investigation
- Appendix D presents the chemical data quality review and laboratory certificate of analysis
- Appendix E presents the TarGOST™ results
- Appendix F presents the CPT results
- Appendix G presents the geotechnical testing report
- Appendix H presents the NAPL physical testing report
- Appendix I presents the piezometer water level data from 2006
- Appendix J presents the calculation sheets from Section 4
- Appendix K presents the historical NAPL sampling and distribution information
- Appendix L presents the response to USEPA comments dated October 3, 2007

2. Exploration and Testing Activities

The exploration and sampling locations for the spring, summer, and winter NAPL investigations are shown on Figures 2-1 through 2-3. The sampling locations and sample identifiers are listed in Table 2-1. Daily field reports and a photographic log of field investigation activities are presented in Appendix A and Appendix B, respectively. Activities carried out during the spring, summer, and winter NAPL investigations are summarized as follows:

- Measured groundwater levels and NAPL thicknesses at monitoring wells
- Sampled and analyzed NAPL from monitoring wells
- Made diver observations of gas bubble and NAPL seepage in the canal
- Sampled and analyzed NAPL deposition on the cap surface
- Sampled and analyzed NAPL seepage
- Carried out TarGOST™ (tar-specific green optical screening tool) and cone penetrometer test (CPT) probing of subsurface soil
- Sampled and analyzed cap and subsurface soil for geotechnical conditions
- Installed piezometers in the canal and on the canal banks to assess groundwater temperatures that may influence hydraulic gradients and measure gas bubble production in the native material
- Conducted additional settlement monitoring of the sand cap

In discussing the transects and specific locations in relation to the transects, we use the following notation system:

- Tx = the transect number; for instance, T10
- Tx+x = the number of feet south of the transect line; for instance, T10+50 is 50 feet south of Transect T10
- Tx+x E/Wx = the number of feet east of the east bank cribbing (indicated by E) or west of the west bank cribbing (indicated by W); for instance, T10+50E20 is a point 20 feet east of the east bank cribbing as measured from 50 feet south of Transect T10

2.1 Groundwater and NAPL Monitoring at Existing Monitoring Wells

Groundwater levels and NAPL thicknesses were gauged in existing monitoring wells during the spring, summer, and winter investigations. The data quality objective (DQO) for the NAPL measurements was to collect data to evaluate the presence and extent of NAPL. To characterize the NAPL, samples were also collected for laboratory analysis.

Groundwater level and NAPL thickness measurements were collected at the monitoring wells on May 1, 2006, August 14, 2006, February 2, 2007, and February 6, 2007. Coordinates for the monitoring well locations were determined in a survey conducted during the spring investigation and are presented in Table 2-2. Monitoring well locations are shown on Figure 2-1.

2.1.1 Groundwater Level and NAPL Thickness Measurements

The extent of potentially mobile NAPL was assessed in part by measuring the thickness of NAPL at the top and bottom of the monitoring wells. Wells RW10+25, RW14, MW17, MW23B, RW9+80, and RW11 (all west of the canal) and wells MW11A, MW11B, MW103B, and MW110 (all on the east bank of the canal) were evaluated for the presence of NAPL and, when NAPL was present, the thickness of NAPL layers was measured. NAPL was not gauged or sampled at well MW11D because this well has been sampled previously by The Johnson Company of Montpelier, Vermont, and groundwater samples from this well have never had detectable concentrations of polycyclic aromatic hydrocarbons (PAHs).

2.1.2 NAPL Sampling and Analysis

During the spring investigation, two NAPL samples were collected, one from observation well RW14 on the west bank and one from monitoring well MW11B on the east bank. No other monitoring wells contained sufficient NAPL for sampling, and no NAPL was observed in canal seeps near Transects T11 and T14. The NAPL samples were submitted for the following analyses to characterize the NAPL's properties:

- Kinematic and dynamic (absolute) viscosity at both method-specified and typical soil temperatures using American Society for Testing and Materials (ASTM) methods
- Density at both method-specified and typical soil temperatures using ASTM methods
- Interfacial tension at both method-specified and typical soil temperatures
- Chemical analysis for PAHs by U.S. Environmental Protection Agency (USEPA) Method 8270C and for benzene, toluene, ethylbenzene, and xylenes (BTEX) by USEPA Method 8260B

NAPL from the site was used as a calibration standard for the laboratory analysis of total petroleum hydrocarbons (TPH) in soil samples. Further details on NAPL sampling and testing are presented in the Work Plan's Field Sampling Plan and Quality Assurance Project Plan (BBL and Hart Crowser 2006b).

2.2 Diver Survey and Sampling Activities

Diver observations and NAPL sampling were performed during the spring and summer investigations to assess the mechanism through which NAPL migrates into the canal and to estimate the mass of NAPL migrating into the canal. The DQO for diver observations and sampling was to collect sufficient data to locate the NAPL seeps, to evaluate the source of NAPL being mobilized by gas bubbles, and to estimate the rate of NAPL release. The survey was repeated in the summer to evaluate whether gas seeps with NAPL appear to be consistently located or whether they migrate.

2.2.1 Diver NAPL and Gas Observations

The diver survey was conducted in two phases. The first phase, consisting of a broad survey, was conducted from the west bank. Sheen and seep observations were made at 50-foot intervals for three minutes per location. Observations were documented using broad survey observation forms. During the summer investigation, nets

were used to move free-floating vegetation toward the bank and away from active seeps to enable direct observation of the water surface.

The second phase of the diver survey was performed following completion of the broad survey. Per the Work Plan, the divers attempted to locate seeps by swimming east to west or west to east across the canal at approximately 20-foot intervals in the north-to-south direction. Because of the low visibility and the presence of vegetation, it was determined that it would be more efficient to locate seeps on the basis of surface observations. The workboat (in the spring) or the barge (in the summer) was piloted down the center of the canal and along the east bank while representatives looked for areas of NAPL seeps and gas ebullition (i.e., bubbling). The rate of NAPL release was estimated at selected seeps. A diver observed a few NAPL seeps in detail and attempted to determine whether gas bubbles bring NAPL up from beneath the cap or whether bubbles pick up NAPL at the cap surface. The diver sometimes observed a seep by wading out to the seep. The water depth in the canal was generally shallow enough to make wading, rather than diving, a more feasible method. Walking on the surface of the cap stirred up sheens that may have temporarily impacted the observations. Seep and gas bubble locations observed during the spring and summer investigations are shown on Figure 2-2. Observations were documented using diver observation forms.

During the spring investigation, the diver survey was conducted between Transects T9 and T14 and was concurrent with swabbing of the cap surface for NAPL and the sampling of water column seeps. The divers marked 14 seep and/or bubble locations observed from the water surface with buoys tied to 2-pound diver weights.

During the summer investigation, the diver survey was conducted between Transects T9 and T12+50. Fifteen seep and/or bubble locations were identified and documented using the diver observation forms.

2.2.2 Cap Surface Swabbing and Analysis for NAPL

Swabbing of the cap surface was performed during the spring and summer investigations to quantitatively characterize the nature and extent of NAPL and PAHs on the cap surface. The primary DQO was to identify NAPL concentration gradients or trends and to estimate the mass of NAPL present on the cap surface. This estimate was made on the basis of the mass of NAPL realized during cap swabbing and the area of the cap that was swabbed.

Swabbing of the cap surface for NAPL was performed in conjunction with diver surveys using the following procedure:

- The cap areas of interest were divided into 1-meter-square (1-m²) grid cells.
- A 1-square-meter frame was created from perforated, small-diameter polyvinyl chloride (PVC) tubing and placed on the surface of the cap at seep locations.
- A Teflon[®] cloth approximately 4 inches by 4 inches, which was placed on the diver's hand by an assistant, was used to wipe the entire surface of the cap within the PVC square.
- The Teflon[®] cloth was then removed from the diver's hand and placed in laboratory-supplied glassware.
- Following sample collection, the sample jars were labeled and packed in ice for shipment to the laboratory under chain of custody.

The samples were submitted to Katahdin Analytical Services of Scarborough, Maine for chemical analysis of PAHs and TPH. The Teflon[®] cloth was also submitted to Katahdin Analytical Services for extraction and analysis of TPH (using representative NAPL from the site as a calibration standard) and PAHs. The locations of cap surface swabs collected during the spring and summer investigations are shown on Figure 2-2.

During the spring investigation, cap surface swab sample locations were co-located with active seep locations. In all, nine samples were collected at five cap locations. During the first six attempts, the Teflon[®] cloth became saturated with NAPL before the entire 1-m² surface area was swabbed. Three additional swabs were collected over areas of less than 1 m² to better assess the amount of NAPL on the cap surface. At PSC-T10+67E20 and PSC-T10+76E20, additional samples were collected from smaller subsets of the frame (one-third and one-ninth of the 1-m² area). At PSC-T11+04E20, a sample of vegetation present on top of the cap was collected for visual observation before the wipe sample was collected. Cap surface samples collected during the spring investigation are identified as CS01 through CS09.

During the summer investigation, cap surface swab locations were co-located with active seep locations as well as with grid sampling of the cap surface to accurately characterize the extent of NAPL. Twenty-nine cap surface swab samples were collected, eight at active seep locations and 21 from the grid locations. None of the grid swab samples was saturated. Cap surface samples are identified as CS10 through CS38. All samples that contained NAPL were submitted for analysis. Selected samples that appeared clean (i.e., did not contain observable NAPL or sheen) were submitted to the laboratory and archived.

2.2.3 Water Column Seep Sampling and Analysis for NAPL

Water column seep sampling for NAPL was performed during the spring and summer investigations to quantitatively characterize the nature and extent of NAPL and PAHs migrating to the surface water of the canal. The DQO was to estimate the mass of NAPL present in the water column. This estimate was made on the basis of the mass of NAPL identified in water column seep sampling and the number of NAPL droplets found during the diver survey.

The seep sampling was performed in conjunction with the diver surveys using the following procedure:

- A Teflon[®] net was placed over the seep to collect 20 NAPL droplets rising through the water column.
- The net was then placed in laboratory-supplied glassware, and the jars were labeled before being packed in ice for shipment to the laboratory under chain of custody.

The samples were submitted to Katahdin Analytical Services for chemical analysis of PAHs and TPH (using representative NAPL from the site as a calibration standard). The amount of time required to collect 20 drops of NAPL was recorded. The locations of seep samples collected during the spring and summer investigations are shown on Figure 2-2.

During the spring investigation, only four water column seeps were sampled, because NAPL seepage was not continuous with respect to time or consistent with respect to location. Water column seep samples are identified as SW01 through SW04.

During the summer investigation, 15 water column seeps were sampled. All samples were collected at active seep locations. Water column seep samples are identified as SW05 through SW19.

2.3 Cap Coring and Chemical Testing to Assess NAPL Migration

Cap coring was performed to assess whether the mechanisms of potential cap recontamination include:

- Migration of NAPL and PAHs to the water column from NAPL deposition on the cap surface, resulting from mobilization by gas bubbles moving upward through the cap
- Migration of NAPL and PAHs to the water column from NAPL below the cap, resulting from compression of the underlying contaminated soils, mobilization by gas bubbles moving upward through the cap, or upward hydraulic gradient
- Migration of NAPL and PAHs to the sand cap laterally through the west bank cribbing.

The primary DQO was to obtain samples from discrete intervals, with sufficient resolution from each interval that analytical results can be used to determine concentration gradients or trends. Average analyte concentrations and standard deviations were calculated for each discrete sample interval, and results were compared to determine whether there is a significant statistical difference between sample intervals.

2.3.1 Spring Investigation

During the spring investigation, cap coring was conducted in conjunction with subsurface probing to minimize cap penetrations (described in Sections 2.4.1 and 2.5.1). The equipment was deployed from a 16-foot by 20-foot barge that was supplied by Atlantic Testing Laboratories of Canton, New York. A CME-45 drilling rig was welded to the deck of the small barge, which was equipped with two winch-operated spuds to hold the barge in place. The barge was prevented from moving during sampling through the use of spud beams partially penetrating the cap. Cap thickness was measured using a graduated pole before the spud beams were deployed. An outboard motor was attached to the barge to power it. The drilling rig rams were used to advance standard-sized CPT rods, which have a cross-sectional area of 10 square centimeters (cm²) and are 1 meter in length.

Cap coring was conducted at 15 points of NAPL seepage as determined through diver observations. The cap samples were collected using a standard 3-inch-diameter split- spoon sampling device. Sampling was planned for the top three 10-cm intervals (i.e., 0 to 10 cm, 10 to 20 cm, and 20 to 30 cm), the middle of the cap, and the bottom three 10-cm intervals. However, because of poor recovery, a limited number of samples were collected from the bottom interval.

The cap coring samples were identified as CP01 through CP14 and CP16. The cap coring locations were co-located with the TarGOST™ locations identified as LIF01 through LIF14 and LIF16, as shown on Figure 2-3. Samples were submitted for the analysis of TPH, PAHs, and total organic carbon (TOC).

2.3.2 Summer Investigation

During the summer investigation, cap coring was conducted at 10 points of NAPL seepage as determined through diver observation with the concurrence of the USEPA field oversight representative. The method for cap coring at nine locations was the same methodology currently being used by The Johnson Company for the compliance monitoring program; the sampling was conducted from the company's barge. However, one of the

sample locations (PSC-T10+50E20-CP27) was within the piezometer clusters, and it was not possible to move the barge without risking damage to the piezometers. The core was therefore pushed by the diver in the water at this location.

Cap core sampling was planned in the top three 10-cm intervals (i.e., 0 to 10 cm, 10 to 20 cm, and 20 to 30 cm), the middle of the cap, and the bottom three 10-cm intervals. However, because of poor recovery, a limited number of samples were collected from the bottom interval.

The cap coring samples were identified as CP17, CP18, and CP20 through CP27. These cap coring locations are shown on Figure 2-2. Samples were submitted for the analysis of TPH, PAHs, and TOC.

2.3.3 Winter Investigation

During the winter investigation, cap coring was conducted at three transects (T10+00, T10+50, and T11+00) along the west bank to determine whether NAPL is migrating laterally through the west bank cribbing to the sand cap. The cap coring locations were determined by considering TarGOST™ probing results, which indicated the highest fluorescence readings beneath the west bank; previously observed seep locations; and safe access. Cap cores were collected east of the west bank cribbing. At each of the three cap coring transects, three cores that were equally spaced between the cribbing and the edge of the ice were hand-driven with a dedicated polyethylene liner to a depth of 5 feet below ground surface (bgs). However, cap sand recovery was always less than 5 feet and ranged from 1.9 feet to 3.2 feet. The cap coring samples were identified as CP100 through CP108. The cap coring locations were east of the TarGOST™ locations identified as TG102B (CP100 through CP102), TG104 (CP103 through CP105), and TG106 (CP106 through CP108), as shown on Figure 2-3.

Prior to subsampling, each core was observed for NAPL and visible preferential pathways. NAPL was observed at Transect T10+50 in cap cores CP103 and CP105 and at Transect T11+00 in cap cores CP107 and CP108. One of the two following subsampling schemes was used:

- If no NAPL was observed in the core, the entire core was subsampled into 6-inch-long samples. Three samples per core were randomly selected for analysis.
- If NAPL was observed in the core, the entire core was subsampled into 6-inch-long samples. For each core, three samples of the intervals with NAPL were submitted for analysis.

Two additional samples from CP104 were submitted for analysis in April 2007. These cap coring locations are shown on Figure 2-3. Cap core samples were submitted for the analysis of TPH and PAHs.

2.4 Subsurface TarGOST™ Probing and Confirmation Borings

To evaluate the extent of mobile NAPL, additional data collection was accomplished using a TarGOST™ attached to a direct-push drilling rig. TarGOST™ is a laser-induced fluorescence screening tool that detects coal tar NAPL in soil; it was developed by Dakota Technologies, Inc. of Fargo, North Dakota. The tool is calibrated to the fluorescence of PAHs in coal tar NAPL. TarGOST™ is a front-face fluorometer that shines excitation light onto a surface and collects emissions from the same surface of soil. The fluorometer then captures light from fluorescing coal tar NAPL. The fluorescence is directed into a spectrophotometer that analyzes the light. TarGOST™ integrates data and produces results for every 1- to 2-inch interval; these results represent

fluorescence response, which is correlated to NAPL concentration, versus depth. This technique allows for the relatively rapid and inexpensive collection of approximate NAPL concentration data.

TarGOST™ probing and borings were completed in the canal during the spring investigation using the barge and drill rig described in Section 2.3. TarGOST™ probing and borings were completed in the east and west banks of the canal during the winter investigation using a CME-45 drilling rig mounted on a Mattracks truck. TarGOST™ results were confirmed by collecting soil samples from borings at approximately 20 percent of the TarGOST™ locations. The DQO was to collect sufficient NAPL data to allow determination of the areal and vertical extent of mobile NAPL.

2.4.1 Spring Investigation

During the spring investigation, TarGOST™ borings were advanced within the canal between Transects T9 and T13. The instrument was mounted inline directly above the CPT apparatus (see Section 2.5), with its window 2.2 feet above the tip of the cone penetrometer. TarGOST™ locations were co-located with CPT and cap coring locations to limit cap penetrations. A TarGOST™/CPT/cap coring “shakedown” hole was advanced in the turning basin before investigation probes were advanced in the canal. Probing was advanced at least 2 feet into the silt unit, immediately below the peat, using a direct-push drilling method. During TarGOST™ and CPT probing, casing was advanced to the geotextile and geomembrane just below the cap. Upon completion of a probe, the TarGOST™ and CPT probes were removed. Drilling rods were lowered through the casing to below the geotextile and geomembrane. Probing was then abandoned by pumping a cement and bentonite grout into the hole, to avoid leaving a preferential transport pathway, while the drilling rod and casing were slowly removed.

Twenty-six TarGOST™ locations were completed in the canal during the spring investigation. Fifteen of these locations, identified as LIF01 through LIF14 and LIF16, were co-located with cap coring locations (see Section 2.3), which were based on diver observations of NAPL seepage. The remaining 11 locations, identified as TG01 through TG11, were located between Transects T9 and T13. Probing locations are shown on Figure 2-3.

TarGOST™ results were confirmed by collecting soil samples from borings at six (approximately 20 percent) of the TarGOST™ locations. The borings, which were selected based on TarGOST™ results, represent a range of samples containing from no or minimal NAPL to high concentrations of NAPL. Boring locations were positioned no more than 3 feet from the original TarGOST™ locations. One combined TarGOST™/confirmation boring was installed at T9+00E60. For this location, a grab sample was collected at a depth of 12.5 to 13.5 feet; a TarGOST™ reading was then taken immediately below the sample depth. Some of the confirmation borings were completed as piezometers in the canal to limit cap penetrations.

The confirmation samples were collected using a standard 3-inch-outer-diameter split-spoon sampler. The Work Plan called for continuous coring with the 3-inch core barrel. However, this method had low recovery rates; in addition, it was not possible to confirm sample depths because of compression of the material within the core barrel. The drilling method was therefore modified to use the spun casing method with a low-pressure Myno pump, in which a 4-inch casing is advanced and the hydraulic pressure within the casing prevents material from entering the casing. Once the sample depth was reached, the sample was collected by advancing the split-spoon sampler ahead of the casing. The revised drilling method was discussed with USEPA representatives in the field.

The locations of confirmation borings are identified as CB02, CB03, CB06, CB07, CB08, and CB10. Locations CB02, CB03, CB06, and CB08 correspond with TarGOST™ locations LIF02, LIF03, LIF06, and LIF08, respectively, and locations CB07 and CB10 correspond with TG07C and TG10, respectively. Confirmation

boring locations are shown on Figure 2-3. Between two and four samples were collected from each confirmation boring. Seventeen samples were selected for laboratory analysis on the basis of probing results and visual observations. The selected samples were analyzed for PAHs, TPH, and TOC.

2.4.2 Winter Investigation

To define the horizontal extent of high-mobility NAPL on the banks, TarGOST™ borings were advanced during the winter investigation between Transects T9 and T12, approximately 5 feet landward from the cribbing, as well as near Transect T14. Based on the 2006 subsurface explorations and three-dimensional (3-D) modeling, the majority of high-mobility NAPL was between T10+60 and T11+50 along the east bank and T10+20 and T11+40 along the west bank. Because of limited access, fewer TarGOST™ borings were completed on the east bank than on the west bank. On the west bank, probings were conducted on 25-foot spacing between T9+00 and T11+75. On the east bank, probings were conducted on 25-foot to 75-foot spacing between T10+00 and T12+50. Probings were also conducted near historically observed seeps from the banks at T9+75, T14+05, T14+27, T14+50, and T14+75 along the west bank and T14+25 along the east bank. A probing was also placed near T11+95 on the east bank at the approximate location of the historically filled-in slip.

Where high-mobility NAPL was encountered within the initial TarGOST™ locations completed on the west and east banks, additional probings were completed to the north or south, as appropriate, along each bank. Three additional probings (TG117, TG118, and TG123) were completed approximately 10 feet to 20 feet west of the initial TarGOST™. However, no additional probings were conducted south of Transect T15, since this is the extent of observed NAPL seeps in the canal. The probings were abandoned by backfilling the boreholes with granular bentonite.

Thirty-two TarGOST™ locations were completed in the canal during the winter investigation. Twenty-four of these locations, identified as TG100, TG101, TG102B, TG103 through TG109, TG110B, and TG111 through TG123, were located on the west bank. The remaining eight locations, identified as TG124 through TG128, TG130, TG131, and TG132, were on the east bank. At TarGOST™ location TG129, located at Transect T10+75, the probe met refusal at approximately 6 feet bgs. Probing locations are shown on Figure 2-3.

TarGOST™ results were confirmed by collecting soil samples from borings at seven (approximately 20 percent) of the TarGOST™ locations. The borings, which were selected based on TarGOST™ results, represent a range of samples containing from no or minimal NAPL to high concentrations of NAPL. Boring locations were positioned no more than 3 feet from the original TarGOST™ locations with the exception of CB131, which was located approximately 27 feet from TG131 to obtain additional subsurface soil conditions for the east bank. The confirmation samples were collected continuously using a standard 3-inch-outer-diameter split-spoon sampler. The borings were abandoned by pumping a cement and bentonite grout into the hole, to avoid leaving a preferential transport pathway.

The locations of confirmation borings are identified as CB100, CB101, CB104, CB120, CB125, CB130, and CB131; these locations correspond with TarGOST™ locations TG100, TG101, TG104, TG120, TG125, TG130, and TG131, respectively. Confirmation boring locations are shown on Figure 2-3. Between three and eight samples were collected from each confirmation boring. Twenty-six soil samples were selected for laboratory analysis on the basis of probing results and visual observations. The selected samples were analyzed for PAHs, TPH, and TOC.

During the winter investigation, ex-situ TarGOST™ screening was conducted on the west bank confirmation soil samples to better correlate the TarGOST™ probing results with the analytical sampling results. The selected

samples were homogenized and tested using the TarGOST™ probe before being placed into sample jars and submitted for environmental analytical testing. The ex-situ screening was performed by placing each soil sample on the TarGOST™ laser window three times, for a total of 60 readings per sample. The results were used to develop the TPH-based and TarGOST™-based NAPL mobility criteria described in Section 4.3.

2.5 Subsurface CPT Probing and Borings to Assess Geotechnical Conditions

The geotechnical conditions of the soil were assessed to confirm whether localized bearing-capacity failures provide a mechanism for NAPL migration. Data collection to address this data gap was accomplished during the spring investigation by completing CPT and subsurface borings in the canal using the barge and drill rig and during the winter investigation by completing subsurface borings on the east and west banks, as described in Section 2.4. The DQO was to collect sufficient geotechnical data to allow evaluation of whether localized bearing-capacity failures and associated disruption to the cap create a NAPL migration mechanism, as well as to confirm stratigraphy. No additional CPT or subsurface borings were advanced during the summer investigation.

2.5.1 Subsurface CPT Probing

During the spring investigation, CPT probes were advanced within the canal between Transects T9 and T12, as well as near T14, to determine the strength and compressibility of the soils underlying the cap. CPT locations were co-located with TarGOST™ and cap coring locations to limit cap penetrations.

CPT is a well-established means of obtaining information in-situ regarding the classification, strength, and compressibility of soils. The equipment consists of a conical tip that is hydraulically pushed through the soil column. The tip's resistance to the "push" is measured. Concurrent with this measurement, an outer sleeve is pushed into the soil such that the frictional resistance of this sleeve is measured. These values are used in conjunction to quantitatively determine the physical geotechnical properties of the soil. CPT locations are shown on Figure 2-3.

The CPT instrument was a 10-ton digital subtraction-type piezocone manufactured by Applied Research Associates in Vermont. Readings of the tip, friction, and pore pressure were taken at 5-cm intervals as the rods were advanced using a depth counter resting on top of the casing. The testing was conducted in accordance with ASTM D-5778 ("Standard Test Method for Performing Electronic Friction Cone and Piezocone Penetration Testing of Soils") and the International Society for Soil Mechanics and Foundation Engineering's "International Reference Test Procedure for Cone Penetration Test."

2.5.2 Geotechnical Confirmation Sampling and Analysis

During the spring investigation, geotechnical samples were collected concurrently at five of the CPT/TarGOST™ borings to confirm the CPT results. Between two and three samples were collected from each of confirmation borings CB02, CB06, CB07, CB08, and CB10. In total, 14 samples were analyzed for geotechnical index parameters, bulk density, and permeability.

During the winter investigation, geotechnical samples were collected concurrently at the seven TarGOST™ confirmation borings. Between three and four samples were collected from each of the confirmation borings CB100, CB101, CB104, CB120, CB125, CB130, and CB131. In total, 27 samples were analyzed for

geotechnical index parameters. One sample from each of three stratigraphic layers (peat, clayey silt, and fill) was analyzed for bulk density and permeability.

2.6 Piezometer and Temperature Probe Installation and Monitoring

Two potential mechanisms of NAPL mobilization and migration at the site are (1) upward groundwater hydraulic gradients and (2) gas bubbles, potentially affected by temperature fluctuations, rising from the native material. To evaluate these potential migration mechanisms, piezometers were installed at the site, both in the canal and on the banks of the canal, to measure hydraulic heads and groundwater temperatures. The piezometers were installed during two separate field investigations. The spring 2006 piezometers were installed in May 2006 and data were collected from mid-May until mid-November 2006, when the piezometers were abandoned. The winter 2007 piezometers were installed in February 2007 and collected data from late April through late October 2007. Piezometer coordinates and screened depths are presented in Table 2-3. Piezometer locations at which data were collected are shown on Figure 2-1. All piezometer locations are shown on Figure 2-3.

2.6.1 Spring 2006 Piezometer Installation

Eight piezometers were installed during the spring 2006 field investigation in the canal in two clusters and screened at four intervals: shallow organic silt/sediment, deep organic silt/sediment, peat, and clayey silt. Based on the CPT results, the piezometer clusters were located at T12+00 E60/40 and T10+50 E20. A combination pressure transducer and temperature probe was installed in each of the piezometers at depths of 1 to 2 feet, 3 to 4 feet, 9 to 10 feet, and 19 to 20 feet below the cap/sediment interface. Temperature probes were installed to determine whether there is a connection between temperature and gas generation rate. Pressure transducers were installed to measure groundwater elevations as a function of time. To track the response of the groundwater elevations and temperature in piezometers with respect to the level of the canal and temperature of the surface water, a stilling well with a transducer was installed next to PZ7.

One complete piezometer cluster was damaged beyond repair during the spring field investigation and subsequent data collection. On May 18, 2006, the PVC riser for PZ1 was broken off near the mudline at the connection between two 10-foot riser sections. This occurred during attempted installation of the transducer in the piezometer, when the skiff being used to gain access to the piezometers drifted into PZ1.

On May 24, 2006, during routine transducer data downloads, it was discovered that the risers on two additional piezometers, PZ2 and PZ4, had broken off. This was most likely due to extreme weather conditions (including heavy rain, high winds, and a rise in canal water elevation) at the site during the previous week. The risers and the transducer cables for PZ2 and PZ4 were retrieved from the bottom of the canal. It appeared that the top riser section of PZ2 had become unthreaded from the bottom portion, because it was still intact. The top riser section of PZ4 appeared to have broken off near the mudline at the riser joint. After these occurrences, The Johnson Company installed chimney rods flush with the piezometers to help support the weight of the transducer cable and stabilize the piezometer stickup.

On June 6, 2006, during reinstallation of compliance monitoring sediment traps by The Johnson Company, PZ3 broke off. The piezometer was damaged when a gust of wind caused the barge being used during sediment trap installation to drift into the piezometer riser. Temperature and pressure data were collected from PZ3 up until it was damaged. The four damaged piezometers were abandoned in place.

Temperature and pressure data were collected from the remaining four transducers installed in PZ5, PZ6, PZ7, and PZ8 from mid-May until the piezometers were decommissioned in mid-November 2006, as discussed

below. Although the piezometer clusters located at T12+00 E60/40 were damaged, the piezometer cluster around T10+50 E20 provided substantial amounts of usable data for the analysis of hydraulic gradients and groundwater temperatures.

2.6.2 Spring 2006 Piezometer Decommissioning

The four piezometers (PZ5, PZ6, PZ7, and PZ8) remaining from the spring 2006 installation were decommissioned by The Johnson Company on November 15 and 16, 2006. The piezometers were removed to avoid damage to them from canal ice. Decommissioning was performed in accordance with the Work Plan (BBL and Hart Crowser 2006b). A report on the decommissioning prepared by The Johnson Company is provided in Appendix A.

2.6.3 Winter 2007 Piezometer Installation

Five piezometers were installed on the banks of the canal during the winter 2007 field investigation. Piezometers PZ100 and PZ101 were installed in a cluster on the west bank of the canal. Piezometers PZ102, PZ103, and PZ104 were installed in a cluster on the east bank of the canal. Piezometers PZ100 and PZ102 were co-located with TarGOST™ confirmation borings CB104 and CB130, respectively. The piezometers were screened in the materials indicated below:

- PZ100: stratified silt and sand
- PZ101: peat
- PZ102: clayey silt
- PZ103: peat
- PZ104: peat

A combination pressure transducer and temperature probe was installed in each of the piezometers in late April 2007. A stilling well with a transducer was also installed during the same field event to collect data on the water level of the canal. The stilling well data were used to track the response of the groundwater elevations in piezometers with respect to the canal surface water elevations.

Pressure data were collected from the five piezometers and stilling well from late April 2007 to late October 2007. The probes were removed from the piezometers and stilling well on October 26, 2007. The stilling well was also removed on this date. The piezometers remain on the site.

2.7 Cap Settlement Plate Installation and Monitoring

Additional settlement monitoring of the sand cap was necessary to evaluate whether the cap's long-term settlement rate had decreased to an insignificant level and whether additional settlement could contribute to additional releases of NAPL to the cap. During the spring investigation, 13 cap settlement plates were installed.

During cap construction in the fall of 2002, temporary settlement plates were installed at Transects T8+50 (center and west), T10+50 (center, west, and east), and T12+50 (center and east). Those temporary plates were later damaged during reinundation of the canal and subsequent ice formation. During the spring investigation, settlement plates were reconstructed at the same approximate locations. Settlement plates were also established at Transects T9+50 and T11+50 near the center of the canal and the west side of the canal. Additional upland

settlement plates were installed along the west bank near Transects 9, 10, 11, and 12. Settlement plate elevations were monitored through October 2006.

3. Field and Laboratory Results

This section summarizes the results of the analyses conducted by Katahdin Analytical Services of Scarborough, Maine; Queen's University of Kingston, Ontario, Canada; and Hart Crowser's geotechnical laboratory in Seattle, Washington, as well as data collected in the field. Tables referenced in this section summarize the key data generated through geotechnical testing, chemical analysis of soil and NAPL, physical analysis of NAPL, and groundwater elevation monitoring conducted in the field. Following data validation, all field and laboratory test measurements were deemed acceptable for use. Complete results and full data validation reports are presented in Appendices D through I. Boring logs are presented in Appendix C.

3.1 Soil Physical Characteristics

The purpose of collecting subsurface geotechnical soil probes was to gather information on the stratigraphy of the canal and the bank sediments and underlying organic peat soils, as well as to evaluate the basic index and geotechnical engineering properties of the site soils. Both disturbed (i.e., grab) and relatively undisturbed (i.e., Shelby tube) samples were collected during the field investigation for testing in the Hart Crowser geotechnical laboratory.

A generalized soil profile was developed for our analysis of subsurface conditions at the site. The general order of soil types encountered by the explorations from ground surface downward was as follows:

Sand Cap Material. Up to about 3 feet of silty, fine sand was encountered between the mudline and the underlying geotextile.

Organic Silt/Sediment. Very soft, wet, dark gray, sandy, clayey, organic silt and silt with scattered root fragments and organic materials were encountered beneath the geotextile. This layer is generally 4 to 8 feet thick.

Peat. A layer of soft, wet, dark brown to black peat underlies the organic silt. This unit is up to about 8 feet thick and is often interbedded with organic silt.

Stratified Silt and Sand. Loose, wet, gray to dark gray, clayey, stratified, very silty, fine sand and sandy, clayey silt underlie the peat unit. In several locations, lenses of silty clay were encountered within this unit. This stratified unit is up to 10 feet thick.

Clayey Silt. Underlying the stratified silt and sand is very soft to soft, wet, gray, stratified clayey silt and silty clay.

In addition, there is a surface layer of fill, silty clay, fine sand, sand and silt, and clayey silt that is called "bank soil" in this report. This layer is primarily located on the east bank, but there is some bank soil located on the west bank as well. The stratigraphy is presented on Figures 3-1 through 3-7.

3.1.1 Data Quality

On the basis of an initial review, the geotechnical data appear generally acceptable. Problematic data and our course of action for each case are summarized below.

In most cases, the initial interpretation of stratigraphy shown on the original CPT logs (created by the CPT subcontractor, Northwest Cone Exploration, Inc. of Snohomish, Washington) is not in agreement with the conditions we observed during drilling of the confirmation borings. To reconcile the data, we developed subsurface profiles at each CPT probe location based on site conditions, field observations, and classification of soil samples obtained during drilling. These profiles have been added to the CPT logs presented in Appendix F.

Hydraulic conductivity for two samples having a water content above the soil liquid limit was determined using a rigid-wall permeameter, rather than a flexible-wall permeameter. Refer to the discussion of hydraulic conductivity in Section 3.1.6.

3.1.2 CPT and Boring Results

CPT logs are presented in Appendix F. Boring logs are included in Appendix C. Soil samples from the explorations were visually classified in the field. Selected soil samples were taken to the Hart Crowser geotechnical laboratory, where the classifications were verified in a controlled environment.

The CPT logs include our generalized interpretation of the subsurface profile at each probe location (see the far right column of the logs). Our interpretation of the stratigraphy is based primarily on the conditions observed during drilling of the confirmation borings and the classification of samples obtained during drilling. The stratigraphy under the canal as presented on Figures 3-2 through 3-4, 3-6, and 3-7 is based on an assumed constant water level in the canal. This is reasonable because the variation of the water level was less than 2 inches during the spring investigation.

In general, the stratigraphy interpreted from the explorations advanced as part of these investigations agrees with historical site data reported by others.

3.1.3 Soil Classification Parameters

Field and laboratory observations include density/consistency, moisture condition, and estimates of grain size and plasticity. These results are shown in Table 3-1 by sampling event and by stratigraphic unit. The soil classification parameters reported in Table 3-1 are in general agreement with historical site data presented in previous reports.

3.1.3.1 Soil Classification

The classifications of selected samples were checked by conducting laboratory tests such as Atterberg limits and grain size analysis. Classifications were made in general accordance with the Unified Soil Classification System, ASTM D 2487, as presented on Figure C-1 in Appendix C.

3.1.3.2 Water Content

Water content was determined for most samples recovered in the explorations as soon as possible following their arrival in the Hart Crowser laboratory; this test was conducted in general accordance with ASTM D 2216. The results of these tests are shown in Table 3-1 and available in Appendix G (on hydraulic conductivity pages G-10 through G-29 for the spring investigation and page G-41 for the winter investigation). In addition, water content is routinely determined in samples subjected to other kinds of testing. These additional results are also presented on the exploration logs. Note that the water content is calculated as a percentage of the weight of water divided by the weight of dry soil grains in a sample, so that values greater than 100 percent are possible. The significance of water content results exceeding 100 percent is indicative of the presence of organic matter or high plasticity clay. In the case of the Pine Street Canal, it is organic matter that is contributing to the values above 100 percent. This is because organics have lower specific gravity than minerals, typically have high void ratios, and retain moisture within the plant fibers. Water contents for organic soil will depend on the amount of organic matter versus mineral and the state of decomposition of the peat. These factors combine to create variable results for water contents in peat, which range up to values that are quite high, as shown in the results.

3.1.3.3 Grain Size Analysis

Grain size distribution was analyzed for representative samples in general accordance with ASTM D 422. Wet sieve analysis was used to determine the size distribution greater than the U.S. No. 200 mesh sieve. The results of the tests are shown in Table 3-1 (as “Soil Description”) and are presented in Appendix G as curves that plot percent finer by weight versus grain size.

3.1.3.4 Atterberg Limits

Atterberg limits were measured for selected fine-grained soil samples. The liquid limit and plastic limit were determined in general accordance with ASTM D 4318-84. The result of the Atterberg limits analyses and the plasticity characteristics are summarized in Table 3-1. The results are also presented on the liquid and plastic limits test report in Appendix G. This report relates the plasticity index (liquid limit minus the plastic limit) to the liquid limit. The results of the Atterberg limits tests are shown graphically on the boring logs, as well as on figures presenting various other test results, where applicable.

3.1.3.5 Bulk Density

We determined the bulk density of each Shelby tube sample by measuring the weight of the tube alone, the weight of the tube with the soil, and the volume of the soil. The results of the bulk density determination are included in Table 3-1 and are also presented on pages G-9 and G-41 in Appendix G.

3.1.3.6 Organic Content

The organic content of selected samples was analyzed using ASTM D 2974 Method C (“Standard Test Methods for Moisture, Ash, and Organic Matter of Peat and Other Organic Soils”). The results of the organic content tests are included in Table 3-1 and on page G-30 in Appendix G.

3.1.4 Compressibility and Consolidation Parameters

Moisture content data (which can be correlated to compressibility for saturated samples), plasticity data, hydraulic conductivity testing, and the CPT data can be correlated with parameters used to assess both magnitude and time rate of consolidation.

Consolidation settlement behavior of cohesive soils is a non-linear relationship between stress and strain. Cohesive soils have relatively low permeability; thus, when they undergo loading (such as the placement of a sand cap), their compression is controlled by the rate at which water is expelled from the pores. The rate at which water is expelled dissipates over time, and so the rate of consolidation also decreases with time. Typically, this time rate of settlement will approach a straight line when settlement is plotted versus the logarithm of time.

The available historical data (The Johnson Company 2003) were used to determine the time rate of settlement during normal (virgin) compression.

Based on The Johnson Company data, we determined the amount of settlement that occurred until October 2003 for nine settlement plates, as described in the Work Plan (BBL and Hart Crowser 2006b). It should be noted that the plates or rods at T8+50E and T10+50E were removed in late March or early April 2003; as such, the total settlement observed at these locations is less than at the other six locations, where data were collected for another six months. When we plot the historical time rate of settlement data for the six locations monitored beyond spring 2003 as a logarithmic regression and apply theoretical extrapolations, we can also estimate the total amount of settlement that has occurred through October 2006 as a result of placement of the cap.

From these estimates of the magnitude of consolidation and phase equations, we can estimate the amount of water and/or NAPL expelled from the pores through October 2003 and through October 2006. This information is summarized in Table 3-2.

When we plot the time rate of settlement data collected for this study (Section 3.1.7), it appears that secondary compression on the order of 0.1 inch per year is occurring. The accuracy of the data from the new settlement plates is such that a definitive trend cannot be discerned. To determine a trend in long-term secondary settlement, the plates would need to be left in place and monitored for a longer period of time. In some of the plates we do see some downward trend. Based on typical behavior of organic silt/sediment and peat deposits of this nature, we know that some secondary compression may be continuing to occur. Given the lack of a discernable trend, it is appropriate to extrapolate the original (i.e., The Johnson Company) data, which would suggest a continuing rate of at least 0.1 inch per year. However, these data cover a relatively short time on the consolidation versus time curve. Over the coming years, further settlement of the ground surface should approach very small values.

3.1.5 Soil Strength Parameters

Tip resistance and friction measurements obtained from CPT testing provide direct data on soil strength and the compressibility of site soils. The CPT logs (Appendix F) present tip resistance data in tons per square foot, as well as friction data as a percentage of the tip resistance. The tip resistance values obtained from cone penetrometer testing indicate very low to low soil strength. The average ranges of CPT tip resistance observed for each layer are as follows:

- Organic silt/sediment: 0.2 to 1.2 tons/square foot (ft²)

-
- Peat: 1.2 to 3.3 tons/ft²
 - Silty sand to sandy silt: 17.4 to 25.1 tons/ft²
 - Stratified silt and sand: 10.6 to 14.6 tons/ft²
 - Clayey silt: 6.3 to 6.8 tons/ft²

Tip resistance of the more cohesive soils can be related to undrained shear strength by empirical methods that account for the total overburden pressure and as empirical cone factor. In general, the values of interpreted shear strength obtained for each soil unit are within the range of strength and compressibility data reported by others from previous site investigations.

A comparison of the distribution of NAPL concentrations with soil strength at the same location shows no discernable trend between soil strength and NAPL concentrations observed at the surface (i.e., on the cap), within the cap, or within the subsurface soils.

3.1.6 Hydraulic Conductivity

During the spring and winter investigations, laboratory hydraulic conductivity tests were conducted on samples from the five upper soil units (cap material, organic silt/sediment, peat, stratified silt and sand, and clayey silt). Hydraulic conductivity tests were conducted in general accordance with ASTM D 5084 Method C (Falling Head, Rising Tailwater) (“Standard Test Methods for Measurement of Hydraulic Conductivity of Saturated Porous Materials Using a Flexible-Wall Permeameter”). Because of the high water content of some soil samples, two samples were tested using ASTM D 5856 Method D (Falling Head, Rising Tailwater) (“Standard Test Methods for Measurement of Hydraulic Conductivity of Porous Materials Using a Rigid-Wall, Compaction Mold Permeameter”). Hydraulic conductivity values determined from laboratory testing on 13 samples are presented in Table 3-3. The results are presented by location (under the canal and under the bank) and by stratigraphic unit. The results are also presented in Appendix G on the pages for hydraulic conductivity test data and the corresponding hydraulic conductivity test report.

Previous site investigations of hydraulic conductivity were reviewed from the following documents:

- “Supplemental Remedial Investigation Final Report: Pine Street Canal Superfund Site,” prepared under USEPA contract number 68-W9-0036. March. (Metcalf and Eddy 1992)
- “Additional Remedial Investigation, Pine Street Canal Superfund Site, Burlington, Vermont.” July 3. (The Johnson Company 1997)

Hydraulic conductivity data reported in these historical documents encompasses both in-situ field test results and undisturbed vertical Shelby tube laboratory tests. Laboratory testing of site soils was performed to determine hydraulic conductivity by PEER in 1990 and Perkins-Jordan in 1984. Perkins-Jordan also conducted two pumping tests to further evaluate the hydraulic conductivity of the peat and sand deposits at the site. In-situ hydraulic conductivity data were collected through pumping tests in 1991 and 1992 by Metcalf and Eddy. These values are reported in Table 3-4. Hydraulic conductivities in feet per day (ft/day) for ARCADIS BBL laboratory test and for historical laboratory tests are summarized below:

- Sand cap layer:
 - 6.09 ft/day (source: ARCADIS BBL; laboratory tests)
- Organic silt/sediment layer:

-
- 0.00176–2.61 ft/day (source: ARCADIS BBL; laboratory tests)
 - Bank Soil Layer (upland):
 - 0.00906 ft/day (source: ARCADIS BBL; laboratory tests)
 - 0.2–1.0 ft/day (source: Metcalf and Eddy 1992; in-situ tests)
 - 0.00037–0.00059 ft/day (source: Perkins-Jordan 1984; laboratory tests)
 - Peat layer:
 - 0.00884–0.433 ft/day (source: ARCADIS BBL; laboratory tests)
 - 0.01–0.5 ft/day (source: Metcalf and Eddy 1992; in-situ tests)
 - 0.0048–0.0054 ft/day (source: Perkins-Jordan 1984; laboratory tests)
 - 0.8 - 0.00008 ft/day under 0.25 – 4.0 kips per square foot (KSF) loading conditions (Metcalf and Eddy 1992)
 - Stratified silt and sand layer:
 - 0.00465–0.00706 ft/day (source: ARCADIS BBL; laboratory tests)
 - 0.02–0.2 ft/day (source: Metcalf and Eddy 1992; in-situ tests)
 - 0.7 ft/day (source: PEER 1990; laboratory tests)
 - 0.0012–0.0057 ft/day (source: Perkins-Jordan 1984; laboratory tests)
 - 0.0021–0.45 ft/day (source: Perkins-Jordan 1984; in-situ tests)
 - Clayey Silt Layer:
 - 0.000453–0.000765 ft/day (source: ARCADIS BBL; laboratory tests)
 - 0.04–0.6 ft/day (source: Metcalf and Eddy 1992; in-situ tests)
 - 0.00002–0.0003 ft/day (source: PEER 1990; laboratory tests)

Table 3-4 also presents a summary of this information. In general, the hydraulic conductivity values reported by others are within one order of magnitude of those determined in this study. It should be noted that in-situ methods for evaluating bulk hydraulic conductivity are considered more representative of actual conditions at the site and that laboratory measured hydraulic conductivities provide valuable order-of-magnitude values for the vertical component of hydraulic conductivity, but may not appropriately characterize anisotropy found in natural systems. Although a broad range of hydraulic conductivities are reported for several of the soil units at the site, only the range of hydraulic conductivities measured from in-situ field tests are used for subsequent calculations and laboratory-measured hydraulic conductivities are presented for reference only.

3.1.7 Cap Settlement Parameters

The Johnson Company has provided data for the cap settlement plates installed in May 2006 for a period of five months. At each settlement plate location, the elevation of a given point on the riser pipe was recorded. This information has been used to determine the elevation change of the individual settlement plates. Table 3-5 summarizes the data for each of 13 settlement plates.

The settlement plate data do not indicate a trend in downward movement given the short monitoring duration and the accuracy of the settlement plate measurements, which is on the order of 0.3 inch. However, extrapolation of historical settlement plate data (see Section 3.1.4) suggests that the current time rate of settlement is about 0.1 inch per year and should steadily decrease in the future.

3.1.8 Cap Thickness Measurement

In 2006, the sand cap thickness was measured at locations where cap corings, TarGOST™ probings, and piezometer installations were carried out. These measurements are summarized in Table 3-6.

3.2 Groundwater Potentiometric and Temperature Data

This section discusses data collected for the purposes of evaluating site hydrogeology. These data include manual groundwater level gauging data, data collected from pressure transducers and temperature probes installed on site, and NAPL thickness gauging data.

3.2.1 Data Quality

Data quality was assessed for each portion of the hydrogeology investigation task, and a determination was made as to whether data quality is considered acceptable and the data are usable for future site evaluation.

As specified in the Work Plan (BBL and Hart Crowser 2006b), groundwater levels and NAPL thickness measurements at monitoring wells were obtained in the field using a Heron H0.1L oil-water interface probe marked at 1/100-foot increments. Volatile organic compounds (VOCs) in the headspace of each monitoring well were measured and recorded in parts per million (ppm) before the well was gauged using a MiniRAE 2000 photoionization detector (PID), which was calibrated before the field measurements were made. The monitoring well and piezometer elevations and horizontal coordinates were surveyed by a surveyor licensed in the State of Vermont. Groundwater elevations and NAPL elevations were calculated from the field measurements and the surveyor's elevation data. The groundwater level and NAPL thickness data presented in this report are considered acceptable and usable for future site evaluation.

Groundwater elevation and temperature data were collected in the field from mid-May 2006 until mid-November 2006 using transducers in the piezometers and a stilling well that indicates the water level at the canal. Piezometers were installed to specifications in the Work Plan and were completed in accordance with the State of Vermont Department of Environmental Conservation's Conservation Practice Standard for Monitoring Well Installation, Code 353. Upon transducer installation, water levels were measured using a Heron water level meter marked at 1/100-foot increments, and piezometers were developed using a disposable bailer. In-situ LevelTroll 500 combination pressure and temperature transducers with data loggers were installed in the piezometers after development and in the stilling well. An additional manual water level measurement was obtained when the transducer unit began logging. The transducers convert pressure readings to depth-to-water measurements based on standard specific gravity for water. Piezometer and stilling well top-of-casing elevations were surveyed by a surveyor licensed in the State of Vermont. Groundwater elevations were calculated from depth-to-water measurements recorded by the transducer, the surveyor's elevation data, and the water level measurements taken at the start of transducer logging.

Although one in-water piezometer cluster was damaged during installation and subsequent field measurement events, the data obtained from the transducers at piezometers PZ5 through PZ8 provide a sufficient basis to characterize potentiometric levels and vertical hydraulic gradients beneath the canal during the monitoring period. Potentiometric data were collected within each hydrogeologic layer beneath the canal (organic silt/sediment, peat, and clayey silt) over an approximately six-month period from May 2006 to November 2006, which covers the transition from wet (spring) conditions to dry (fall) conditions. Because one complete cluster

of piezometers remained active throughout the monitoring period, data are available to evaluate hydraulic interactions between the subsurface layers and the canal.

Prior to removing the pressure transducers and abandoning the in-water piezometers, The Johnson Company collected additional water level and transducer depth data to confirm the placement elevation of the transducers. The final transducer elevations were compared to the transducer elevations recorded at the time of installation to determine whether any transducer “drift” occurred during the course of deployment. The difference between the final transducer elevation reading and the manual reading was 0.037 foot for PZ5, 0.08 foot for PZ6, and 0.094 foot for the stilling well. The difference between the transducer elevation reading and the manual reading was 0.17 foot for PZ8 and 0.56 foot for PZ7. A linear correction was applied to all of the piezometer data over the period of record to account for these differences.

Water level spikes in PZ5 and PZ7, which were considered anomalies, were removed from the data set for gradient calculations and presentation of maximum and minimum water level elevations. The full data set, including the anomalous water level spikes, is presented in Appendix I.

Upon review of the complete, corrected PZ5 data set, we determined that the water level data were unusable for hydrogeologic calculations. The data from mid-May through August 2006 showed extremely slow recovery, which made the early part of the data set unusable for calculation of vertical gradients or correlation with canal surface water levels. In the latter part of the data set, from the end of August through November 2006, the water level in the peat piezometer dropped significantly to a level below the surface water, suggesting that the reference level (top of casing) had changed. It is likely that the piezometer settled into the peat during this time as a result of the high compressibility potential of the peat. This settling may have also contributed to the break in the seal around the piezometer casing, allowing for hydraulic communication of the peat piezometer to the surface water. This would account for the close correlation between the peat and canal surface water levels in the second half of the data set. The complete data set for peat water levels is plotted along with the other piezometer data sets in Appendix I.

Sharp water level rises, or “spikes,” were observed in the transducer data on September 29, October 4, and October 20, 2006. These spikes were observed at all of the piezometers and the stilling well. The cause of the spikes is unknown; three possibilities are seiche events, changes in barometric pressure, or a combination of both.

A seiche is a standing wave in a closed body of water, such as Lake Champlain, that results from high winds. A review of wind records for the Burlington area from weather gauges reporting to Weather Underground (www.weatherunderground.com) indicates that high wind events did occur on September 29, October 4, and October 20. The average high wind speeds and high wind gust speeds on these dates were among the top five wind speeds and wind gusts for September, October, and November, when the piezometers were removed. Since the stilling well spikes are smaller than the spikes at the other measurement points, however, it is unlikely that all three events were related to seiche events.

Another possible cause of the spikes is changes in barometric pressure. As the barometric pressure declines, water levels in piezometers may rise. Weather Underground’s records of barometric pressure for September 29, October 4, and October 20 indicate that the barometric pressure was generally the lowest recorded for the September and October time period. In any case, because these brief spikes were observed in all of the water level data sets, they are interpreted as part of the representative data set and were included in the assessment of water level ranges and hydraulic gradients.

Groundwater elevation data were collected in the bank piezometers and stilling well from late April 2007 until late October 2007. Data collected from the bank piezometers and stilling well in 2007 were acceptable for use without qualification.

Data obtained from previous site investigations were not specifically evaluated for data quality.

3.2.2 Depth to Groundwater and Groundwater Elevation Data

Groundwater elevation data collected at the site are discussed below.

3.2.2.1 Monitoring Well Data

Table 3-7 presents the monitoring well data collected during the spring, summer, and winter investigations, including water level data. Water levels at individual monitoring wells were consistent during all three rounds of measurements, typically within 0.5 foot or less. The depth of groundwater ranged from approximately 3.98 to 7.61 feet below top of casing during these measurement events.

3.2.2.2 Piezometer Data

2006 Piezometer Installations

Graphs of the groundwater elevations¹ in the various piezometers and stilling well are presented on Figure 3-8. The data discussed below include data downloaded from the transducers through November 16, 2006, when the spring 2006 piezometers were abandoned.

- Groundwater elevations in PZ3, screened in the clayey silt, ranged from 98.06 feet to 99.27 feet.
- Groundwater elevations in PZ7, screened in the clayey silt, ranged from 97.25 feet to 99.93 feet.
- Groundwater elevations in PZ8, screened in the deep organic silt/sediment, ranged from 95.49 feet to 99.21 feet.
- Groundwater elevations in PZ6, screened in the shallow organic silt/sediment, ranged from 96.30 feet to 99.23 feet.
- Surface water elevations in the stilling well ranged from 96.39 feet to 99.10 feet.

The water levels measured at the stilling well and piezometers indicate temporal fluctuations, but the general order of water levels is consistent with upward groundwater flow. The greatest potentiometric levels were recorded in the deepest piezometer (PZ7), and the lowest levels were generally recorded in the stilling well.

¹ All elevations provided in Section 3.2.2.2 are in 1988 North American Vertical Datum.

Winter 2007 Piezometer Installations

Graphs of the groundwater elevations in PZ100, PZ101, PZ102, PZ103, and PZ104 and the stilling well for the six-month period from late April 2007 to late October 2007 are presented on Figure 3-9. Locations and screen depths of these piezometers are presented in Table 2-3. The data discussed below include data downloaded from the transducers through October 26, 2007, when the pressure transducers were removed.

- Groundwater elevations in PZ100, screened in the stratified silt and sand on the west bank, ranged from 96.47 feet to 100.38 feet.
- Groundwater elevations in PZ101, screened in the peat on the west bank, ranged from 96.45 feet to 102.09 feet.
- Groundwater elevations in PZ102, screened in the clayey silt on the east bank, ranged from 97.34 feet to 100.25 feet.
- Groundwater elevations in PZ103, screened in the peat on the east bank, ranged from 96.93 feet to 99.89 feet.
- Groundwater elevations in PZ104, screened in the peat on the east bank, ranged from 96.26 feet to 100.27 feet.
- Surface water elevations in the stilling well ranged from 96.36 feet to 100.24 feet.

Vertical hydraulic gradients are discussed in Section 4.7.1 and presented in Table 3-8. Horizontal hydraulic gradients are discussed in Section 4.7.2. Historical hydraulic gradients are discussed in Section 4.7.1 and 4.7.2 and presented Table 3-4. Digital files of raw data collected from the transducers are available upon request. Piezometer boring logs are presented in Appendix C.

3.2.3 Surface Water Elevations

Water level data were collected in the canal during the 2006 and 2007 data collection periods as described above. Canal water levels were compared to water levels reported by the USGS for Lake Champlain (USGS ECHO station at the Leahy Center for Lake Champlain located at One College Street, Burlington, VT, Figure 3-10). The weir separating the canal from the lake is at an elevation of 96.5 feet (NAVD88). This weir typically keeps the canal water levels substantially higher than lake levels during the dry season, however in the wet season when lake levels are higher than the top of the weir, the hydraulic connection between the canal and the lake causes the surface water levels to remain closely matched. During the dry season, when lake levels fall 2 or more feet below the top of the weir, surface water gradients from the canal to the lake are very high, but flow is controlled by the weir. The exception is from July to October, 2007, when beavers built a dam east of the weir, which resulted in water levels in the canal higher than the weir elevation. The comparison of these surface water elevations contributes to the general understanding of the interactions between these two water bodies; however, groundwater gradients in the west bank as determined from bank piezometers provide a more accurate characterization of groundwater gradients adjacent to the canal.

3.2.4 Groundwater Temperature Data from Spring 2006 Piezometers

Temperature variations in the piezometers and stilling well are presented on Figure 3-11.

- Groundwater temperatures in PZ3, screened in the clayey silt, ranged from 9.97 degrees Celsius (C) to 10.10 degrees C. Data for this piezometer are only available through June 2006.
- Groundwater temperatures in PZ7, screened in the clayey silt, ranged from 9.99 degrees C to 10.38 degrees C.
- Groundwater temperatures in PZ5, screened in the peat, ranged from 9.66 degrees C to 11.26 degrees C.
- Groundwater temperatures in PZ8, screened in the deep organic silt/sediment, ranged from 9.64 degrees C to 16.30 degrees C.
- Groundwater temperatures in PZ6, screened in the shallow organic silt/sediment, ranged from 10.56 degrees C to 18.62 degrees C.
- Surface water temperatures in the stilling well ranged from 5.52 degrees C to 27.35 degrees C.

As expected, the range in recorded temperatures is greatest in the stilling well and decreases with increasing depth below the mudline, as discussed below. Also, the timing of the temperature peak occurs earliest (in July) at the stilling well. The magnitude of the peak temperature decreases with increasing depth, and the timing of the peak temperature is later with increasing depth. The deepest unit (clayey silt) shows little change in temperature during the monitoring period. Digital files of raw data collected from the transducers are available upon request.

3.2.4.1 Groundwater and Surface Water Temperature Comparison from Spring 2006 Piezometers

Groundwater and surface water temperatures recorded in the piezometers and stilling well were compared for the period of mid-May to mid-November 2006 (Figure 3-11). Surface water temperatures generally increased from May until the beginning of August, decreased until the end of the period, and varied by 21.83 degrees C. During the same period, groundwater temperatures in the shallow and deep organic silt/sediment increased until late August and then began to decrease. Groundwater temperatures in the shallow organic silt/sediment varied by 8.06 degrees C, and groundwater temperatures in the deep organic silt/sediment varied by 6.66 degrees C. Groundwater temperatures in the peat and clayey silt during the same period remained relatively constant, varying by only 1.60 degrees C in the peat and 0.39 degree C in the clayey silt. PZ5 (screened in the peat layer) was excluded from the hydraulic gradient evaluation because it appeared that the piezometer had settled slightly into the peat layer. Also, the head data collected after early August 2006 showed a surprising correlation to the data in the stilling well in the canal, suggesting that the hydraulic seal along the piezometer had been compromised. However, the temperature data at PZ5 showed no change in trends, and no significant correlation with the temperature at the stilling well. Including the data from PZ5, the temperature data all showed less fluctuation and more time lag with increasing depth below the canal. Thus, the temperature data recorded at PZ5 are still considered representative of the temperature in the peat. These data indicate that the temperature of the deeper soil layers at the site is constant and is not influenced by surface water temperatures.

Groundwater and surface water temperatures were recorded during seasonal variations from the spring through the fall months. A complete set of temperature data for all soil layers in the canal, as well as for the surface water, has been collected.

3.2.5 NAPL Thickness Data

Table 3-7 presents the NAPL thickness data collected during the spring, summer, and winter investigations. During the May 2, 2006 gauging event, a sheen or film was recorded at four wells: MW17, RW9+80, RW11, and RW14. A measurable thickness of NAPL was recorded at the bottom of two wells on May 2, 2006: approximately 11 feet of NAPL at well MW11B and 8 inches of NAPL at well RW14. In addition, NAPL droplets were observed at wells MW17 and MW23B. PID readings for VOCs in the wells ranged from 0.0 ppm to 10.7 ppm.

During the August 14, 2006 gauging event, NAPL droplets, sheens, or films were observed at four wells: MW17, RW10+25, RW11, and RW14. A measurable thickness of NAPL was observed at the bottom of two wells: 10 feet of NAPL at well MW11B and 6 inches of NAPL at well RW14. In addition, NAPL droplets were observed at wells MW17 and MW23B, and a trace of NAPL was recorded at well RW10+25. PID readings for VOCs in the wells ranged from 0.0 to 55.7 ppm.

During the February 2 and 6, 2007 gauging event, NAPL droplets, sheens, films or NAPL residual on the oil/water interface probe were observed at four wells: MW17, RW9+80, RW10+25, and RW14. A measurable thickness of NAPL was observed at the bottom of three wells: 9.4 feet of NAPL at well MW11B, 0.1 inch of NAPL at well MW23B, and 1.0 foot of NAPL at well RW14. In addition, NAPL was observed on the tip of the oil/water interface probe at well MW17. NAPL measurements could not be taken at wells RW10+25 and RW11 due to frozen water in the well riser. PID readings for VOCs in the wells ranged from 0.0 to 3.0 ppm.

Available historical NAPL thickness data were reviewed and summarized in Appendix K. According to compliance monitoring data for 2000 to spring 2006, NAPL thicknesses have generally decreased in monitoring wells (The Johnson Company 2006e).

3.3 NAPL Sampling and Analysis

During the spring investigation, samples of NAPL were collected from wells MW11B and RW14 using disposable Teflon[®] bailers. The NAPL in each well was dark brown and slightly viscous. A sample from each well was submitted to Katahdin Analytical Services for chemical analysis of PAHs and BTEX and to Queen's University for analysis of physical properties, including viscosity, density, and interfacial tension.

3.3.1 NAPL Sampling Data Quality

A quality assurance (QA) review of laboratory data was performed for the chemical analysis of free-phase NAPL samples collected from the site. Katahdin Analytical Services analyzed the samples and reported the results as sample delivery group PS-01. The data were reviewed in accordance with the project-specific Quality Assurance Project Plan (QAPP).

The NAPL samples were analyzed for PAHs using USEPA Method 8270C and for BTEX using USEPA Method 8260B. Reporting limits for PAHs were higher than those specified in the QAPP because sample extracts required dilution due to the presence of high concentrations of hydrocarbons. Surrogate recoveries were not applicable because of sample dilution. The overall objectives for the data quality indicators² (DQIs) as set forth in the project QAPP were met, and the data are acceptable for use as qualified. The completeness for these data is 100 percent. Detailed discussions of DQIs are presented in Appendix D for each analytical procedure.

3.3.2 NAPL Sampling Analytical Data

This section presents the analytical data for the NAPL samples. NAPL chemistry results are presented in Table 3-9. NAPL physical properties are presented in Table 3-10. Available historical data are also included in Appendix K for comparison. A summary of that evaluation is included in the following sections. The data quality of these historical samples was not reviewed as part of this work and is therefore unknown. These data were evaluated against the ARCADIS BBL data for comparison purposes only.

As described in the QAPP, NAPL samples will be considered to be generally comparable if the standard deviation of the physical and chemical parameters is less than 25 percent of the average values.

3.3.2.1 NAPL Sampling PAH Results

PAH results for the two NAPL samples (MW11B and RW14) collected in 2006 were similar. All PAHs for which the samples were analyzed were detected in the two NAPL samples except benzo(k)fluoranthene, benzo(g,h,i)perylene, dibenzo(a,h)anthracene, and indeno(1,2,3-cd)pyrene. However, these compounds were subject to elevated detection limits because of sample dilution. Sample RW14 contained greater concentrations of individual PAHs than did sample MW11B, excepting 2-methylnaphthalene and naphthalene. Total PAH concentrations ranged from 135,500 to 147,000 milligrams per kilogram (mg/kg) in samples MW11B and RW14, respectively.

The PAH concentrations for the two NAPL samples were evaluated for similarity, as described in the QAPP. Total PAHs differed by approximately 10 percent and individual concentration of PAHs were within an order of magnitude between the two samples. The standard deviation for individual compounds was less than 25 percent of the average value, excepting acenaphthylene (53 percent), benzo(a)pyrene (30 percent), fluoranthene (28 percent), and pyrene (28 percent). Based on this analysis, the PAH concentrations are considered comparable, but not uniform, between the two NAPL samples.

Historical results from four samples collected in 1990 and one sample collected in 2002 were evaluated for comparability in Appendix K. In summary, the 1990 PAH data were not comparable to either the 2002 or 2006 results. The PAH concentrations for the sample collected in 2002 was considered comparable with the two 2006 samples.

² Quality control parameters such as matrix spikes, surrogates, laboratory control samples, and duplicates that are used to assess data quality, precision, accuracy, and reproducibility.

3.3.2.2 NAPL Sampling BTEX Results

All the BTEX compounds were detected in the two NAPL samples collected in 2006. Sample RW14 contained higher concentrations of individual BTEX compounds than did sample MW11B.

The BTEX concentrations for the two NAPL samples were evaluated for similarity, as described in the QAPP. The standard deviation for individual compounds was less than 25 percent of the average value, excepting benzene (45 percent), ethylbenzene (31 percent), and toluene (56 percent). Based on this analysis, the BTEX concentrations are considered comparable between the two NAPL samples.

Historical results from one sample collected in 1990 were evaluated for comparability in Appendix K. In summary, the one NAPL sample collected by The Johnson Company from the sediment surface was not comparable with the 2006 samples. Benzene and toluene were not detected in this sample and the other BTEX compounds were approximately an order of magnitude less than the 2006 samples. The difference in BTEX concentrations between the 2002 and 2006 samples is likely due to differences in sample location and method. The 2006 samples were collected from monitoring wells, while the 2002 sample was collected from a pool of NAPL on the sediment surface. The 2002 sample may have lower BTEX concentrations due to dissolution from the pool of NAPL into the canal water or volatilization during sampling.

3.3.2.3 NAPL Sampling Physical Results

Density, viscosity, and interfacial tension results were similar between the two NAPL samples collected in 2006. The physical parameters for the two NAPL samples were evaluated for similarity, as described in the QAPP. The standard deviation for density and interfacial tension was less than 2 percent of the average value for the samples. The standard deviation for viscosity was less than 10 percent of the average value for the samples. Based on this analysis, the physical parameters are considered comparable between the two NAPL samples. Density results indicate that NAPL is denser than water.

Historical results from one sample collected in 1990 were evaluated for comparability in Appendix K. In summary, physical testing was conducted on two samples collected in 2003 by The Johnson Company from a NAPL puddle on the ground surface and from a NAPL puddle on the canal cap surface. The standard deviations for physical parameters were less than 25 percent of the average value for all parameters. Based on this analysis, the physical parameters are considered comparable between the two NAPL samples collected in 2003 and are considered comparable to the samples collected in 2006.

3.4 Diver Survey and Sampling Activities

Diver survey and sampling activities were carried out during both the spring and the summer investigations as documented in Section 2.2. Diver seep observations and seep sampling activities for the spring investigation are summarized in Table 3-11. Diver seep observations and seep sampling activities for the summer investigation are summarized in Table 3-12. Sampling locations are shown on Figure 2-2.

3.4.1 Data Quality

3.4.1.1 Spring Investigation

A QA review of the laboratory data generated through analysis of cap surface and water column seep samples was performed. Katahdin Analytical Services analyzed the samples and reported the results as sample delivery group PS-01. The data were reviewed in accordance with the project-specific QAPP.

The Teflon[®] swab samples were submitted for analysis of PAHs using USEPA Method 8270C and TPH using USEPA Method 8015 and site-specific NAPL for calibration. Reporting limits for PAHs were higher than specified in the QAPP because sample extracts required dilution due to the presence of high concentrations of hydrocarbons. Surrogate compounds were not added to these samples because the same extracts were used for both PAH and TPH analysis; surrogate compounds would have caused analytical interference in the TPH analysis. The overall objectives for the DQIs as set forth in the project QAPP were met and the data for this project are acceptable for use as qualified. The completeness for these data is 100 percent. Detailed discussions of DQIs are presented in Appendix D for each analytical procedure.

3.4.1.2 Summer Investigation

A QA review of laboratory data was performed for the chemical analysis of cap surface and water column seep samples. Katahdin Analytical Services analyzed the samples and reported the results as laboratory batches WW4274 and WW4275. The data were reviewed in accordance with the project-specific QAPP.

The Teflon[®] swab samples were submitted for analysis of PAHs using USEPA Method 8270C and TPH using USEPA Method 8015 and site-specific NAPL for calibration. Reporting limits for PAHs and TPH were higher than specified in the QAPP because sample extracts required dilution due to the presence of high concentrations of hydrocarbons. Results for several PAHs were qualified as estimated due to exceedances of initial calibration criteria. Surrogate compounds were not added to these samples because the same extracts were used for both PAH and TPH analysis; surrogate compounds would have caused analytical interference in the TPH analysis. The overall objectives for the DQIs as set forth in the project QAPP were met and the data for this project are acceptable for use as qualified. The completeness for these data is 100 percent. Detailed discussions of DQIs are presented in Appendix D for each analytical procedure.

3.4.2 Observations

3.4.2.1 Spring Investigation

NAPL seeps were intermittent; seeps observed at one location on a given day did not necessarily occur at the same location on following days. This was particularly noticeable at locations marked by the divers with buoys. When these locations were revisited on following days, no seeps were observed. As a result, 14 seep and/or bubble locations were identified during the survey and four water column seep samples were taken.

3.4.2.2 Summer Investigation

The water column seeps and cap surface swabs were sampled during the diver survey. Fifteen seep and/or bubble locations were identified and documented using the diver observation form. The northern portion of the canal (north of the piezometers at approximately Transect T10+50) appeared to be less active than the southern portion of the canal (south of the piezometers at approximately Transect T10+50). The majority of the seeps with associated NAPL were viewed between Transects T10+50 and T11+50.

Twenty-nine cap surface swab samples were collected, 21 from the grid locations shown on Figure 2-2. None of the grid swab samples was saturated, indicating that the NAPL observed on the cap surface during the spring investigation appears to be focused between Transects T10+50 and T11+00 on the western half of the canal.

When the divers disturbed the cap surface on the western edge of the canal, large sheens were produced. In addition, it was observed that the elevation of the cap varied as much as approximately 3 feet. Elevation dips in the cap were noted as the divers progressed north to south along the western edge of the canal.

3.4.3 Cap Surface Swab Analytical Data

This section presents the analytical data for the cap surface swabs. Details concerning the cap swab samples are presented in Table 3-13. Analytical results are presented in Table 3-14. Sample locations are shown on Figure 2-2.

3.4.3.1 Cap Surface Swab PAH Results

Spring Investigation

All PAHs for which the samples were analyzed were detected in the cap surface swab samples excepting benzo(k)fluoranthene, benzo(g,h,i)perylene, dibenzo(a,h)anthracene, and indeno(1,2,3-cd)pyrene. However, these compounds were subject to elevated detection limits because of sample dilution. The greatest concentrations of PAHs occurred in samples from locations T10+96E30, T10+98E40, and T11+4E20. Total PAH concentrations on the surface of the cap within a 1-m² area ranged from 523,200 to 1,118,000 micrograms per wipe (µg/wipe).

Cap surface swab samples collected from surface areas of less than 1 m² contained lower PAH concentrations than samples collected from a full square meter. Cap surface swab samples collected from one-third of a square meter (sample CS07) and one-ninth of a square meter (sample CS08) at location T10+67E20 contained, on average, 11 percent and 17 percent, respectively, of the PAHs in the full square meter sample (CS01). The cap surface swab sample collected from one-third of a square meter (sample CS09) at location T10+76E20 contained, on average, 23 percent of the PAHs in the full square meter sample (CS02).

The cap surface swab sample collected from the vegetation on the surface of the cap (sample CS06) contained 18,440 µg/wipe of total PAHs.

Summer Investigation

For the cap swab samples located in the grid pattern (CS10 to CS30), all PAHs for which the samples were analyzed were detected excepting dibenzo(a,h)anthracene. Of the 13 samples that appeared clean, six were analyzed by the laboratory. The greatest concentration of PAHs on samples that appeared clean was 1,622 µg/wipe. For the grid locations, total PAH concentrations in a 1-m² area ranged from 98 to 235,100 µg/wipe, with the greatest concentrations between Transects T10 and T11.

For the cap swab samples co-located with seep observations (CS31 to CS38), the greatest concentrations of PAHs occurred in samples from locations T10+65E20, T11+00E40, and T11+25E50. Total PAH concentrations on the surface of the cap in a 1-m² area ranged from 1,967 to 971,000 µg/wipe.

3.4.3.2 Cap Surface Swab TPH Results

Spring Investigation

TPH was detected in all the cap surface swab samples. The greatest concentrations of TPH were in samples from locations T10+96E30, T10+98E40, and T11+4E20. TPH concentrations on the surface of the cap in a 1-m² area ranged from 180,000 to 5,800,000 µg/wipe.

At location T10+67E20, cap surface swab samples collected from surface areas of less than 1 m² contained lower concentrations of TPH than did samples collected from a full square meter. For this location, the samples collected from one-third of a square meter (sample CS07) and one-ninth of a square meter (sample CS08) contained, on average, 11 percent and 19 percent, respectively, of the TPH in the full square meter sample (CS01). However, the cap surface swab sample collected from a surface area of less than 1 m² at location T10+76E20 contained greater concentrations of TPH than did the sample collected from a full square meter. For this location, the sample collected from one-third of a square meter (sample CS09) contained about five times the concentration of TPH detected in the full square meter sample (CS02).

The cap surface swab sample collected from the vegetation on the surface of the cap (sample CS06) contained 100,000 µg/wipe of TPH.

Summer Investigation

For the cap swabs located in the grid pattern (CS10 to CS30), TPH was detected in all samples. Of the 13 samples that appeared clean, six were analyzed by the laboratory. The greatest concentration of TPH in samples that appeared clean was 26,000 µg/wipe. TPH concentrations in a 1-m² area for the grid locations ranged from 1,500 to 2,000,000 µg/wipe, with the greatest concentrations between Transects T10 and T11.

For the cap swab samples co-located with seep observations (CS31 to CS38), the greatest concentrations of TPH occurred in samples from locations T10+65E20, T11+00E40, and T11+25E50. Total TPH concentrations on the surface of the cap in a 1-m² area ranged from 25,000 to 11,000,000 µg/wipe.

3.4.4 Water Column NAPL Seep Analytical Data

This section presents the analytical data for the water column NAPL seep samples. Analytical results are presented in Table 3-15. Sample locations are shown on Figure 2-2.

3.4.4.1 Water Column NAPL Seep PAH Results

Spring Investigation

All PAHs for which the samples were analyzed were detected in the water column NAPL seep samples excepting benzo(g,h,i)perylene, dibenzo(a,h)anthracene, and indeno(1,2,3-cd)pyrene. In addition, benzo(k)fluoranthene was not detected in sample SW04. Total PAH concentrations ranged from 2,411 µg/wipe (sample SW01) to 18,140 µg/wipe (sample SW04).

Summer Investigation

All PAHs for which the samples were analyzed were detected in the water column NAPL seep samples excepting dibenzo(a,h)anthracene. Total PAH concentrations ranged from 10 µg/wipe (sample SW14) to 5,985 µg/wipe (sample SW11).

3.4.4.2 Water Column NAPL Seep TPH Results

Spring Investigation

TPH was detected in all the water column NAPL seep samples at concentrations ranging from 20,000 to 100,000 µg/wipe.

Summer Investigation

TPH was detected in all the water column NAPL seep samples at concentrations ranging from 570 to 53,000 µg/wipe.

3.5 Cap Sand Quality Characteristics

This section presents the analytical results for the cap core samples collected from within the canal and on the west bank cap. Cap core samples were collected during the spring, summer, and winter investigations using different methodologies, as described in Section 2.3. Cap core sample locations are presented on Figure 2-2 for the summer investigation and on Figure 2-3 for the spring and winter investigations.

The last portion of the sample identification number indicates the depth in feet below the sediment surface (bss) at which the cap core was collected. For example, T11+70E30-CP14-0-0.32 indicates the cap core sample was collected from cap core location 14 (T11+70E30) at a depth of 0 to 0.32 foot bss. Note that for samples collected in the canal, the sediment surface used in the sample designation is equivalent to the mudline (top of the sand cap) and does not correspond to the organic silt/sediment layer, which is below the sand cap.

The west bank cap samples were collected from depths below ground surface. For example, sample designation T10+00-CP102-2.5-3 indicates that the west bank cap core sample was collected from cap core location 102 (T10+00) at a depth of 2.5 to 3 feet bgs.

The samples were submitted to Katahdin Analytical Services for chemical analysis. Cap core chemistry results are presented in Tables 3-16, 3-17, and 3-18 for the spring, summer, and winter investigations, respectively. The west bank cap core log is presented in Appendix C.

3.5.1 Cap Sand Data Quality

3.5.1.1 Spring Investigation

A QA review of laboratory data was performed for the chemical analysis of cap sand samples. Katahdin Analytical Services analyzed the samples and reported the results as sample delivery groups PS-02, PS-03, and PS-04. The data were reviewed in accordance with the project-specific QAPP.

Cap sand samples were submitted for analysis of PAHs using USEPA Method 8270C, TPH using USEPA Method 8015 and site-specific NAPL for calibration, and TOC using the Lloyd-Kahn method. Reporting limits for PAHs were higher than specified in the QAPP because sample extracts required dilution due to the presence of high concentrations of hydrocarbons. Surrogate recoveries were not applicable because of sample dilutions. The overall objectives for the DQIs as set forth in the project QAPP were met and the data are acceptable for use as qualified. The completeness for these data is 100 percent. Detailed discussions of DQIs are presented in Appendix D for each analytical procedure.

3.5.1.2 Summer Investigation

A QA review of laboratory data was performed for the chemical analysis of sand cap samples collected from the Pine Street Canal Superfund Site. Katahdin Analytical Services analyzed the samples and reported the results as sample delivery groups WW4280 and WW4281. The data were reviewed in accordance with the project-specific QAPP.

Cap samples were submitted for analysis of PAHs using USEPA Method 8270C, TPH using USEPA Method 8015 and site-specific NAPL for calibration, and TOC using the Lloyd-Kahn method. Reporting limits for PAHs were higher than specified in the QAPP because sample extracts required dilution due to the presence of high concentrations of hydrocarbons. Results for several PAHs were qualified as estimated due to exceedances of initial calibration criteria. Surrogate recoveries were not applicable in most samples because of sample dilutions. The overall objectives for the DQIs as set forth in the project QAPP were met and the data for this project are acceptable for use as qualified. The completeness for these data is 100 percent. Detailed discussions of DQIs are presented in Appendix D for each analytical procedure.

3.5.1.3 Winter Investigation

A QA review of laboratory data was performed for the chemical analysis of the west bank cap samples. Katahdin Analytical Services analyzed the samples and reported the results as sample delivery group SA0750. The data were reviewed in accordance with the project-specific QAPP.

West bank cap samples were submitted for analysis of PAHs using USEPA Method 8270C and TPH using USEPA Method 8015 and site-specific NAPL calibration. Reporting limits for some PAHs were higher than specified in the QAPP because sample extracts required dilution due to the presence of high concentrations of

hydrocarbons. Surrogate recoveries in some samples were not applicable because of sample dilutions. The overall objectives for the DQIs as set forth in the project QAPP were met and the data are acceptable for use as qualified. The completeness for these data is 100 percent. Detailed discussions of DQIs are presented in Appendix D for each analytical procedure.

Two archived west bank cap samples were selected for TPH analysis on the basis of results for sample delivery group SA0750.

3.5.2 Cap Sand TarGOST™ Results

During only the spring investigation, TarGOST™ probes were made at 13 locations within the sand cap in the course of completing 11 TarGOST™ explorations (TG01 through TG11); at two locations, multiple probes were necessary to achieve the required depth. TarGOST™ results are presented in Appendix E. TarGOST™ results through the cap generally show elevated signals at the surface of the cap. The signals within the cap are generally very low, with localized occurrences of elevated signals.

3.5.3 Cap Sand PAH Results

3.5.3.1 Spring Investigation

Total PAH concentrations in cap core samples ranged from not detected to about 2,279,000 micrograms per kilogram ($\mu\text{g}/\text{kg}$). PAH concentrations in surface cap core samples do not indicate the presence of an isolated PAH hot spot. The data indicate sporadic elevated PAH concentrations in the surface of the cap with areas of low PAH concentration between the elevated concentrations.

The cap core data generally indicate that the maximum total PAH concentrations occur at the surface and total PAH concentrations decrease with depth. The exceptions are locations CP06, CP08, and CP09:

- At location CP06, three cap core samples were collected from 0 to 0.32 foot, 0.32 to 0.64 foot, and 0.64 to 0.9 foot bss; the maximum total PAH concentration occurs in the interval from 0.64 to 0.9 foot bss.
- At location CP08, three cap core samples were collected from 0 to 0.32 foot, 0.32 to 0.64 foot, and 0.64 to 0.85 foot bss; the maximum total PAH concentration occurs in the interval from 0.32 to 0.64 foot bss.
- At location CP09, two cap core samples were collected from 0 to 0.32 foot and 0.32 to 0.64 foot bss; the maximum total PAH concentration occurs in the interval from 0.32 to 0.64 foot bss.

3.5.3.2 Summer Investigation

Total PAH concentrations in cap core samples ranged from 981 to about 3,247,000 $\mu\text{g}/\text{kg}$.

For cap core locations where two samples were collected, the maximum total PAH concentration generally occurs at the surface, and total PAH concentrations decrease with depth. The exceptions are locations CP18 and CP23, which had little difference in total PAH concentrations between intervals.

At four cap core locations, three samples were collected. Cap core locations CP24 and CP27 displayed maximum total PAH concentrations at the surface. Cap core locations CP17 and CP21 displayed maximum total PAH concentrations in the interval from 0.66 to 0.8 foot bss and 0.66 to 0.99 foot bss, respectively.

3.5.3.3 Winter Investigation

Total PAH concentrations in the west bank cap core samples ranged from 5 to 2,183,900 µg/kg.

Three of the nine cap core locations (CP103, CP105, and CP107) contained a distinct interval of visible NAPL; an additional location (CP108) contained visible NAPL, but not within a discrete interval. The intervals with visible NAPL were preferentially sampled, and chemistry results showed PAH concentrations decreasing above and below the visible NAPL. For west bank cap core locations without visible NAPL within the core, total PAH concentrations were highest in the samples closest to the surface and tended to decrease with depth.

3.5.4 Cap Sand TPH Results

3.5.4.1 Spring Investigation

TPH was detected in all the cap core samples at concentrations ranging from 4.6 to 9,300 mg/kg. Concentrations of TPH in surface cap core samples do not indicate the presence of an isolated hot spot of elevated TPH. The data indicate sporadic elevated TPH concentrations in the surface of the cap, with locations of low TPH concentration between the elevated concentrations.

The cap core data generally display the maximum TPH concentration at the surface, and TPH concentrations decrease with depth. The exceptions are locations CP01, CP02, CP08, and CP09, where the maximum TPH concentrations occur in the subsurface.

3.5.4.2 Summer Investigation

TPH was detected in all the cap core samples at concentrations ranging from 14 to 1,000 mg/kg.

For the cap core locations where two samples were collected, the maximum TPH concentration generally occurs at the surface, and TPH concentrations decrease with depth. The exception is location CP18, which showed little difference in total TPH concentrations between intervals. At four cap core locations, three samples were collected. Cap core locations CP24 and CP27 displayed maximum TPH concentrations at the surface. Cap core location CP17 displayed the maximum TPH concentration in the interval from 0.66 to 0.8 foot bss, while cap core location CP21 displayed the maximum TPH concentration in the interval from 0.33 to 0.66 foot bss.

3.5.4.3 Winter Investigation

TPH was detected in 16 of the 28 cap core samples at concentrations ranging from 6 to 19,000 mg/kg.

TPH concentrations ranged from 4,600 to 19,000 mg/kg in the west bank cap core samples with discrete, visible NAPL intervals. TPH concentrations decreased in the samples above and below the discrete NAPL intervals by

one to two orders of magnitude. For the west bank cap core locations without visible NAPL, TPH concentrations tended to be highest near the cap surface and decrease by one to two orders of magnitude with depth.

3.5.5 Cap Sand TOC Results

TOC was detected in cap core samples at concentrations ranging from 470 to 13,000 mg/kg during the spring investigation and from 470 to 19,000 mg/kg during the summer investigation. West bank cap core samples collected during the winter investigation were not analyzed for TOC.

3.6 Subsurface Soil Quality Characteristics

Confirmation boring samples were collected during the spring and winter investigations. The samples were submitted to Katahdin Analytical Services for chemical analysis and Hart Crowser's geotechnical laboratory for geotechnical analysis. Discussion of geotechnical results is presented in Section 3.1.

3.6.1 Subsurface Soil Data Quality

3.6.1.1 Spring Investigation

A QA review of laboratory data was performed for the chemical analysis of soil samples. Katahdin Analytical Services analyzed the samples and reported the results as sample delivery groups PS-02, PS-03, and PS-04. The data were reviewed in accordance with the project-specific QAPP.

Soil samples were submitted for analysis of PAHs using USEPA Method 8270C, TPH using USEPA Method 8015 and site-specific NAPL for calibration, and TOC using the Lloyd-Kahn method. Reporting limits for PAHs were higher than specified in the QAPP because sample extracts required dilution due to the presence of high concentrations of hydrocarbons. Surrogate recoveries were not applicable because of sample dilutions. The overall objectives for the DQIs as set forth in the project QAPP were met and the data are acceptable for use as qualified. The completeness for these data is 100 percent. Detailed discussions of DQIs are presented in Appendix D for each analytical procedure.

3.6.1.2 Winter Investigation

A QA review of laboratory data was performed for the chemical analysis of soil samples. Katahdin Analytical Services analyzed the samples and reported the results as sample delivery groups SA0661 and SA0797. The data were reviewed in accordance with the project-specific QAPP.

Soil samples were submitted for analysis of PAHs using USEPA Method 8270C, TPH using USEPA Method 8015 and site-specific NAPL for calibration, and TOC using the Lloyd-Kahn method. Reporting limits for some PAHs were higher than specified in the QAPP because sample extracts required dilution due to the presence of high concentrations of hydrocarbons. Surrogate recoveries in some samples were not applicable because of sample dilutions. The overall objectives for the DQIs as set forth in the project QAPP were met and the data are

acceptable for use as qualified. The completeness for these data is 100 percent. Detailed discussions of DQIs are presented in Appendix D for each analytical procedure.

3.6.2 Subsurface Soil TarGOST™ Results

3.6.2.1 Spring Investigation

TarGOST™ probes were made at 32 locations in the canal in the course of investigating 26 TarGOST™ explorations (at some locations, multiple probes were necessary to achieve the required depth). TarGOST™ results are presented in Appendix E. Cross sections with TarGOST™ results posted on them are presented on Figures 3-1 through 3-7. The TarGOST™ results generally show elevated NAPL concentrations in the peat and low NAPL concentrations in the remaining units.

3.6.2.2 Winter Investigation

TarGOST™ probes were made at eight locations along the east bank of the canal and 24 locations along the west bank of the canal (at some locations, multiple probes were necessary to achieve the required depth). TarGOST™ results are presented in Appendix E. Similar to the spring investigation, the TarGOST™ results generally show elevated NAPL concentrations in the peat and low NAPL concentrations in the remaining units. The results also indicate that the NAPL concentrations along the banks are generally lower and less uniform than the NAPL concentrations beneath the canal.

3.6.3 Subsurface Soil Confirmation Borings

This section presents the results of the confirmation borings. The confirmation sample chemistry results are presented in Table 3-19 for the spring investigation and Table 3-20 for the winter investigation. The confirmation boring sample locations are presented on Figure 2-3.

The last portion of the sample identification number indicates the depth at which the sample was collected. For example, T9+48E20-CB02-7-9 indicates the sample was collected from confirmation boring location 2 from 7 to 9 feet bss. The east bank and west bank confirmation borings were collected from depths below ground surface. For example, WB-T10+00-CB120-14.9-15.4 indicates that the sample was collected along the west bank (indicated by WB) at Transect T10+00 from confirmation boring location 120 at a depth of 14.9 to 15.4 feet bgs.

3.6.3.1 Subsurface Soil PAH Results

Total PAH concentrations in confirmation boring samples ranged from approximately 15,000 to 100,650,000 µg/kg in the spring investigation and from 395 to 109,850,000 µg/kg in the winter investigation.

3.6.3.2 Subsurface Soil TPH Results

TPH concentrations in confirmation boring samples ranged from 240 to 650,000 mg/kg in the spring investigation and from 18 to 830,000 mg/kg in the winter investigation.

3.6.3.3 Subsurface Soil TOC Results

TOC concentrations in confirmation boring samples ranged from 1,800 to 790,000 mg/kg in the spring investigation and from 2,600 to 990,000 mg/kg in the winter investigation.

4. Evaluation and Discussion of Results

This section evaluates and discusses the data presented in Section 3, with emphasis on what the data collected during the spring, summer and winter investigations, in some cases in combination with previously collected data, indicate about the location and migration of NAPL. Calculation sheets that accompany these results are provided in Appendix J.

4.1 Methodology

The following information provides a basis to evaluate and select NAPL controls at the site and is generally conservative with respect to the extent and mass of NAPL. The values depicting location and mass of NAPL are derived using conservative (high-end) assumptions. However, in some cases, a range of values or an average value is also presented.

To evaluate NAPL location and mass with respect to the potential for NAPL seepage into the canal, a grid was projected onto the canal. Each cell in the grid is 25 feet by 25 feet in plan view. Cell numbering corresponds to transect numbering. From north to south, grid identification is 9.1 through 12.3. From west to east, grid identification is A, B, and C. The grid and individual cells in the grid are discussed in more detail in the following sections.

It is assumed that the mass of NAPL is equal to the mass of TPH measured in the various environmental matrices. This is a reasonable assumption since the TPH measurements are based on an analytical method calibrated using NAPL from the site.

This section presents analyses of the relative order-of-magnitude masses of NAPL within different stratigraphic layers at the site. This does not represent a mass balance. Since these masses are order-of-magnitude estimates, the actual NAPL mass or seepage associated with each cell may be lower or higher. The following is discussed:

- Estimated residual saturation criteria for coal tar NAPL, which are used to define the difference between mobile and immobile NAPL
- Potentially mobile subsurface NAPL, including the location and mass of mobile NAPL in the subsurface
- NAPL within the sand cap, including the extent and mass of NAPL in the sand cap
- NAPL deposition on the surface of the cap, including the extent and mass of NAPL on the sand cap surface
- NAPL seepage in the canal, including the extent and rate of NAPL seepage into the canal
- Hydrogeologic considerations for NAPL mobility, including estimates of horizontal and vertical gradients

4.2 Estimated Residual Saturation Criteria for Coal Tar NAPL

NAPL is mobile in soil and sediment matrices at concentrations above residual saturation (Mercer and Cohen 1990; USEPA 1990; Huling and Weaver 1991). At concentrations at or below residual saturation, NAPL is trapped within soil pores by capillary forces, which are greater than gravity or hydraulic forces, and the NAPL is immobile. This section presents the estimation of TPH-based and TarGOST™-based NAPL mobility criteria, which define NAPL mobility—i.e., NAPL concentrations above the mobility criteria have potential to be mobile and NAPL concentrations below the mobility criteria will generally not be mobile.

4.2.1 TPH-based NAPL Mobility Criteria

A recent study by the Electric Power Research Institute (EPRI) found that residual NAPL saturation concentrations for coal tar in fine-grained material ranged from 25,000 to 72,000 mg/kg (mass of coal tar NAPL per mass of soil) (EPRI 2004). The range shows that the residual saturation (RS) is dependent on soil conditions and NAPL characteristics. This study showed that RS is correlated with soil grain size and organic content and with NAPL viscosity and interfacial tension. However, other researchers have shown that RS values appear to be insensitive to NAPL properties and very sensitive to soil properties, especially heterogeneities (Huling and Weaver 1991). Because the EPRI study is based on multiple sites exhibiting a range of soil conditions and NAPL characteristics, its values cannot be used to estimate the residual saturation of coal tar NAPL at the Pine Street Canal Superfund Site. However, these values can be used for comparison to a site-specific estimate of residual saturation.

Residual saturation is defined as the volume of immobile, residual NAPL trapped in the pores relative to the total volume of pores (Huling and Weaver 1991) and is calculated as follows:

$$RS = \frac{V_{NAPL}}{V_{Pores}}$$

Where: RS = residual saturation (dimensionless)
V_{NAPL} = volume of residual NAPL trapped in the pores (liters, L)
V_{Pores} = total volume of pores (L)

Mercer and Cohen (1990) summarize the range of NAPL residual saturation values as 0.10 to 0.20 in the vadose zone and 0.15 to 0.50 in the saturated zone. Thus, the capacity for retention of NAPL in the unsaturated zone is less than the capacity in the saturated zone. These RS values were established for fine- to coarse-grained materials. In the spring and winter investigations, the peat had bulk weights ranging from 65 to 70 pounds per cubic foot (pcf), with high moisture contents (250 to 550 percent) and low dry unit weights (10 to 18 pcf). Dr. Bernard H. Kueper, Ph.D., P.Eng, of Queen's University has recommended an RS value of 0.10 for the Pine Street Canal Superfund Site (Kueper 2007b). To reflect the heterogeneity of the subsurface at the site, we selected a conservative RS value of 0.05 for all soil layers. This conservative RS value was selected for design purposes. Using the dry unit weight for the three stratigraphic layers containing the bulk of the NAPL (the organic silt/sediment, the peat, and the stratified silt and sand), we calculated the following range of NAPL residual saturations for the site:

Parameter	Organic Silt/Sediment	Peat	Stratified Silt and Sand
Residual saturation	0.05	0.05	0.05
Dry unit weight (kilograms per liter, kg/L)	0.366	0.227	1.071
Specific gravity of solids *	1.35	1.35	2.65
Residual concentration (mg/kg)	103,000	195,000	31,000

*Brady 1974

Compaction of the soil would reduce the void ratio and promote NAPL displacement out of the peat. Since the residual saturation estimate is based on dry unit weight measured from soil samples collected from the spring investigation, and thus after much of the compaction of the soil has occurred, the residual saturation estimate is believed to be representative of existing conditions.

4.2.2 TarGOST™-based Mobility Criteria

Data generated from TarGOST™ and co-located confirmation borings from the spring and winter investigations were used to establish a relationship between the TarGOST™ fluorescence readings and measured NAPL concentrations in the subsurface. Data generated during the winter investigation, when homogenized soil samples collected along the west bank were screened ex-situ with the TarGOST™ probe prior to their submittal to the laboratory, were also used. The data sets available for the analysis were therefore:

- Spring investigation co-located, in-situ TarGOST™ probes and confirmation boring samples
- Winter investigation co-located, in-situ TarGOST™ probes and confirmation boring samples
- Winter investigation ex-situ TarGOST™ screening and confirmation boring samples

Prior to assessing the NAPL mobility criteria, we evaluated the statistical distribution of the TarGOST™ and TPH results, the reproducibility of the data between investigations, and the variability between the in-situ and ex-situ TarGOST™ results. The findings of this evaluation are summarized below:

- The statistical distribution of the winter data was tested for normal or lognormal (natural logarithm) distribution using USEPA proUCL version 3.0 software. The analysis showed that the majority of the TarGOST™ data were lognormally distributed except for TarGOST™ fluorescence in the sand (identified as normal). The TPH chemistry results were identified as neither normal nor lognormal distribution. Based on these results, all data were treated as lognormally (using the natural logarithm) distributed.
- The amount of scatter within the TarGOST™ plots indicates the reproducibility between two events. Similar scatter was detected for both in-situ investigations. The results are considered reproducible.
- Significant variability was observed between the ex-situ TarGOST™ screening results and the associated in-situ results, confirming previous field observations that the subsurface is highly heterogeneous. The subsurface heterogeneity makes it difficult to compare TarGOST™ fluorescence results from one borehole to TPH concentrations at a nearby second borehole, even when the samples were collected from the same depth interval, because the soil could be significantly different just a few feet away.

Due to the scatter of the data and the heterogeneity of the subsurface soil, the TarGOST™-based NAPL mobility criteria were calculated using all winter investigation ex-situ TarGOST™ screening data and

confirmation boring chemistry results for samples taken in the peat and the stratified silt and sand. All co-located, in-situ TarGOST™ and confirmation boring chemistry results from the spring investigation were used for the sediment samples.

The data were graphed separately for peat, stratified silt and sand, and sediment (see Figure 4-1), and the TPH-based NAPL mobility criteria were added for each soil layer. We selected the TarGOST™-based NAPL mobility criteria at the threshold values above which all of the ex-situ winter investigation points exceeded the TPH-based NAPL mobility criteria discussed above. Although the in-situ data are impacted by subsurface heterogeneity, it is important to note that the majority of the samples exceeding the TarGOST™-based NAPL mobility criteria also exceeded the TPH-based NAPL mobility criteria.

4.2.3 Results

We selected the following criteria to estimate the location and mass of mobile NAPL, as detailed in Sections 4.2.1 and 4.2.2:

Soil Layer	TPH-based Mobility Criteria	TarGOST™-based Mobility Criteria
Organic silt/sediment	100,000 mg/kg TPH	160 %RE*
Bank soil	100,000 mg/kg TPH	160 %RE
Peat	200,000 mg/kg TPH	160 %RE
Stratified silt and sand	30,000 mg/kg TPH	200 %RE
Clayey silt	30,000 mg/kg TPH	200 %RE

*RE = reference emission

The TPH-based mobility criteria were rounded to one significant figure as order-of-magnitude estimates of the residual concentrations presented in Section 4.2.1. The bank soil NAPL mobility criteria were assumed to be similar to those for the organic silt/sediment, and the clayey silt NAPL mobility criteria were assumed based on the stratified silt and sand results. These TPH-based and TarGOST™-based NAPL mobility criteria provide a conservative estimate of mobile NAPL at the site. We assume that NAPL concentrations below the mobility criteria will generally not be mobile and that NAPL concentrations above the mobility criteria have potential to be mobile.

4.3 Potentially Mobile Subsurface NAPL

This section evaluates the location of potentially mobile subsurface (i.e., beneath the cap) coal tar NAPL and estimates its mass. This evaluation is based on the subsurface soil TarGOST™ data presented in Section 3.6.2 and the subsurface confirmation boring data presented in Section 3.6.3.

4.3.1 Location of Subsurface NAPL

Documenting the location of subsurface coal tar NAPL at the Pine Street Canal Superfund Site is relatively complex because of the uncertain release and surface transport history, NAPL behavior, and variable subsurface stratigraphic conditions. Our initial characterization relied on two-dimensional cross sections (Figures 3-1 through 3-7) showing the subsurface stratigraphy along with the TarGOST™ results. To better document the

NAPL distribution, ARCADIS BBL developed a fully three-dimensional data visualization model to depict spatial distribution of the TarGOST™ data.

4.3.1.1 3-D Modeling Methodology

The modeling was performed using the latest version of Mining Visualization System (MVS). MVS is a state-of-the-art computer software that combines numerical modeling and graphics to depict environmental data (C Tech 2006).

The 3-D data visualization model was used to depict the subsurface data collected during the NAPL investigation. This method of data depiction provides an effective means for analyzing and understanding the distribution of TarGOST™ screening data with respect to the geologic units in all three dimensions. The MVS software processor uses finite element networks containing up to three million data nodes. The 3-D hydrogeology and NAPL distribution are then analyzed from a full range of 3-D vantage points.

Before developing the 3-D data visualization model, available information and data were gathered for review, including:

- TarGOST™ data collected in May 2006 and February 2007 (Appendix E)
- Subsurface stratigraphy data collected in May 2006 based on CPT results (Appendix F), February 2007 continuously logged confirmation borings, and the interpretation presented on the two-dimensional profiles and cross sections (Figures 3-1 through 3-7)
- On-site 3-D survey coordinates determined by a surveyor licensed in the State of Vermont

The data contained in these sources were electronically prepared for input to the MVS software.

The 3-D data visualization model includes geologic layer elevation data. The available soil boring and monitoring well data, along with actual ground survey contour elevation data, were used to define the elevations of the subsurface geologic contacts and ground surface. The geologic surfaces were interpolated into the MVS software and converted to a digital mesh representing each geologic layer in 3-D. Each geologic model layer contains a network of quadrilateral cells between the upper and lower contacts.

The vertical structure of the numerical model grid includes five model layers. The model layer geometry was defined based on geologic data from the CPT boring logs and cross sections obtained from previous site investigations. The five model layers are:

- Sand cap material
- Organic silt/sediment and bank soil layer
- Peat layer
- Stratified silt and sand layer
- Clayey silt layer

The geologic layer structure is described in greater detail in Section 3.1.

The MVS software was used to assess the distribution of TarGOST™ data with respect to geologic units at the site in 3-D. The TarGOST™ data were depicted using colored, cylindrical 3-D objects along each surveyed drilling location. These data were posted in the 3-D MVS model along 2-cm vertical depth intervals.

The 3-D presentation of TarGOST™ sample locations and fluorescence values appears on Figure 4-2 (southwest perspective) and Figure 4-3 (southeast perspective). To provide a means for visualizing where large ranges of fluorescence values were present at each TarGOST™ drilling location, the cylindrical objects on these figures have been colored and scaled (by diameter), e.g., the minimum fluorescence values are colored blue and have small radii.

Using the 3-D geologic framework, the TarGOST™ database was interpolated within the geologic model using the MVS software's kriging tool. Kriging is a geostatistical interpolation algorithm that estimates the distribution of a parameter in regions between locations in the nodal grid where the parameter was measured. After estimating the value inside the geologic model, the MVS software assigned the kriged distribution to the grid nodes in the 3-D TarGOST™ NAPL model. The kriged TarGOST™ distribution and stratigraphy are presented on Figure 4-4 (southwest perspective) and Figure 4-5 (southeast perspective).

The 2-D profiles and cross sections of the kriged TarGOST™ distribution and stratigraphy are presented on the following figures:

- Figure 4-6: view of Section A-A' on Figure 2-3
- Figure 4-7: view of Section B-B' on Figure 2-3
- Figure 4-8: view of Section C-C' on Figure 2-3
- Figure 4-9: view of Section D-D' on Figure 2-3
- Figure 4-10: view of Section E-E' on Figure 2-3
- Figure 4-11: view of Sections F-F' and G-G' on Figure 2-3
- Figure 4-12: view of Section H-H' on Figure 2-3

4.3.1.2 3-D Model Results

The general areas with potentially mobile NAPL, as interpreted based on the TarGOST™ data, are indicated by the orange volumes. This is the material with fluorescence values above the TarGOST™-based mobility criteria presented in Section 4.2.3. As shown on the figures, the bulk of the mobile NAPL is located in the peat layer, with lesser quantities in the lower portion of the organic silt/sediment layer and into the upper portion of the stratified silt and sand layer. The TarGOST™ probe is sensitive to very high PAH and TPH concentrations and as a result, the output can have many sharp spikes. The MVS modeling is not significantly affected by this since the majority of the spikes are greater than the TarGOST™-based mobility criteria of 160%-200% fluorescence, which was used to classify potentially mobile NAPL in the subsurface.

The material interpreted to contain immobile NAPL is shown in blue. Based on the 3-D model results, the units containing negligible amounts of mobile NAPL are:

- Most of the sand cap
- The upper portion of the organic silt/sediment layer
- The lower portion of the stratified silt and sand layer
- The entire clayey silt layer

Comparing the 2-D sections within the canal (Figures 4-7, 4-8 and 4-9) to the sections along the banks (Figures 4-6 and 4-10) shows that there is less mobile NAPL along the banks than beneath the canal. The thickness of the mobile NAPL layer in the canal ranges up to 10 feet, while the thickness of the mobile NAPL layer on the banks ranges up to 6 feet.

The extent of mobile NAPL along in the canal extends north and south of the investigation area. The thickness of the mobile NAPL in the peat is generally 5 to 10 feet and is relatively consistent between the western side, the center, and the eastern side of the canal. Potentially mobile NAPL does not appear to extend vertically up into the upper portion of the organic silt/sediment, except in a few locations where there are localized volumes and these are between Transects T10+00 and T11+25.

The extent of mobile NAPL along the east bank profile is from T11+25 to T13+25. Due to site constraints, no offset TarGOST™ probes were completed along the east bank. The 3-D model also shows an area of potentially mobile NAPL extending from the canal into the east bank peat layer on Section F-F' (Figure 4-11) and at T10+75 on Section E-E' (Figure 4-10). This is a product of the kriging effects of TG11 located in the canal along the cribbing, which had TarGOST™ results that indicated potentially mobile NAPL. The potentially mobile NAPL likely does not extend into the east bank because the cribbing acts to isolate NAPL in the canal. This is supported by data from probing TG130 that did not contain mobile NAPL and is located on the east bank, approximately 25 feet south of Section F-F'.

Along the west bank profile, the extent of mobile NAPL is from T9+50 to T12+75. Three TarGOST™ locations along the west bank cribbing were offset with an additional exploration 10 to 15 feet landward. The TarGOST™ results along the west bank cribbing showed mobile NAPL layers with thicknesses ranging from 2 to 6 feet. Two of these offset locations did not have mobile NAPL and the third location had a thinner mobile NAPL layer (reduced from 6 feet to 2 feet).

4.3.2 Mass of Subsurface NAPL

An estimate of the mass of potentially mobile NAPL in the canal and banks subsurface was calculated based on the 3-D modeled TarGOST™ results and the NAPL mobility criteria analysis of the TarGOST™ data and confirmation boring data. This estimate is not part of a mass balance. It was done to evaluate NAPL migration mechanisms and to select and design NAPL controls.

Several assumptions were made in the mass calculations. First, the volumes estimated by the model for the four stratigraphic units and the NAPL mobility zone were extracted for use in estimating the mass in each cell. The canal was divided into cells according to the description in Section 4.1. Since the TarGOST™ results have shown a decrease in the volume of mobile NAPL landward from the cribbings, each cell along the west and east banks was 25 feet by 20 feet in plan view. Following a similar grid identification described in Section 4.1, the canal cells were calculated from 9.1 through 12.3. The west bank cells were calculated from 8.2 through 14.4 and the east bank cells were calculated from 10.1 to 14.2, which represent the extent of data collected along each bank. The plan view of the cells is provided in Figure 4-13. The MVS software was used to compute the volume of soil containing NAPL within each grid cell in support of a detailed evaluation of alternatives. MVS was then used to calculate volume estimates for various regions in the 3-D data visualization model. Finally, MVS was used to isolate and “cut out” specific 3-D model subregions and then compute the volume of soil containing modeled TarGOST™ data inside those targeted subregions. The modeled volumes between grid cells 9.1 and 12.3 are presented below. All modeled volumes are available in Appendix J.

Layer	Volume of Soil Beneath Canal with Mobile NAPL (cubic meters, m ³)	Volume of Soil Beneath West Bank with Mobile NAPL (cubic meters, m ³)	Volume of Soil Beneath East Bank with Mobile NAPL (cubic meters, m ³)
Organic Silt/Sediment	1,120	Not applicable	Not applicable
Bank Soil	Not applicable	48	4
Peat	3,110	557	482
Stratified Silt and Sand	226	117	82
Total	4,460	723	569

Next, the average NAPL concentration within each NAPL mobility zone was used to estimate the mass in each cell. The mass of NAPL within each cell and stratigraphic unit was calculated using the following equation:

$$M_{SS} = C_{SS} \times \rho_{soil} \times V_{SS} \times \frac{35.315}{10^6 \times 2.2}$$

Where: M_{SS} = calculated mass of NAPL in the subsurface within the cell area (kg)
 C_{SS} = average concentration for NAPL mobility zone (mg/kg)
 ρ_{soil} = dry unit weight of each stratigraphic unit (pounds per cubic foot, lb/ft³)
 V_{SS} = volume from 3-D model for the four stratigraphic units (m³)
35.315 = unit conversion (ft³/m³)
10⁶ = unit conversion (mg/kg)
2.2 = unit conversion (pounds per kilogram, lb/kg)

The average concentration for the NAPL mobility zone was calculated for each stratigraphic layer by averaging results for the spring and winter investigation chemistry samples. Due to the difference in TPH concentrations in the peat between the canal, east bank, and west bank samples, the C_{SS} was calculated separately for each of these areas. TPH results greater than the mobility criteria established in Section 4.3.1 were used in the calculation. The following summarizes the equation inputs and details regarding calculations are provided in Appendix J.

Layer	C_{SS} Beneath Canal (mg/kg)	C_{SS} Beneath West Bank (mg/kg)	C_{SS} Beneath East Bank (mg/kg)	ρ_{soil} for Each Layer (lb/ft ³)
Organic Silt/Sediment	302,985	Not applicable	Not applicable	22.8
Bank Soil	Not applicable	100,000	100,000	110.2
Peat	533,188	406,494	260,000	14.2
Stratified Silt and Sand	75,330	75,330	75,330	66.8

Table 4-1 shows the estimated mobile NAPL masses calculated for each cell in the canal and bank between 9.1 and 12.3. The overall mass of mobile NAPL in the canal and banks subsurface is presented below.

Layer	Mass of Mobile NAPL Beneath the Canal (kg)	Mass of Mobile NAPL Beneath the West Bank (kg)	Mass of Mobile NAPL Beneath the East Bank (kg)
Organic Silt/Sediment	124,000	Not applicable	Not applicable
Bank Soil	Not applicable	8,600	724
Peat	379,000	51,600	28,500
Stratified Silt and Sand	18,300	9,460	6,660
Total	521,000	69,700	36,000

The general distribution of potentially mobile NAPL mass within the canal subsurface is shown on Figure 4-13. The following criteria were used for classifying the potential within a cell area:

- Low relative mass of mobile NAPL in the canal subsurface is defined as less than 5,000 kg.
- Medium relative mass of mobile NAPL in the canal subsurface is defined as greater than 5,000 kg and less than 15,000 kg.
- High relative mass of mobile NAPL in the canal subsurface is defined as greater than 15,000 kg.

4.3.3 Discussion of Subsurface NAPL

The 3-D model figures clearly indicate that NAPL concentrations increase with depth to approximately mid-depth and then decrease to non-detect in the lower portion of the explorations, with the bulk of the potentially mobile NAPL located in the peat layer. On Figures 4-2 and Figure 4-3, some explorations in the canal show slightly elevated fluorescence values at the top, which is consistent with the observation of NAPL on the surface of the cap. Although there may be limited, localized pools of mobile NAPL at the interface between organic silt/sediment and sand cap, the potentially mobile NAPL in the organic silt/sediment is generally not in direct contact with the sand cap. The model also shows that the vertical extent of NAPL beneath the canal has been documented.

On a cell basis, the maximum mass of mobile NAPL in the canal subsurface was 17,200 kg on the western side of the canal near Transect T10+50 (Cell 10.3A). The other cells with the highest mass of subsurface mobile NAPL are generally in the middle of the canal. Approximately 70 percent of the total mass of mobile NAPL within the canal subsurface is found in the peat layer.

The extent of mobile NAPL is defined to be within T9+50 to T12+75 along the west bank. Offset TarGOST™ probing indicates that the volume of mobile NAPL decreases landward from the west bank cribbing. The calculated mass of mobile NAPL beneath the west bank (69,700 kg) is 11 percent of the total mass of mobile NAPL (this includes mobile NAPL beneath the canal and both banks and is 627,000 kg). The cells with the highest mass of subsurface NAPL are 9.4 and 10.3, which are both generally in the area with the highest seepage.

The extent of mobile NAPL is defined to be within T10+50 to T13+25 along the east bank. Section D-D' in the canal (Figure 4-9) and Section E-E' along the east bank (Figure 4-11) indicate that the volume of mobile NAPL decreases away from the cribbing toward land. The calculated mass of mobile NAPL beneath the east bank (36,000 kg) is 6 percent of the total mass of mobile NAPL (this includes mobile NAPL beneath the canal and both banks). These results indicate NAPL concentrations beneath the east bank decrease with distance away from the canal. The exception to this is along area of the former slip where the highest masses of subsurface NAPL are in Cells 11.4, 12.1, and 12.2, which indicate potentially mobile NAPL at similar concentrations to the adjacent location within the canal. This is supported by the NAPL thicknesses in monitoring well MW11B ranging from 9 to 11 feet.

The west bank and east bank results indicate that the mass on NAPL along the banks is at least approximately an order of magnitude less than within the canal. The extent of the mobile NAPL along the banks is considered defined within these ranges based on the winter investigation TarGOST™ results.

These TarGOST™ results are generally consistent with historical NAPL observations that indicated nearly the entire canal subsurface contains NAPL; and within the area of interest, NAPL beneath the banks is also located in the peat layer but is of very limited extent (The Johnson Company 1997). The areal extent of historical NAPL observations east of the canal was heterogeneous, as NAPL was not observed in numerous borings. On the east bank, NAPL was historically observed in a relatively small area adjacent to the former slip and in a larger area near the former MGP. Along the west bank away from the canal, historical observations generally indicated that NAPL was not present. This historical data is in agreement with the results of the TarGOST™ probings completed in the canal, the west bank, and the east bank. The historical and TarGOST™ data combined show that most of the NAPL is in the peat in the canal and a more limited area of NAPL is present along the banks of the canals. The historical data are further discussed in Appendix K.

While the TarGOST™ data provided a useful basis for assessing the general distribution and relative saturation of NAPL beneath the canal and the banks, these data do not supersede direct observations and measurements of the presence and mobility of NAPL. For example, although the 3-D figures do not show interpreted mobile NAPL in the sand cap, localized, sporadic NAPL seeps have been directly observed above the cap during diver surveys and the rate of NAPL seepage has been measured. Gas bubbles can pick up NAPL that would not be classified as mobile according to the NAPL mobility evaluation. NAPL mobility is a function of the NAPL migration mechanism.

4.4 NAPL within the Sand Cap

The following discussion examines how NAPL within the sand cap interacts with the NAPL migration by looking at the locations and mass of NAPL within the upper and lower portions of the canal sand cap, the current thickness of the canal sand cap relative to the original design thickness, and the locations of NAPL within the west bank cap.

4.4.1 NAPL within the Canal Sand Cap

NAPL has been observed in the upper portion of the sand cap; the upper cap is defined as the top 4 inches of the sand cap, and the lower cap is defined as the portion below the top 4 inches. This section evaluates the locations of NAPL and estimates the mass of NAPL within the sand cap. The upper portion of the cap generally had high concentrations of TPH, which may be due to NAPL deposition on the cap surface that has settled into the top few inches of the sand cap via gravity. To accurately indicate locations where NAPL is migrating upward through the cap, the mass of NAPL in the upper and lower portions of the sand cap were calculated separately.

4.4.1.1 Locations of NAPL within the Canal Sand Cap

In 2006, the concentrations of NAPL within the sand cap were evaluated using corings at 25 locations between Transects T9 and T12. The distribution of NAPL within the lower portion of the sand cap is shown on Figure 4-14, which illustrates the relative concentrations of NAPL (classified as low, medium, or high, as defined in Section 4.4.1.2) by cell based on the total calculated mass of NAPL within the lower cap.

To assess whether NAPL is migrating upward through the cap, cap coring locations were examined for vertical gradation of NAPL concentrations in which elevated NAPL concentrations are at the bottom of the sand cap. Excluding samples from the upper cap, five cap coring locations exhibited either NAPL concentrations greater than 5,000 mg/kg in the deepest sample or NAPL concentrations in the deepest sample that were one order of

magnitude greater than the concentration in the sample above the deepest sample. These five locations include samples CP09 (Cell 11.1A), CP17 (Cell 11.2B), CP18 (Cell 11.2A), CP21 (Cell 11.1A), and CP24 (Cell 10.4C). These results indicate that NAPL may be migrating upward through the cap at these locations.

However, the observed vertical gradation along the west side of the canal may be a remnant of the construction conducted in June and July 2004 to address observed NAPL seepage along the west cribbing (The Johnson Company 2004a). Additional sand was placed from T9+50 to T14+20 and extended approximately 15 feet from the west bank. The eastern edge of the cap was tapered west to meet existing grade. Prior to this installation of the west bank cap, NAPL was removed from pools and the ground surface using commercial divers and a vacuum system. However, some residual NAPL may have remained and could be part of the NAPL detected in the cap in 2006.

To further assess whether a seepage path was apparent within the collected cores, the cap coring locations were examined for horizontal gradation of NAPL based on the photographic logs. Cap coring locations CP18 (Cell 11.2A), CP21 (Cell 11.1A), and CP23 (Cell 10.4A) exhibited visible NAPL seepage paths. Although other corings were co-located with observed seeps, seepage paths were not visible in cores from the other locations. There are three possible explanations for the absence of a visible seepage path in a cap core:

1. Seep location and frequency have been intermittent. Seeps observed in one location on a given day are not necessarily observed in the same location on the next day.
2. The seep may not consistently occur in the same location. Many of the cap corings contained NAPL throughout the cross section. This suggests that a general area, as opposed to a specific location, may exhibit seepage.
3. NAPL seepage may not always be entirely vertical, i.e., NAPL can migrate vertically and horizontally. This pathway would not be captured in a vertical core.

Compliance monitoring events conducted by The Johnson Company included two cap coring events (October 2004 and July 2005) that occurred after construction of the west bank cap in July 2004. The coring locations were not co-located with seeps. In nearly all corings, PAH concentrations were greater in the upper cap sample than in the mid-cap sample. These samples were not analyzed for TPH.

4.4.1.2 Mass of NAPL within the Canal Sand Cap

An estimate of mass of NAPL in the sand cap was calculated. This estimate is not part of a mass balance. It was done to evaluate NAPL migration mechanisms and to select and design NAPL controls. Data used for this calculation included:

- Cap coring chemistry data from the spring investigation (Table 3-16)
- Cap coring chemistry data from the summer investigation (Table 3-17)
- The Johnson Company's cap coring chemistry data from the following reports:
 - Compliance Monitoring Report Fall 2004 (The Johnson Company 2005a)
 - Compliance Monitoring Report Fall 2005 (The Johnson Company 2005c)

Several assumptions were made in calculating the mass of NAPL in the cap. First, we assumed that the bulk density of the cap is 120 lb/ft³ and that this parameter is not significantly affected by the concentration of NAPL. Second, we assumed that the thickness of the cap at the coring location could be applied over the cell area. Third, we used NAPL concentrations from corings co-located with seeps to estimate the mass for the entire cell area, resulting in a conservative estimate (i.e., overestimation of the mass of NAPL in the cap).

Because visual observations show that the majority of the NAPL is within the upper cap samples, two equations were used to calculate the mass of NAPL in the cap: one for the upper cap (i.e., the top 4 inches) and one for the lower cap (i.e., below the top 4 inches). The thickness of the recovered cap cores was often less than the thickness of the cap. To account for this in the mass calculation, the lower cap sample lengths were expanded to represent the cap thickness below the top 4 inches. The upper cap sample lengths were not expanded because NAPL in the upper cap core samples is primarily on the surface of the core, so expanding the upper cap sample lengths would have biased the mass calculations high. The mass of NAPL within the upper cap per unit area of the sand cap was calculated using the following equation:

$$M_{CP-top} = C_{CP-top} \times L_{CP-top} \times \rho_{cap} \times A_{cell} \times \frac{1}{10^3 \times 2.2}$$

Where: M_{CP-top} = calculated mass of NAPL in the upper cap within the cell area (grams, g)
 C_{CP-top} = concentration of NAPL in the upper cap sample based on dry unit weight of sand (mg/kg)
 L_{CP-top} = thickness of the top sample in the coring (ft)
 ρ_{cap} = dry unit weight of cap sand (lb/ft³)
 A_{cell} = area of the cell (ft²)
 10^3 = unit conversion (milligrams per gram, mg/g)
 2.2 = unit conversion (lb/kg)

The mass of NAPL in the lower cap was also calculated. At multiple locations, more than one sample was collected in the lower cap. To calculate the total mass of NAPL within the lower cap, the mass of NAPL within each sample (m_{CP}) was first estimated and then those values were summed to estimate the mass for the entire lower cap. This approach accounts for the wide range of TPH concentrations in each core by summing a depth-weighted mass estimate of the multiple samples within the lower cap. The mass of NAPL in each sample, corrected for the difference between the cap thickness and the recovery thickness, was calculated using the following equation:

$$m_{CP} = C_{CP} \times \frac{L_{CP} \times (L_{cap} - L_{CP-top})}{(L_{recovery} - L_{CP-top})} \times \rho_{cap} \times \frac{1}{10^3 \times 2.2}$$

Where: m_{CP} = mass of NAPL in the lower cap sample per unit area (grams per square foot, g/ft²)
 C_{CP} = concentration of NAPL in the lower cap sample based on dry unit weight of sand (mg/kg)
 L_{CP} = thickness of the lower cap sample in the coring (ft)
 L_{cap} = thickness of the cap (ft)
 L_{CP-top} = thickness of the upper cap sample in the coring (ft)
 $L_{recovery}$ = thickness of the coring recovery (ft)
 ρ_{cap} = dry unit weight of cap sand (lb/ft³)
 10^3 = unit conversion (mg/g)
 2.2 = unit conversion (lb/kg)

The total mass of NAPL per cell within the lower cap was calculated based on addition of the samples below the upper cap sample using the following equation:

$$M_{CP} = [(m_{CP})_1 + (m_{CP})_2 + \dots(m_{CP})_n] \times A_{cell}$$

Where: M_{CP} = calculated mass of NAPL in the lower cap within the cell area (g)
 A_{cell} = area of the cell (ft²)

Some of the cells did not include cap coring locations. The mass of NAPL within the sand cap for cells where sampling was not conducted was estimated by averaging neighboring cell mass, factoring in the presence or absence of NAPL seeps observed in 2006, and examining the results of previous cap corings conducted by The Johnson Company.

Table 4-1 shows the masses calculated for each cell. The average, maximum, and minimum mass calculations for the upper and lower cap are summarized below.

Sand Cap Layer	Total Mass of NAPL (grams)	Mass of NAPL per Cell, M_{CP} (grams/cell)		
		Average	Maximum	Minimum
Upper (the top 4 inches)	756,000	16,800	158,000	556
Lower (below the top 4 inches)	2,400,000	53,400	1,450,000	399

The relative mass of NAPL in the upper cap, shown on Figure 4-15, was evaluated based on the mass calculated in the upper cap and the cap surface swab data presented in Section 4.5.1. The following criteria were used for classifying the potential for seepage:

- Low relative mass of NAPL in the upper cap is defined as less than 5 kg.
- Medium relative mass of NAPL in the upper cap is defined as greater than 5 kg and less than 50 kg.
- High relative mass of NAPL in the upper cap is defined as greater than 50 kg.

The potential for the residual NAPL in the lower cap to indicate NAPL migration into the canal, shown on Figure 4-14, was evaluated based on concentrations from cap coring chemistry results in the lower cap. The following criteria were used for classifying the potential for seepage:

- Low relative NAPL concentration in the lower cap is defined as less than 100 mg/kg.
- Medium relative NAPL concentration in the lower cap is defined as greater than 100 mg/kg and less than 1,000 mg/kg.
- High relative NAPL concentration in the lower cap is defined as greater than 1,000 mg/kg.

4.4.1.3 Discussion of NAPL within the Canal Sand Cap

On a cell basis, the maximum mass of NAPL in the upper portion of the sand cap is 158 kg on the western side of the canal near Transect T11+25 (Cell 11.2A). The maximum mass of NAPL in the lower portion of the sand cap is 1450 kg on the western side of the canal near Transect T11+00 (Cell 11.1A). Approximately 77 percent of

the total estimated mass of NAPL within the lower cap is found in Cells 10.4A, 10.4C, and 11.1A. Cell 11.1A alone contains approximately 1,450,000 grams of the total mass. Mass calculations for Cell 11.1A were based on location CP21, which had visible NAPL at the base of the coring.

A significant portion of the total mass of NAPL is within the upper cap. For each cell, the percentage of NAPL mass within the upper cap was calculated and compared to the mass of NAPL within the entire cap depth. For each cell, an average 54 percent of the NAPL was in the upper cap. Based on the total mass in the cap, 24 percent of the NAPL was in the upper cap. The average thickness of the cap was approximately 2.0 feet.

4.4.2 Thickness of the Canal Sand Cap

The thickness of the sand cap varies along the canal. This section identifies locations where the thickness of the sand cap is less than the minimum design thickness of 1.5 feet (The Johnson Company 2004a). The purpose of this evaluation is to assist in determining the mechanisms of NAPL migration into the canal. For design of NAPL controls within the canal, a bathymetric survey of the cap surface will be necessary.

4.4.2.1 Distribution of the Sand Cap Thickness

In 2006, 42 cap thickness measurements were taken at different locations within the canal between Transects T9 and T12+50. Cap thickness is summarized below.

	Average (ft)	Maximum (ft)	Minimum (ft)
Cap Thickness	2.1	5.5	0.7

Ten of the 42 cap thickness measurements were less than the minimum design thickness for the sand cap of 1.5 feet; eight of these locations were between Transects T9+48 and T10+76 and 20 feet from the west bank. The other two locations were at T11+00E40 and T11+25E50.

The relative thickness of the sand cap is shown on Figure 4-16. The following criteria were used to classify the relative thickness:

- Low relative thickness of the sand cap is defined as greater than 1.5 feet.
- Medium relative thickness of the sand cap is defined as greater than 1.0 foot and less than 1.5 feet.
- High relative thickness of the sand cap is defined as less than 1.0 foot.

In cells for which multiple measurements were made in 2006, the smallest measurement was used to classify the relative thickness. In cells that lack measurements, thickness was calculated using the average of neighboring cells for which measurements had been made. These assumptions are consistent with other evaluations in this report in their focus on providing a conservative design basis for NAPL controls.

4.4.2.2 Discussion of the Sand Cap Thickness

Ten sand cap thickness measurements were less than 1.5 feet. Of these 10, three associated cap corings had high relative NAPL concentrations in the lower cap, five had medium relative NAPL concentrations in the lower cap, and two had low relative NAPL concentrations in the lower cap.

Following construction of the sand cap and the west bank cap, The Johnson Company carried out cap thickness measurements. Within the canal, cap thicknesses ranged from 1.5 feet to 5 feet, with the greatest thicknesses occurring from T10+80 to T11+60 and up to approximately 10 feet from the west cribbing. For the cells along the western side of the canal, it is likely that the sand cap thicknesses within 15 feet of the cribbing are greater than 1.5 feet. Although this is not represented in Figure 3-10, it will be incorporated into future NAPL controls design. At the locations where the sand cap thickness was less than 1.5 feet as measured in 2006, The Johnson Company measured cap thicknesses ranging from 2 feet to 4 feet after completion of the cap.³ Future design of NAPL controls will need to examine the possible reasons for the decrease in sand cap thickness and protect the surface from potentially further thinning.

4.4.3 NAPL within the West Bank Cap

NAPL has historically been observed in seeps along the west bank following placement of the sand cap within the canal. The west bank was capped in 2004 to prevent further NAPL migration through the west bank. Each set of three cap corings from the winter investigation (Section 2.3.3) was evaluated for NAPL potentially migrating through the west bank cap (west bank cap results are discussed in Section 3.5). This evaluation is presented below. Due to the generally isolated seep locations, a total mass of NAPL within the west bank cap was not calculated.

4.4.3.1 Locations of NAPL within the West Bank Cap

The west bank cap coring results are presented in Table 4-2 by elevation. At Transect T10+00 (CP100, CP101, and CP102), no intervals with visible NAPL were observed. Two of the cap cores had minimal TPH concentrations in the surface sample.

At Transect T10+50 (CP103, CP104, and CP105), CP103 and CP105 had discrete intervals of visible NAPL approximately 2 inches thick, while CP104 midway between the cribbing and canal did not have visible NAPL. The elevations⁴ of the discrete intervals were between 94.3 feet near the cribbing and 93.4 feet near the canal. The TarGOST™ probe results (TG104) from the west side of the cribbing at this transect show potentially mobile NAPL at an elevation of 94 to 94.5 feet (see Figure 3-1).

At Transect T11+00 (CP106, CP107, and CP108), only midway core CP107 had a 3-inch-thick, visible NAPL interval. The elevation of the discrete NAPL interval was 94.1 feet to 94.4 feet. The TarGOST™ probe results (TG106) from the west side of the cribbing at this transect show potentially mobile NAPL at an elevation of 93 feet (see Figure 3-1).

³ These findings appear in Appendix A of the Action Plan (BBL and Hart Crowser 2006a).

⁴ All elevations in Section 4.4.3.1 are in 1988 North American Vertical Datum

Discrete intervals of NAPL can form when a disturbance in the subsurface creates a layer of less resistance. NAPL tends to pool and can migrate through this disturbed layer more easily. Prior to the placement of the west bank cap, the surface elevation of the west bank was 94 feet to 95 feet in the area where these cap cores were taken. Additionally, tension cracks resulting from differential settlement were observed on the west bank cap in the region of Transect T10+50 following installation.

Given that consolidation occurred during the placement of the west bank cap, the elevations of the discrete intervals of NAPL in the cap cores are approximately at the elevation of the interface between the bottom of the cap and the former west bank soil surface. Because NAPL is not observed in all cap cores, any NAPL migration through the west bank cap is likely very localized.

4.5 NAPL Deposition on Cap Surface

NAPL has been observed on the cap surface. This section evaluates the locations of NAPL deposition and estimates the mass of NAPL deposition on the cap surface. NAPL deposition is defined as the NAPL that could be assessed using cap swabs.

4.5.1 Locations of NAPL Deposition

In 2006, NAPL deposition on the cap surface was sampled by taking cap swabs at 38 locations between Transects T9 and T13. Cap swabs provide the means for both a qualitative (i.e., visual) evaluation of the presence of NAPL and a quantitative (i.e., chemical analysis) evaluation. The distribution of NAPL deposition on the cap surface is shown on Figure 4-15, which illustrates the relative mass of NAPL deposition (classified as low, medium, or high, as defined in Section 4.5.2) by cell.

The majority of the NAPL deposition that could be assessed using cap swabs was observed between Transects T10+50 and T11+50. A lesser but significant amount of NAPL deposition was observed between Transects T9 and T10+50 along the west bank. A third location with notable NAPL deposition was at Transect T12 along the east bank and next to the former slip.

Analytical results for cap surface swab samples were greater in samples collected from locations that were co-located with seeps than in samples from locations that were not co-located with seeps (grid samples). This suggests that in some areas, NAPL deposition is related to NAPL seepage into the canal.

Four compliance monitoring events (August and October 2004; March and June 2005) conducted by The Johnson Company included cap probings, which provide a visual evaluation of the presence of NAPL, along the canal. These events took place following construction of the west bank cap in July 2004 and subsequent NAPL vacuuming of the cap surface around areas T9+80, T10+80, and T11+30. Of the approximately 240 probing locations throughout the canal between Transects T9 and T12, spots of NAPL were detected on the probe fabric at 72 locations.⁵ Generally, locations where NAPL was detected in these compliance monitoring events compare well with the 2006 spring and summer investigation data used to produce Figure 4-15.

⁵ These findings appear in Appendix A of the Action Plan (BBL and Hart Crowser 2006a).

4.5.2 Mass of NAPL Deposition

An estimate of the mass of NAPL on the cap surface was calculated. This estimate is not part of a mass balance. It was done to evaluate NAPL migration mechanisms and to select and design NAPL controls. Data used for this calculation include:

- Cap surface swab chemistry data (Tables 3-13 and 3-14)
- The Johnson Company's 2004/2005 cap probing observations discussed above

In making the mass calculations, we assumed that (1) the mass of NAPL is equal to the mass of TPH measured in a sample and (2) the mass collected in one sample can be used to estimate the mass in the entire cell. For each cap swab sample, the mass of NAPL deposition on the cap was calculated using the following equation:

$$M_{CS} = \frac{m_{CS}}{A_{CS}} \times A_{cell} \times \frac{1}{10^6 \times 10.764}$$

Where: M_{CS} = calculated mass of NAPL on the cap surface within the cell area (g)
 m_{CS} = mass of NAPL on the wipe ($\mu\text{g/wipe}$)
 A_{CS} = area of the cap surface sampled (m^2)
 A_{cell} = area of the cell (ft^2)
 10^6 = unit conversion (micrograms per gram, $\mu\text{g/g}$)
 10.764 = unit conversion (ft^2/m^2)

The area of each cell was 625 ft^2 . For cells where multiple cap surface swab samples were collected, the maximum mass of NAPL within the cell was used to determine the potential for NAPL deposition to contribute to NAPL migration into the canal.

Six cap surface swab samples (CS01 through CS06) were completely saturated after 1 m^2 was sampled. The associated mass deposition for these samples was estimated using three additional samples (CS07 through CS09) collected from smaller areas. The maximum mass of NAPL per unit area of the additional samples was derived from sample CS09 with an estimated mass of 7,650,000 micrograms per square meter ($\mu\text{g/m}^2$). This value was used to estimate the mass of NAPL associated with samples CS01 through CS06.

The average, maximum, and minimum mass calculations for cap surface NAPL are presented below.

Cap Swab Locations	Mass of NAPL per Square Meter, m_{CS}/A_{CS} ($\mu\text{g/m}^2$)		
	Average	Maximum	Minimum
Grid Samples	203,000	2,000,000	1,500
Seep Co-located Samples	4,710,000	11,000,000	25,000

The maximum mass of NAPL per square meter was 11,000,000 $\mu\text{g/m}^2$ for sample CS35 (in Cell 11.1B). Using a NAPL density of 1.06 kg/L, this corresponds to a thickness of 0.0104 millimeters of NAPL on the surface of the cap at location CS35.

The estimated NAPL mass on the cap surface is summarized below.

	Total Mass of NAPL (grams)	Mass of NAPL per Cell, M_{CS} (grams/cell)		
		Average	Maximum	Minimum
Cap Surface	2,480	55.1	639	0.1

Table 4-1 shows the mass of NAPL calculated for each cell. Of these, 18 cells did not contain any cap surface swab sampling locations. Mass deposition calculations were estimated for those 18 cells by averaging neighboring cell mass depositions, factoring in the presence or absence of NAPL seeps observed in 2006, and examining the results of previous cap probings conducted by The Johnson Company. The majority (80 percent) of the cap swab NAPL mass was located in nine cells: 10.4A through C, 11.1A through C, and 11.2A through C. Another 15 percent of the total cap swab NAPL mass was located along the west bank in five cells: 9.3A, 9.4A, 10.1A, 10.2A, and 10.3A.

The relative mass of NAPL deposited on the cap surface is shown on Figure 4-15. The following criteria were used for classifying the relative mass:

- Low relative mass of NAPL deposited on the cap surface is defined as less than 0.010 kg within a cell area (625 ft²).
- Medium relative mass of NAPL deposited on the cap surface is defined as greater than 0.010 kg and less than 0.100 kg within a cell area (625 ft²).
- High relative mass of NAPL deposited on the cap surface is defined as greater than 0.100 kg within a cell area (625 ft²).

The classifications shown on Figure 4-15 were upgraded to account for the mass of NAPL estimated in the upper portion of the cap, as described in Section 4.4.

4.5.3 Discussion of NAPL Deposition on Cap Surface

On a cell basis, the estimated maximum mass of NAPL deposition is 0.5 kg, which occurred on the western side of the canal near Transects T10+75 and T11 (Cells 10.4A and 11.1A). The majority of NAPL deposition was observed between Transects T10+50 and T11+50. Cap surface swab results were greater at sample locations co-located with seeps than at sample locations not co-located with seeps (grid samples). The mass of NAPL deposition appears to be correlated with the observed seepage locations. The cap surface swab samples taken within the canal at grid intervals generally had NAPL masses one order of magnitude less than did the samples co-located with observed seepage.

4.6 NAPL Seepage into the Canal

NAPL is migrating into the canal via NAPL seeps and gas bubbles. This section evaluates the locations of NAPL seepage and estimates the rate (mass per unit time) of NAPL seepage into the canal.

4.6.1 Locations of NAPL Seepage

NAPL seepage into the canal was observed between Transects T9 and T12 in 2006. Two mechanisms of NAPL seepage were observed:

- Direct NAPL seepage from the cap to the surface of the canal
- The migration of gas bubbles, carrying NAPL on the bubble surface, from the cap to the surface of the canal

During construction of the cap, the majority of NAPL observations occurred between Transects T9+50 and T12, and were primarily concentrated along the west bank cribbing. Most of these observations were associated with groundwater flowing into the canal between the cribbing posts (see Figure 4; The Johnson Company 2003). Post construction monitoring of NAPL in surface water associated with gas bubbles was performed by The Johnson Company from 2003 through 2006. Most of the observed NAPL seeps were located between Transects T10 and T12 (see Figure A.6-1 of the Action Plan; BBL and Hart Crowser 2006a).

In 2006, the majority of NAPL seepage was observed in the western portion of the canal between Transects T10 and T11. However, NAPL seepage was also observed in the middle and eastern portions of the canal and between Transects T9 and T12. On August 8, 2007, the USEPA and The Johnson Company observed two locations of NAPL seepage at Transects T11 and T12, each approximately 20 feet west of the east bank.

4.6.2 Rate of NAPL Seepage

This estimate is not part of a mass balance. It was done to evaluate NAPL migration mechanisms and to select and design NAPL controls. An estimate of the rate of NAPL seepage into the canal was calculated based on the following data:

- Water column NAPL seep chemistry data (Table 3-15)
- Diver observations (Tables 3-11 and 3-12)
- Seep observations from the following inspection reports:
 - January 24, 2006 (The Johnson Company 2006a)
 - March 1, 2006 (The Johnson Company 2006b)
 - June 8, 2006 (The Johnson Company 2006c)
 - June 21, 2006 (The Johnson Company 2006d)
 - July 19, 2006 (The Johnson Company 2006f)
 - August 25, 2006 (The Johnson Company 2006g)
 - September 17, 2006 (The Johnson Company 2006h)

It was assumed that the mass of NAPL was equal to the mass of TPH measured in a water column seep sample. The rate of NAPL seepage was calculated using the equations presented below.

The following equation gives the mass of NAPL per droplet of NAPL:

$$m_{SW-d} = \frac{SW}{n_d}$$

Where: m_{SW-d} = mass of NAPL per droplet of NAPL (micrograms per droplet, $\mu\text{g}/\text{droplet}$)
 SW = water column seep chemistry data ($\mu\text{g}/\text{wipe}$)
 n_d = number of NAPL droplets in the water column seep sample based on diver observation (unitless)

Using the above equation, the average, maximum, and minimum mass per NAPL droplet from 19 water column seeps sampled during the spring and summer investigations were calculated as presented below.

	Average Mass ($\mu\text{g}/\text{droplet}$)	Maximum Mass ($\mu\text{g}/\text{droplet}$)	Minimum Mass ($\mu\text{g}/\text{droplet}$)
NAPL Droplets	1,150	5,000	29

The rate of NAPL seepage into the canal (mass per second) for each water column seep sample was estimated using the following equation:

$$r_{SW-Ts} = \frac{SW}{t}$$

Where: r_{SW-Ts} = rate of NAPL seepage (micrograms per second, $\mu\text{g}/\text{second}$)
 SW = water column seep chemistry data ($\mu\text{g}/\text{wipe}$)
 t = time to collect water column seep sample based on diver observation (seconds)

The total rate of NAPL seepage into the canal (mass per year) for each water column seep sample was estimated using the following equation:

$$R_{SW} = \frac{r_{SW-Ts} \times 43,200 \times D}{10^6}$$

Where: R_{SW} = rate of NAPL seepage in years (grams per year, g/yr)
 r_{SW-Ts} = rate of NAPL seepage in seconds ($\mu\text{g}/\text{second}$)
43,200 = unit conversion (seconds/day)
 D = unit conversion (days/year) (see discussion below)
 10^6 = unit conversion ($\mu\text{g}/\text{g}$)

A value of 12 hours per day, not 24 hours per day, was used to make the conversion from seconds to days. Based on field observations, seeps tend to be more active in the afternoon than in the morning, and seeps are not consistently active throughout a 24-hour day. Twelve hours was chosen to conservatively represent the daily period of seep activity. Two different conversion factors were used, one for water column seep samples collected in the spring, another for samples collected in the summer. For spring samples, we assumed that the seep was continuously active eight months of the year, so a conversion of 243 days per year was used for D . For summer samples, we assumed that the seep was continuously active four months of the year, so a conversion of 122 days per year was used for D . Some of the spring seeps were also observed in the summer (and were sampled in both the spring and summer investigations).

The rate of NAPL seepage was also estimated for seeps that were observed but not sampled (including observations by both ARCADIS BBL and The Johnson Company) using the average mass of NAPL per droplet. If a quantitative observation of the rate of seepage was available, it was used in calculating the mass. If a qualitative observation of the rate of seepage was available, an average rate of seepage based on the rate of seepage from sampled seeps was used. Once the calculation was performed for each water column seep sample, the rate of NAPL per seep was summed to estimate the total rate of NAPL seepage into the canal per year, as presented below. These calculations are provided in Appendix J.

	Rate of NAPL Seepage, R_{sw} (g/yr)
Total Combined NAPL Seepage	111,000

Note that this estimated rate of NAPL seepage (converted for discussion to 111 kilograms/year [kg/yr]) is based on conservative assumptions (i.e., continuous seepage) for the purpose of selecting and designing NAPL controls.

Table 4-1 shows the rate of NAPL seepage calculated for each cell. The relative rate for NAPL seepage into the canal, shown on Figure 4-17, is based on the rate calculation and the number of seeps observed in a cell. The following criteria were used to classify the relative rate of NAPL seepage:

- Low NAPL seepage is defined as cells that had no observed seeps.
- Medium NAPL seepage is defined as cells that had at least one observed seep and the estimated mass of NAPL seepage per year for all seeps within the cell was less than about 5 kg/yr.
- High NAPL seepage is defined as cells that had at least one observed seep and the estimated mass of NAPL seepage per year for all seeps within the cell was greater than about 5 kg/yr.

For cells with multiple seep samples or seep observations, the total mass of NAPL within the cell was used to determine the relative NAPL seepage into the canal. The exception is Cell 12.1C where the USEPA and The Johnson Company observed NAPL seepage in August 2007. This cell was classified as medium NAPL seepage to reflect this observation. Cell 11.1C was already classified as medium NAPL seepage so no change was made based on USEPA's observation.

4.6.3 Discussion of NAPL Seepage into the Canal

The estimate maximum rate of NAPL seepage per cell was 32 kg/yr, which occurred on the western side of the canal near Transect T10+75 (Cell 10.4A). The majority of NAPL seepage in 2006 was observed in the western portion of the canal between Transects T10 and T11.

This estimated rate of NAPL seepage is evenly distributed between seeps observed in the spring and seeps observed in the summer. Spring seeps, assuming they are active eight months of the year, contribute 55,000 g/yr of TPH to the canal. Summer seeps, assuming they are active four months of the year, contribute 56,000 g/yr of TPH to the canal. Although there are fewer spring seeps than summer seeps, the spring seeps are active twice as long as the summer seeps.

As shown above, the mass contributions of the spring and summer seeps are similar. Based on an average density of the NAPL of 1.06 kg/L at 10 to 20 degrees C, the rate of NAPL seepage can also be expressed as approximately 104 liters (27 gallons) per year. It is noted that the NAPL seepage at the site is variable and the

resulting observations have a high level of uncertainty. As a result, this mass contribution represents an order-of-magnitude estimation.

Most cells that exhibited high relative NAPL seepage rates (Figure 4-17) also had low sand cap thickness (Figure 4-16) and high relative NAPL concentrations in the lower cap (Figure 4-14).

Based on the information presented in Table 4-1, a significant portion of the total mass of NAPL is within the subsurface of the canal. Based on the estimated rate of NAPL seepage (111 kg/yr) and the estimated mass of mobile NAPL in the canal subsurface (about 521,000 kg), the annual seepage rate is about 0.02 percent of the mass present in the subsurface.

In August 2007, the USEPA and The Johnson Company observed NAPL seepage near MW11B at Transect T12, 20 feet from the east bank. Significant NAPL of varying thickness, ranging from 9.4 to 11 ft, was observed in monitoring well MW11B during the spring, summer, and winter investigations. This NAPL may be associated with the NAPL in the peat.

4.7 Hydrogeologic Considerations for NAPL Mobility

Hydrogeologic factors effecting NAPL mobility include hydraulic gradients, which were calculated from field-measured water levels. Hydraulic gradients in the vertical and horizontal directions can be affected by soil anisotropy, stratigraphy, and natural or constructed barriers to groundwater flow. In addition, the NAPL properties control the relative effects of vertical and horizontal gradients on the potential for NAPL mobility resulting from hydraulic gradients.

4.7.1 Vertical Hydraulic Gradient Data Calculated Using Spring 2006 Piezometers

Vertical hydraulic gradients were estimated from groundwater elevations calculated from pressure transducer data and piezometer completion data from the spring 2006 piezometers. Table 3-8 summarizes the vertical hydraulic gradients. For each piezometer, groundwater elevation differences were calculated by subtracting the groundwater elevation at the deeper piezometer from the groundwater elevation at the shallower piezometer. A positive vertical hydraulic gradient value indicates downward groundwater flow, and a negative vertical hydraulic gradient value indicates upward groundwater flow. The maximum and minimum elevation differences were chosen for estimating vertical gradients to capture the complete range of conditions observed during the monitoring period. Groundwater elevation differences were then divided by the vertical distance between the midpoint elevations of the piezometer screened intervals to calculate the magnitude of the vertical hydraulic gradient.

Gradients were evaluated between the deep organic silt/sediment (PZ8, shallower) and the clayey silt (PZ7, deeper) and between the shallow organic silt/sediment (PZ6, shallower) and the deep organic silt/sediment (PZ8, deeper), as shown on Figure 4-18. Vertical hydraulic gradients between the deep organic silt/sediment layer and the clayey silt layer ranged between -0.18 foot/foot (ft/ft) and -0.035 ft/ft, with an average vertical hydraulic gradient of -0.052 ft/ft. This indicates consistent upward groundwater flow between the deep organic silt/sediment and the clayey silt. Vertical hydraulic gradients between the shallow organic silt/sediment and the deep organic silt/sediment layers ranged between -0.28 ft/ft and 0.26 ft/ft, with an average vertical hydraulic gradient of 0.00031 ft/ft. This indicates variable gradient conditions, with periods of upward and downward flow. These observations are consistent with previous site investigations, which are presented in Table 3-4.

Historical results were variable in the shallower layers and generally upward in the deeper layers (Metcalf and Eddy 1992; Perkins-Jordan 1984).

4.7.1.1 Groundwater Fluctuation with Change in Surface Water Elevation Using Spring 2006 Piezometers

A strong linear relationship between surface water elevation and groundwater elevation was observed in the clayey silt (PZ7), the deep organic silt/sediment layer (PZ8), and the shallow organic silt/sediment layer (PZ6), with $R^2 = 0.99$ for all of these comparative data sets⁶. When surface water elevations changed, groundwater elevations changed in a similar manner, as demonstrated on Figure 3-8. This indicates that the organic silt/sediment layer and the clayey silt layer are hydraulically connected to and influenced by variations in surface water elevation. This finding is consistent with previous investigation results at the site.

4.7.2 Horizontal Hydraulic Gradients Calculated Using Spring and Winter 2007 Piezometers

Groundwater generally flows in a westerly or northwesterly direction on the site, with horizontal hydraulic gradients ranging from 0.004 ft/ft to 0.0360 ft/ft (Metcalf and Eddy 1992; Perkins-Jordan 1984). Horizontal hydraulic gradients at the banks of the canal were determined in this study to evaluate the potential for NAPL to be mobilized into the canal by horizontal gradients at the site.

Figure 4-19 presents the horizontal hydraulic gradients calculated between the bank piezometers and the canal. The horizontal gradients were calculated based on the water levels measured in the canal and at the following piezometers:

- PZ100: The horizontal gradients in the stratified silt and sand layer on the west bank of the canal ranged between -0.0450 ft/ft and 0.0397 ft/ft, averaging 0.0080 ft/ft during the period of record.
- PZ101: The horizontal gradients in the peat layer on the west bank of the canal ranged between -0.0523 ft/ft and 0.0446 ft/ft, averaging 0.0059 ft/ft during the period of record.
- PZ104: The horizontal gradients in the peat layer on the east bank of the canal ranged between -0.1843 ft/ft and 0.0290 ft/ft, averaging -0.0153 during the period of record.

Negative gradients indicate that the gradient is from the canal to the bank (eastward in the east bank and westward in the west bank). Positive gradients indicate that the hydraulic gradient is into the canal from the bank.

The results of these gradient calculations show that horizontal hydraulic gradients in the west bank are towards the canal during the wet season when rainfall infiltration in the west bank causes groundwater mounding and surface water levels in the canal are approximately matched by water levels in the lake. Dry season gradients in the west bank tend to be negative indicating a hydraulic gradient from the canal into the bank. Low lake water levels, the absence of significant recharge in the west bank, and the artificially high water levels maintained in the canal by the weir during the dry season appear to cause hydraulic gradients in both the stratified silt and sand

⁶ R^2 is the regression coefficient; a value of 1 reflects a perfect correlation.

and the peat in the west bank to be from the canal to the lake. Average horizontal hydraulic gradients in the west bank over the course of the entire monitoring period, which encompassed the wet and dry seasons between April and October 2007 were gentle and towards the canal for both the stratified silt and sand and the peat.

Horizontal hydraulic gradients in the east bank peat layer largely mirror the pattern observed in the west bank. During the wet season groundwater recharge resulting from rainfall infiltration creates consistently positive horizontal hydraulic gradients from the banks to the canal. In the dry season this pattern is reversed as the horizontal hydraulic gradient in the east bank becomes negative, indicating that the gradient is from the canal into the east bank. This appears to be a combined result of the weir maintaining the canal surface water elevations above the lake water elevations in the dry season and the temporary effects of the canal conveying stormwater from the City of Burlington. Water levels measured in PZ104 towards the end of the monitoring period were increasingly deep, generating increasingly negative gradients from the canal to the east bank during the months of September and October 2007. This trend in the data renders the average gradient negative over the duration of the monitoring period, indicating that the average gradient in the east bank was from the canal to the east bank. In spite of this conclusion derived from the available data set, it is inferred that the long-term average gradient is from the east bank towards the canal.

Horizontal hydraulic gradients calculated for PZ102 and PZ103 were deemed not representative of actual horizontal hydraulic gradients present between the banks and the canal. PZ102 had the deepest screened interval of all of the piezometers, and PZ103 had the deepest screened interval of all of the peat piezometers. It is recognized that the majority of the head loss between these deeper layers and the canal may relate to the upward vertical flow beneath the canal. Therefore, only the horizontal gradients measured in shallower piezometers (PZ100, PZ101, and PZ104) are considered to be reliable. Because the general trends are similar across all of the piezometers, the results from PZ100, PZ101 and PZ104 are considered representative of approximate horizontal gradients in the deeper stratigraphic zones.

These observations are consistent with previous site investigations, which are presented in Table 3-4. Historical results were generally west in the shallower layers and north to northwest in the deeper layers (Metcalf and Eddy 1992; Perkins-Jordan 1984).

5. Update of Conceptual Site Model

This section updates the conceptual site model for NAPL migration at the Pine Street Canal Superfund Site that was originally presented in the Action Plan (BBL and Hart Crowser 2006a). The conceptual site model is based on the data presented in Section 3, the evaluations presented in Section 4, and information from other NAPL sediment sites discussed in Section 4 of the Action Plan. The conceptual site model focuses on potential NAPL migration mechanisms, including:

- NAPL migration via hydraulic gradient
- NAPL migration via localized bearing-capacity failures
- NAPL migration via preferential pathways
- NAPL migration via gas bubble-induced transport

NAPL has been observed migrating to the surface water of the canal as discrete droplets with gas bubbles and independent of gas bubbles. NAPL migration tends not to be continuous, and weather conditions can make it difficult to observe. NAPL has also been observed on the surface of the cap, within the cap, and beneath the cap.

The objective of the historical conceptual site model presented in the Action Plan (reproduced on Figure 5-1 of this report) was to identify data gaps. The identified data gaps were used to determine spring, summer, and winter investigation activities. In this section, the conceptual site model is reevaluated to determine whether it is still valid in light of data generated in the spring, summer, and winter investigations. We conclude from this reevaluation that while all NAPL migration mechanisms may be occurring, only one migration mechanism—NAPL migration via gas bubble-induced transport—is contributing significant NAPL migration into the canal.

Conclusions from the reevaluation discussed here will be used in the NAPL controls report to evaluate NAPL control options.

5.1 NAPL Migration via Hydraulic Gradient

Soil samples obtained in the canal and TarGOST™ boring results suggest that a substantial mass of mobile NAPL is present in the area beneath the canal. In addition, diver surveys identified several locations with active NAPL seeps during spring and/or summer conditions and areas with NAPL deposition on the surface of the cap. One of the driving forces that could potentially cause NAPL to migrate upward into the canal is the vertical component of the hydraulic gradient.

NAPL migration can also be effected by horizontal hydraulic gradients which could act to mobilize sufficiently large pools of NAPL present in the banks towards the canal.

5.1.1 NAPL Migration via Vertical Hydraulic Gradient

The ability of mobile NAPL to migrate upward will depend on the balance between the magnitude of the upward hydraulic gradient component and the downward driving force associated with the NAPL density. If the upward gradient is insufficient, then the NAPL density prevents upward movement. Upward NAPL migration would not occur under the following condition (Cohen and Mercer 1993):

$$i_{v,up} < \Delta\rho_{NAPL}/\rho_w$$

Where: $i_{v,up}$ = the upward component of the hydraulic gradient
 $\Delta\rho_{NAPL}$ = the difference between the NAPL and water densities ($\rho_{NAPL} - \rho_w$, approximately 0.06 gram/milliliter [g/mL] based on site-specific data)
 ρ_w = the density of water (assumed to be 1 g/mL)

The term $\Delta\rho_{NAPL}/\rho_w$ on the right side of the equation is sometimes referred to as the gradient due to gravity, i_g (Cohen and Mercer 1993). Therefore, an upward hydraulic gradient component exceeding 0.06 (dimensionless) across the NAPL would be required to mobilize it upward beneath the canal. It is recognized that the hydraulic gradient acting on the NAPL could be enhanced by a reduction in the permeability of water within the NAPL-containing material. Assuming the gradient across the NAPL may be magnified by a factor of three relative to the general hydraulic gradient (within materials lacking NAPL) (Kueper 2007a), a measured upward gradient of 0.02 or more may mobilize NAPL upward. Using the convention adopted in Section 3.2.2.3, in which gradients with upward flow have a negative sign, the upward gradient would have to be less than -0.02 to have the potential to mobilize NAPL upward.

Based on hydrologic data from the site (discussed in Section 3.2), the sand cap, organic silt/sediment, and clayey silt layers appear to be hydraulically connected to and influenced by variations in canal surface water elevation. The vertical component of the gradient was characterized as follows based on hydraulic head data measured at piezometers installed beneath the canal (note that negative values indicate upward flow and positive values indicate downward flow):

- The upward hydraulic gradient component from the clayey silt (PZ7, deeper) to the deep organic silt/sediment (PZ8, shallower) ranged from **-0.18** to **-0.035**, with an average vertical hydraulic gradient component of **-0.052**.
- The upward gradient component from the deep organic silt/sediment (PZ8) to the shallow organic silt/sediment (PZ6) ranged from **-0.28** to 0.26, with an average vertical hydraulic gradient component of 0.00031.

The numbers in boldface type meet the criterion for potential upward mobilization. Thus, the upward vertical gradient appears to be consistently strong enough to potentially contribute to upward NAPL movement between the clayey silt layer and the deep organic silt/sediment layer. In addition, the upward vertical gradient appears to be sufficient, during some time intervals, to contribute to upward movement between the deep organic silt/sediment layer and the shallow organic silt/sediment layer. Thus, NAPL could incrementally migrate upward through the organic silt/sediment because of upward vertical hydraulic gradients.

The vertical hydraulic gradient within the sand cap material was not explicitly measured, but it can be estimated based on the relative hydraulic conductivity values of the sand cap and the underlying soils and the vertical gradients measured within the soils. The vertical component of the specific discharge (q_v) within the sand or the subsurface soil can be calculated using a form of Darcy's Law, as follows:

$$q_v = K_v i_{v,up}$$

Where: K_v = the vertical component of the hydraulic conductivity

Assuming that the specific discharge (volume per unit area per unit time) is consistent between the organic silt/sediment and the sand cap, the upward vertical gradient within the sand cap can be estimated as:

$$i_{v,up, sand\ cap} = (K_v\ sediment / K_v\ sandcap) i_{v,up\ sediment}$$

Table 3-3 summarizes laboratory measurements of hydraulic conductivity that ARCADIS BBL obtained for the sand cap and various geologic units beneath the canal. The hydraulic conductivity of the sand cap material (sample CB-06 S-1) was measured as approximately 6 ft/day. The geometric mean of three hydraulic conductivity measurements for the organic silt/sediment (samples CB-06 S-2, CB-07 S-2, and CB-08 S-1) is approximately 0.1 ft/day. Thus, the hydraulic conductivity of the sand cap material is approximately 60 times more permeable than the underlying sediment. Based on the equation above, the upward vertical gradient within the sand cap is estimated as approximately one-sixtieth (1/60) of the upward vertical gradient within the organic silt/sediment. Thus, the following upward vertical gradients are estimated for the sand cap:

- The upward gradient component within the sand cap is estimated to range from -0.0047 to 0.0043, with an average vertical hydraulic gradient component of 0.000052.

Even the strongest estimated upward hydraulic gradient within the sand cap (-0.0047) is insufficient (by a factor of approximately four) to contribute to upward NAPL movement. Again, this calculation accounts for gradient magnification within the NAPL-containing medium due to reduced water permeability. The NAPL is likely to be non-wetting within the sand cap (based on the physical properties of the NAPL and the sand cap); it is unlikely that the NAPL would wick into the sand cap. In the presence of an upward driving force (hydraulic gradient), however, NAPL may migrate into the coarser sand cap layer from the finer underlying organic silt/sediment.

Under current conditions and based on the available data, upward NAPL movement within the sand cap material appears to be unlikely due to hydraulic gradients within the sand cap alone. However, it cannot be ruled out that short-term vertical gradients may have been enhanced upon cap emplacement, due to consolidation of underlying materials with low bearing capacity. In addition, other modes of NAPL migration through the sand cap may be occurring, as discussed below. Lastly, as noted above, current upward hydraulic gradients do appear to be sufficient to potentially promote upward NAPL movement between the clayey silt and the deep organic silt/sediment and between the deep organic silt/sediment and the shallow organic silt/sediment. Thus, NAPL may migrate upward into the base of the cap due to hydraulic gradients within the underlying sediment. This process, if it is occurring, could produce an accumulation of NAPL within the base of the cap over time and may cause NAPL “breakthrough” where the cap is relatively thin.

5.1.2 NAPL Migration via Horizontal Hydraulic Gradient

This section presents an evaluation of the potential for NAPL to migrate toward the canal from areas beneath the west and east banks of the canal – i.e., horizontal NAPL mobility due to horizontal hydraulic gradients. This evaluation includes an assessment of the size of NAPL pools that may be mobile, and their velocities (if mobile), under average and also conservative assumptions regarding hydraulic conductivity and hydraulic gradient.

NAPL migration due to horizontal hydraulic gradient occurs when the horizontal hydraulic gradient across a zone sufficiently saturated with NAPL (known as a NAPL pool) is high enough that the pool exceeds the capillary resistance of formation. The maximum stable pool length of a NAPL pool situated on a horizontal layer is inversely proportional to the horizontal hydraulic gradient. The higher the hydraulic gradient, the smaller a NAPL pool needs to be for it to be stable. NAPL pools that are longer than the maximum stable length, calculated for a specific magnitude of horizontal gradient, are mobile. NAPL pools that are shorter than or equal to the maximum stable pool length are immobile. The pool length referred to here is calculated in the direction of groundwater flow.

The relative potential for NAPL to be mobilized by horizontal hydraulic gradients adjacent to the canal can be evaluated using the site-specific horizontal gradients, bulk hydraulic conductivities calculated from in-situ field tests, the measured NAPL properties at the site, and the size of the zone of potentially mobile NAPL identified based on the TarGOST™ study.

Maximum stable NAPL pool lengths were calculated for each unit in which potentially mobile NAPL was identified adjacent to the canal. These calculations were performed for the east bank and the west bank areas:

- the average and maximum horizontal gradients
- geometric mean and the maximum measured in-situ hydraulic conductivity value (from Perkins-Jordan 1984, and Metcalf and Eddy 1990)

Note that laboratory hydraulic conductivity values were not used in this analysis, as they represent order-of-magnitude estimates of vertical hydraulic conductivity, and thus are not applicable to horizontal calculations. The NAPL properties, including density and viscosity, are described in Section 3.3.2. To be conservative, the minimum interfacial tension and viscosity values were used in the calculations.

The calculations that are based on the geometric mean hydraulic conductivity and average horizontal gradient provide a representative assessment for the maximum stable NAPL pool length (Appendix J, Table J-1). Using these representative parameters, the calculated maximum stable pool length, and associated NAPL pool velocity (applicable to pools longer than the maximum stable pool length, if any) are as follows:

- East bank, peat – the average measured gradient in this unit was in the direction away from the canal; thus, under this scenario, from the standpoint of protecting the canal, the assessment of maximum stable pool length is not applicable
- West bank, stratified silt and sand – maximum stable pool length 846 ft, velocity (if mobile) 0.002 feet/year (ft/yr)
- West bank, peat – maximum stable pool length 781 ft, velocity (if mobile) 0.004 ft/yr

These calculations suggest that, under representative average site conditions, NAPL pools would have to be very long to be mobile, and it is very unlikely that any pools are present at lengths greater than the calculated maximum stable pool lengths near the canal.

The combination of maximum hydraulic conductivity and maximum horizontal gradient provides the most conservative (smallest) estimate for the maximum stable pool length (Appendix J, Table J-2). Using these conservative parameters, the calculated maximum stable pool length, and associated NAPL pool velocity (applicable to pools longer than the maximum stable pool length, if any) are as follows:

- East bank, peat – maximum stable pool length 79 ft, velocity (if mobile) 0.1 ft/yr
- West bank, stratified silt and sand – maximum stable pool length 58 ft, velocity (if mobile) 0.2 ft/yr
- West bank, peat – maximum stable pool length 50 ft, velocity (if mobile) 0.2 ft/yr

These calculations suggest that, under the most conservative conditions, NAPL pools lengths would have to be in the tens of feet to be mobile, and their maximum estimated velocities would be very low. The primary reasons for the extremely slow NAPL velocity (if temporarily mobile on an intermittent basis) include low hydraulic conductivities for the subject geologic layers and the high viscosity of the coal tar.

Based on the results of the winter investigations and the TarGOST™ modeling, the volume of potentially mobile NAPL is greatest beneath the canal and decreases away from the canal towards the upland on either side of the canal. Two of the three TarGOST™ probes conducted 10 to 15 feet west of the west bank cribbing did not show potentially mobile NAPL; the third showed a significant decrease in thickness, indicating the zone of mobile NAPL was pinching out and of limited extent in the west bank. TarGOST™ results indicate that NAPL in the east bank also tends to decrease with distance from the bank; however, NAPL pools large enough to be mobilized towards the canal by horizontal hydraulic gradients may exist in the east bank.

Based on the available data characterizing the distribution of potentially mobile NAPL at the site, it is considered unlikely that a significant number of NAPL pools (if any) beneath the west bank of the canal are of sufficient size to promote movement by horizontal hydraulic gradient, even with the most conservative estimates of stable NAPL pool lengths.

Although there may be mobile NAPL pools present in the east bank, these are likely of limited extent in the direction parallel to the canal, and their mobility is likely to be limited to intermittent periods of elevated gradient magnitude.

It is important to recall that the maximum measured hydraulic gradients in each unit occur briefly, and on an intermittent basis. Even under these conditions, the NAPL velocity in the most permeable zones is estimated as very low, less than 1 ft/yr. These calculations indicate little or no overall mobility of NAPL toward the canal from either bank.

5.2 NAPL Migration via Localized Bearing-Capacity Failures and Consolidation Settlement

Bearing-capacity failures and/or consolidation settlement in canal soils may result in NAPL migration into the canal. During the spring and summer investigations and sampling for the additional remedial investigation, sheens were frequently observed during coring (The Johnson Company 1997). Sheens were observed during mobilization for the additional remedial investigation, apparently the result of trucks driving near the canal shoreline in the vicinity of Transect T9 and barge spuds inserted into the soils (The Johnson Company 1997). Sheens were also observed during construction of the cap, apparently in response to the weight of the cap and the additional surcharge induced by the construction equipment, which may have caused localized failures.

The upper geologic materials at the site consist of highly organic peat soils that occupy the upland areas on either side of the canal. A portion of this peat material was removed for the original construction of the canal. The canal was originally dredged between the cribbing walls approximately 10 to 15 feet into the underlying sphagnum peat. The dredged material was placed beyond the cribbing on the sides of the canal, and additional fill was placed at later dates along the east side. The peat extends 5 to 10 feet below the original dredged bottom of the canal at approximately 80 feet above the 1988 North American Vertical Datum (NAVD88). The canal has subsequently been infilled with a very soft and highly organic silt/sediment. From a geotechnical perspective, the key considerations in identifying the mechanism by which NAPL may have invaded the sand cap are the strength, compressibility, and thickness of the organic silt/sediment and underlying peat soils. Vane shear testing was performed for the original design. Peak shear strengths of the organic silt/sediment of less than 50 psf occurred in the upper portions, with 50 to 100 psf to significant depths of 8 to 10 feet near Transects T10 and T11. CPT indicates strengths in the organic silt/sediment as low as 20 psf. However, in general, the tip resistance measured was on the order of 1,200 psf. These strengths are considered low. In addition, low shear strength is generally commensurate with higher water content and higher compressibility for a given soil type. This higher compressibility has been substantiated by the significant amount of settlement of the cap in this area, observed by monitoring of the settlement plates.

Field monitoring of cap settlement indicated that a significant magnitude of consolidation settlement (on the order of 1 to 3 feet) occurred within several months of cap construction. The underlying organic silt/sediment and peat soils are highly organic and, as a result, very compressible and tend to undergo consolidation settlement as load is transferred to this material. This is referred to as primary consolidation and occurs as quickly as water (and NAPL) can be squeezed out of the soil mass. Settlement data indicate that this process occurred over a period of months following cap construction. Organic soils will exhibit a tendency toward secondary consolidation, which is a time-dependent phenomenon of organic soils in which settlement will continue to occur at an ever-decreasing rate over time. The magnitude of this secondary settlement over time tends to be greater for organic soils than for inorganic soils. This too will lead to squeezing of water (and possibly NAPL) over a long period of time at an ever-decreasing rate. The excess water and NAPL will migrate both laterally and predominantly upward, thus potentially migrating through the cap via fissures (i.e., zones of weakness and/or structural irregularities) in the cap or zones of higher permeability, such that the water and NAPL may become concentrated in isolated, or “focused,” areas on top of the cap, where the water and NAPL can further migrate horizontally. One of these isolated areas may very well be the cribbing along the west side of the canal where the appearance of NAPL was noted during early cap construction (2003/2004) and where differential settlement of the cap in relation to the cribbing resulted in exposure of portions of the cribbing. Since then, the cribbing has been capped and no evidence of NAPL seepage in this area has been observed.

In comparing the distribution of NAPL concentrations to soil strength at the same locations, we find no discernable trend between soil strength and NAPL concentrations observed at the surface (on the cap), within the cap, or within the subsurface soils. Mud boils and localized failures of the cap were noted in some areas during cap construction. Although there does not appear to be a trend between soil strength and NAPL concentrations, given the relatively low strength of the organic silt/sediment in general, as well as the greater thickness of the cap, it is possible that localized failures of the cap occurred; this could result in the formation of preferential pathways for water and NAPL to escape during consolidation and could also result in direct contamination of the cap surface as NAPL is forced up through the cap. It has been suggested that, in general, consolidation of soil after cap placement may result in migration of NAPL that was previously stable (Reible 2005).

The data suggest that substantial consolidation of the underlying organic silt/sediment and NAPL-rich peat soils has occurred as a result of placement of the cap material. Using the time rate of consolidation trends observed after cap placement, we can estimate the amount of settlement that has occurred at several locations in the canal. From the magnitude of consolidation values and phase equations, we can estimate that the amount of water and/or NAPL expelled from the pores to the present date is on the order of 1.0 to 2.8 cubic feet per square foot of cap surface. The estimated settlement and expelled fluid at nine locations are summarized in Table 3-2 based on the thickness of cap reported by The Johnson Company. Recent measurements of cap thickness indicate that the cap is thinner than when originally constructed (Section 4.4.2). It is possible that NAPL has migrated to the surface in these thinner capped areas due to consolidation.

Based on the foregoing analysis, both localized cap failure and greater magnitudes of consolidation (which expelled NAPL-rich porewater) cannot be eliminated as reasonable causative mechanisms for the presence of NAPL in and on the sand cap.

5.3 NAPL Migration via Preferential Pathways

Preferential pathways for NAPL migration include cribbing along the canal banks and vertical seeps at specific points. Gaps or holes in the old wood cribbing (such as may be caused by tree roots), which was installed in the 1890s, may create a preferential pathway along or through which NAPL can migrate into the canal. NAPL may be more likely to migrate along this preferential pathway when combined with other factors, such as an increase in piezometric head within the soil mass associated with an increase in overburden. As the weight of cap is placed on the underlying peat and organic silt/sediment, this increase in overburden pressure is initially carried by the porewater in the saturated organic silt and peat. This results in a temporary upward (and lateral) hydraulic gradient due to the temporarily higher piezometric head within the soil mass. NAPL seepage through the cribbing was observed during construction of the cap when the canal was dewatered (i.e., increase in hydraulic head from the soil to the canal, through the cribbing) (The Johnson Company 1997). NAPL seepage through the cribbing may also have occurred when the cap was placed on top of and behind the cribbing (i.e., increased overburden weight and preferential migration along and through the cribbing).

NAPL wicking may explain the NAPL migration along the wooden cribbing. It is possible that the NAPL is preferentially wetting the wooden cribbing in the presence of water. If this is the case, then it is reasonable to assume that the NAPL would wick along the cribbing due to preferential wetting. Since NAPL seems to be predominantly associated with the peat, NAPL wicking may also be a migration mechanism within the peat. It is possible that, due to the high organic content of the peat, the NAPL is preferentially wetting on the peat in the presence of water.

As discussed above, consolidation of the underlying peat and organic silt/sediment may enhance the short-term upward gradient as water is squeezed from the soil mass. As the water moves upward through the cap, some hydraulic fracturing of the cap can occur, which provides a preferential flow path. Similarly, the water will take the path of least resistance, which may also include zones of higher permeability in the cap material itself (i.e., sandier zones and zones of lower silt content). This can result in “pipes” within the mass of the sand cap that will then act as long-term pathways.

Preferential flow paths may have also been created in areas of vertical seeps at specific point locations, such as along the east side of the canal (i.e., Transect T14+30) and in the vicinity of the former slip on the east side of the canal. Based on information provided by The Johnson Company, we understand that low-density polyethylene (LDPE) liner material was placed in the area of Transect T14+30 and then weighted down with gabions. According to the project records, location T14+30 is coincident with the southern end of the LDPE liner. It is possible that the weight of the gabion may be forcing water and NAPL around the edge of the LDPE liner in this area. The former slip may also provide a preferential pathway, because the fill material may have contained NAPL and may be more permeable than the surrounding soil. During the spring and summer investigations, sheens were not observed in the vicinity of Transect T14+30 or the former slip. During the cap coring events, plant roots were generally not found at depth with the sand cap corings. Thus, plant roots are not believed to be a significant preferential flow path in the cap.

Gas bubbles may also create preferential pathways. The gas bubbles may physically disrupt the sediment as the bubbles rise, creating a track of high-porosity sediment along the path of the bubble migration. The high-porosity track may increase the migration of NAPL (Reible 2005). Laboratory observation of bubble growth in natural sediments indicates that the sediment fractures as the gas bubble forms and migrates out of the sediment (Johnson et al. 2002). Observations indicate that bubble growth by sediment fracturing should correspond to bubbles that are coin- or disk-shaped (Johnson et al. 2002). These bubble shapes have been observed at other sediment sites, including Eckernförde Bay and Anacostia River (Johnson et al. 2002; Reible 2005). It is

unknown what shape gas bubbles take at the Pine Street Canal Superfund Site, because low visibility in the canal makes it impossible to observe bubble shape.

Based on the foregoing analysis, preferential pathways have the potential to facilitate NAPL migration into the canal. This type of NAPL migration would result in contamination of the cap surface (cap swabbing indicates that NAPL is present on the surface of the cap), with possible seepage of NAPL into the cap. Data from the spring and summer investigations indicate that preferential pathways provide a potential NAPL migration pathway.

5.4 NAPL Migration via Gas Bubble-induced Transport

Methane is produced in sediment through the anaerobic degradation of organic matter (Martens and Klump 1984; Adams et al. 1990; Howard et al. 1971). If sufficient methane is produced, it will form gas bubbles that migrate out of the sediment, through the water column, and to the air (Amos and Mayer 2006). Ebullition is the vertical transport of gas bubbles driven by buoyancy forces. As gas bubbles migrate through the sediment, they can pick up NAPL in the sediment or on the surface of the cap, carrying the NAPL to the water surface. Gas bubbles form in the sediment when the partial pressure of the gas in the bubbles exceeds the atmospheric and hydrostatic pressures above the sediment (Reible 2005; Heslein 1976; Fendinger 1981; Adams et al. 1990). Gas bubbles are hydrophobic and can accumulate hydrophobic organic contaminants (such as coal tar NAPL) and colloids from porewaters (Reible 2005; Adams et al. 1990). However, gas bubbles may not be the only migration mechanism, because NAPL migration independent of gas bubbles has been observed at the site.

In freshwater sediments with high organic content, methane is likely the gas that controls bubble formation because of its abundance in freshwater anoxic sediment and its low solubility (Heslein 1976). Measurements of the contents of gas bubbles from freshwater sediments indicate that the bubbles consist primarily of methane, with a small amount of nitrogen and possibly trace amounts of carbon dioxide (Chau et al. 1977; Adams et al. 1990; Howard et al. 1971; Ward and Frea 1979; Amos and Mayer 2006).

NAPL migration may be temperature-dependent as a result of the production of gas bubbles being temperature-dependent. If NAPL is transported via gas bubbles, there is then a greater likelihood of NAPL transport during periods of warmer temperature and higher gas bubble production. The seasonal rate of methane gas bubble production has been evaluated in freshwater and marine sediments, and gas ebullition occurs primarily in summer months (Kipphut and Martens 1982; Kelly and Chynoweth 1981). The effects of temperature and the supply of organic carbon on methane generation from sediment were evaluated for two Michigan lakes (Kelly and Chynoweth 1981). Methane production increased during warmer months (Kelly and Chynoweth 1981; Heslein 1976), as did the supply of organic carbon (Kelly and Chynoweth 1981), and the supply of organic carbon controlled the rate of methane production (Kelly and Chynoweth 1981). In warmer months, when the supply of organic carbon was higher, methane production increased (Kelly and Chynoweth 1981). At the Pine Street Canal Superfund Site, the supply of organic carbon from the stormwater system may be similar throughout the year (assuming the organic carbon content of stormwater does not vary by much throughout the year). However, the supply of organic carbon from algae and water plants is likely highest during warmer months, when photosynthesis is at its peak. The increased supply of organic carbon during the warmer months may result in increased methane production at the site during warmer months. Thus, more gas bubbles and more NAPL transport are observed at the site during the summer.

One source of methane at the Pine Street Canal Superfund Site may be the peat, which contains high organic concentrations and is likely anoxic. These conditions allow for methane generation via anaerobic degradation of organic matter. The organic silt/sediment may also be a source of gas bubbles, as described below.

Gas bubbles have the potential to carry NAPL into the canal. This type of NAPL migration may result in NAPL contamination of the cap from the bottom of the cap to its top, if the source of NAPL is in the underlying organic silt/sediment layer below the cap. If the source of NAPL is on the surface of the cap, gas bubbles would not affect the concentration of NAPL in the cap. Gas bubbles, both with and without NAPL, have been observed at the site since completion of the cap. Gas bubbles were also observed at the site prior to construction of the cap (USEPA 2005). Site data indicate that gas bubbles are a NAPL migration pathway into the canal by carrying NAPL from the organic silt/sediment layer, through the cap and at times picking up NAPL on the surface of the cap.

During cap coring at the site, a number of locations contained sheen along the length of the cap core, indicating NAPL was migrating through the cap. In addition, a number of cap core locations contained maximum concentrations of total PAHs and TPH in the subsurface, also suggesting that NAPL was migrating through the cap. The limited number of cap cores having a clear gradient from subsurface to surface may be the result of multiple factors:

- Gas bubbles may migrate along small-diameter pathways at isolated locations in the canal. The likelihood of capturing a small pathway during cap coring is low. Thus, the majority of cap coring data may not be indicative of NAPL migration through the cap.
- NAPL may be migrating into the canal via multiple pathways (such as gas bubbles and preferential pathways), thus confounding the concentration gradient in the cap.

The transport of NAPL via gas bubbles also appears to be temperature-dependent. As reported in the October 21, 2005, biweekly inspection report (The Johnson Company 2005b), fewer gas bubbles were observed during the inspection period than in earlier inspections when the temperature was warmer. In areas where there were gas bubbles, no NAPL migration was observed, which may be related to the cooler temperatures. NAPL seeps and gas bubbles were more abundant in the summer investigation than in the spring investigation, again suggesting that temperature may contribute to NAPL migration and gas bubble generation. Temperature data collected from the piezometers indicate that the cap and organic silt/sediment are affected by fluctuations in the surface water temperature. The peat and silt layers maintain a constant temperature and are not influenced by surface water temperatures.

If gas bubbles are generated in the cap or organic silt/sediment, the rate of gas generation may be affected by fluctuations in surface water temperature. If gas bubbles are generated in the peat or silt layers, the rate of gas generation is not controlled by temperature fluctuation because the peat and silt layers have a fairly constant temperature. All layers likely have sufficient organic matter to produce methane via anaerobic degradation. The cap has organic matter in the form of NAPL, deposited algae and plant material, and stormwater deposition. The organic silt and peat are, by definition, high in organic matter. It is possible that methane is produced in any of these layers.

Based on the foregoing analysis, the spring and summer investigation data indicate that NAPL migration via gas bubble-induced transport is a NAPL migration pathway. The data indicate that gas bubbles carry NAPL through the cap and/or pick up NAPL on the surface of the cap. The ebullition rate, if ebullition is occurring in the cap or organic silt/sediment, may be affected by temperature. If gas bubble generation is occurring in the peat or silt layers, the temperature data recorded at PZ5, although damaged, indicate that the rate of bubble generation is not controlled by temperature.

5.5 Summary of NAPL Migration Mechanisms

Based on the available data, all of the following pathways are potential NAPL migration mechanisms:

- **NAPL migration via vertical hydraulic gradient.** Based on available data, vertical hydraulic gradients in the clayey silt and organic silt/sediment are sufficient for upward NAPL movement to the base of the sand cap. This mechanism makes it possible for localized pools of NAPL to form at the interface between the organic silt/sediment and the sand cap. Upward NAPL movement through the sand cap via hydraulic gradient is unlikely due to hydraulic gradients. Once the NAPL is at the base of the sand cap, other NAPL migration mechanisms may then cause the NAPL to migrate into the canal.
- **NAPL migration via horizontal hydraulic gradient.** Based on available data, horizontal hydraulic gradients in both the east and west banks fluctuate seasonally, correlating with surface water levels and groundwater recharge. Gradients capable of mobilizing NAPL towards the canal are likely not present or are only present intermittently.
- **NAPL migration via localized bearing-capacity failures.** Based on available data, consolidation settlement may have contributed to NAPL migration through the sand cap in the past. It appears that current settlement rates have approached secondary compression. It is anticipated that under current conditions, consolidation settlement will play an ever-decreasing role in NAPL migration to the canal. NAPL migration to the canal may occur along localized bearing-capacity failures.
- **NAPL migration via preferential pathways.** NAPL wicking along the cribbing and NAPL migration via preferential flow paths (such as hydraulic fractures and high-porosity zones) are potential NAPL migration mechanisms to the canal.
- **NAPL migration via gas bubble-induced transport.** Gas bubbles are an observed method of NAPL migration to the canal.

The overall conclusion is that NAPL may have migrated from the NAPL-rich peat layer to the organic silt/sediment layer and the base of the sand cap due to consolidation and is continuing to migrate due to the effect of vertical hydraulic gradients. At that point, gas bubbles carry the NAPL through the cap into the canal. The effect is most pronounced where the cap is thinnest. NAPL migration via gas bubble-induced transport appears to be the most significant of the potential ongoing NAPL migration pathways and is the primary pathway that the NAPL controls must address. The NAPL controls must also address the secondary migration mechanisms. This conclusion is depicted on Figure 5-2, which illustrates the revised conceptual site model.

5.6 Combined Evaluation of Location and Migration of NAPL

The evaluation and discussion of results presented in Section 4, and the updated conceptual model presented above, were considered for use in evaluating potential NAPL controls. Two forms of NAPL control are potentially needed at the site:

- Control of NAPL already on the surface of the cap
- Control of migration of NAPL into the canal

NAPL has been observed on the cap surface (combined deposition and upper portion of the sand cap). The extent of NAPL on the cap surface is presented on Figure 5-3. These areas will likely require control of NAPL on the cap surface. The contiguous area of cap surface requiring control is approximately 10,000 ft², or one-quarter of an acre.

The remaining analyses of the location and migration of NAPL, including NAPL seepage into the canal, NAPL within the sand cap, and potentially mobile subsurface NAPL, have also been synthesized on Figure 5-3. To accomplish this synthesis, the classification for each analysis and each grid cell was tabulated. Each classification was assigned a number, indicating its relative importance in contributing to NAPL migration. For example, observed NAPL seepage into the canal was assigned a higher number than was potentially mobile subsurface NAPL. These numbers were summed. Each grid cell was then classified as low, medium, or high for its potential for NAPL migration based on the grid cell sum. This classification is provided in Appendix J.

Figure 5-3 depicts the potential for NAPL migration (i.e., low, medium, or high). Areas with high and medium potential for NAPL migration will likely require control of NAPL migration into the canal. The contiguous area of the canal requiring control of NAPL migration is approximately 14,000 ft², or one-third of an acre. The extent of NAPL on the cap surface, discussed above, is within this area.

6. Conclusions

This NAPL investigation report evaluates data collected during the spring, summer, and winter investigations and updates the conceptual site model with respect to NAPL migration mechanisms. All estimates of NAPL location and mass presented in this report are based on conservative assumptions for the purpose of selecting and designing NAPL controls. The estimated NAPL masses do not represent a mass balance. Since these masses are order-of-magnitude estimates, the actual NAPL mass or seepage associated with each cell may be lower or higher.

Based on the information presented here, we have developed the following conclusions with respect to data gaps identified in the Work Plan (BBL and Hart Crowser 2006b) for this NAPL investigation:

NAPL Seepage into the Canal

- The approximate annual rate of NAPL seepage into the canal is estimated to be on the order of 111 kg/yr. Based on 2006 observations of NAPL seepage, the area of greatest seepage is centered between Transects T10 and T11, focused in the center and western portion of the canal. There is also seepage extending 50 feet north of Transect T10 and 50 feet south of Transect T11.
- Seepage was mostly associated with gas bubbles in 2006 and varied in location, timing, and rate. Limited NAPL seeps also occur as globules rising to the canal surface without gas bubbles.
- Recent measurements of sand cap thickness indicate that the cap is thinner in some locations than when it was originally constructed (Figure 4-16). Generally, NAPL seepage rates are relatively high at locations with the thinner cap.
- Based on a grid classification of post-construction and 2006 seepage observations, approximately 5,000 ft² of the canal appear to have a relatively higher NAPL seepage rate and 9,000 ft² of the canal appear to have a relatively lower NAPL seepage rate (Figure 4-17). Based on observed seepage, the overall area of potential seepage is approximately 14,000 ft², or about one-third of an acre.

NAPL Deposition on the Cap Surface

- The majority of NAPL deposition was observed between Transects T10+50 and T11+50 and appears to be correlated with the observed seepage locations from 2006.
- We estimate that the mass of NAPL deposition on the top of the cap is on the order of 2.5 kg in the area of interest. This is the amount of NAPL that can be quantified using cap swabs.

NAPL in the Sand Cap

- Based on 2006 sampling conducted to characterize the presence of NAPL on the surface and in the upper portion (i.e., the top 4 inches) of the sand cap, the area of observed NAPL is generally similar to and coincident with the area of observed NAPL seepage into the canal. The approximate mass of NAPL on the surface and in the upper layer of the sand cap is estimated to be on the order of 760 kg.

-
- Based on 2006 sampling conducted to characterize the presence of NAPL in the lower portion (i.e., below the top 4 inches) of the sand cap, the area of observed NAPL is generally similar to and coincident with the area of observed NAPL seepage into the canal. The approximate mass of NAPL in the lower portion of the sand cap is estimated to be on the order of 2,400 kg. Based on the mass of NAPL within the pore space of the sand (generally less than 20,000 mg/kg), this mass is residual NAPL and is generally not expected to be mobile.
 - Five cap coring locations in the canal exhibit increased NAPL concentrations toward the bottom of the cap, indicating that NAPL may be migrating upward through the cap at these locations. However, NAPL is also present at some locations due to deposition during construction. Generally, the cap coring locations did not show visible horizontal gradation of NAPL. A visible horizontal gradation of NAPL, indicative of a vertical seepage path, could be observed in the corings from only a few locations.
 - During the winter investigation an additional nine cap cores (on three transects) were conducted in the west bank cap. The west bank cap coring results indicate that limited, localized, discrete intervals of NAPL are present at the apparent interface between the base of the cap and the underlying soil. However, no continuous pathway of NAPL from the cribbing to the canal was observed.

Thickness of the Sand Cap

- Forty-two sand cap thickness measurements were obtained. Of these, 10 measurements were less than 1.5 feet, the cap's minimum design thickness. Most cells with low sand cap thickness also exhibited NAPL seepage and relatively high NAPL concentrations within the cap.

Potentially Mobile NAPL in the Subsurface

- Based on 2006 subsurface explorations beneath the canal and three-dimensional modeling, the area of mobile NAPL within the subsurface (Figure 4-13) is larger than the area of observed NAPL seepage (Figure 4-17). The approximate mass of mobile NAPL in the canal subsurface is estimated to be on the order of 521,000 kg. Approximately 70 percent of the mobile NAPL is found in the peat layer. Approximately 24 percent of the mobile NAPL is found in the organic silt/sediment layer, the majority of which is in the lower portion of the organic silt/sediment layer.
- Investigation data indicate that there is a significant mass of potentially mobile NAPL present beneath the canal. It generally does not appear to extend into the stratified silt and sand or clayey silt layers underlying the peat (Figures 4-4 to 4-12). Therefore, the vertical extent of potentially mobile NAPL has been defined at the site.
- Although the horizontal extent of potentially mobile NAPL along the canal has not been completely defined at the site, the limited observations of NAPL seepage north or south of the spring investigation boundaries indicate that the horizontal extent of potentially mobile NAPL along the canal length has been adequately defined for the purposes of this study.
- Based on the winter investigation, the horizontal extent of mobile NAPL along the banks of the canal is less than the extent of mobile NAPL beneath the canal. Furthermore, NAPL concentrations beneath the banks decrease quickly with distance away from the canal. In the vicinity of documented seepage to the canal, the only significant NAPL observed beneath the banks is in the former slip on the east bank, and even here NAPL concentrations are lower than beneath the canal. The calculated mass of mobile NAPL beneath the west and east banks is 11 percent and 6 percent, respectively, of the total mass of mobile

NAPL beneath the canal and banks. Historical data supports these results. On the east bank, NAPL was historically observed in a relatively small area adjacent to the former slip and in a larger area near the former MGP. Along the west bank away from the canal, historical observations generally indicated that NAPL was not present.

NAPL Migration Mechanisms

- The following mechanisms may contribute to NAPL migration mechanisms at the Pine Street Canal Superfund Site:
 1. Vertical hydraulic gradient (within the geologic units below the sand cap, but not within the cap)
 - The cap sand, organic silt/sediment, and clayey silt layers are hydraulically connected to and influenced by variations in surface water elevation in the canal. The vertical hydraulic gradient provides a NAPL migration pathway within the geologic layers beneath the cap sand. However, the average estimated upward component of the hydraulic gradient within the cap sand does not appear to be sufficient to mobilize NAPL upward through the sand cap.
 - NAPL is migrating upward into the organic silt layer and to the base of the cap due to hydraulic gradients within the underlying soils. This process, if it is occurring, could produce an accumulation of NAPL within the base of the cap over time and may cause NAPL “breakthrough” where the cap is relatively thin.
 2. Horizontal hydraulic gradient (within the banks of the canal – towards the canal)
 - Horizontal hydraulic gradients in both the east and west bank fluctuate seasonally, correlating with seasonal changes in surface water levels and groundwater recharges.
 - NAPL with pool lengths greater than the maximum stable pool lengths calculated for stratified silt and sand in the west bank, peat in the west bank, and peat in the east bank are not likely to be present. If sufficient gradients exist to mobilize NAPL by this mechanism they exist only intermittently and do not likely contribute to significant NAPL mobility at the site.
 3. Localized bearing-capacity failures and consolidation settlement
 - Localized bearing-capacity failures provide a potential NAPL migration pathway to the canal. In comparing the distribution of NAPL concentrations to the soil strength at the same locations, no discernable trend was observed between soil strength and NAPL concentrations at the surface (on the cap), within the cap, or within the subsurface soils. However, given the relatively low strength of the organic silt/sediment, it is possible that localized bearing-capacity failures of the cap have occurred, which could result in the formation of preferential pathways for water and NAPL to escape. The current and future significance of this NAPL migration pathway is likely of secondary importance, unless redistribution of loading occurs as a result of future capping or other activities.
 - Consolidation settlement provides a potential NAPL migration pathway to the canal. Substantial consolidation of the underlying organic silt/sediment and peat has occurred as a result of placement of the cap material. The current and future significance of this NAPL migration pathway, under existing conditions, is likely of secondary importance.

-
- Implementation of the selected NAPL controls has the potential to create NAPL migration from either of these mechanisms. Therefore, approaches that reduce the risk of inducing these pathways will be factored into the design. Certain construction methods that apply heavy loads to the bank or directly to the cap must be avoided. Similarly, a heavy capping material or the application of the capping material non-uniformly must also be avoided.
4. Preferential pathways
- Potential preferential pathways for NAPL migration to the canal include cribbing along the canal banks and vertical seeps at specific points. Some cores did show traces of vertical pathways. Although no direct evidence for some of these pathways was observed, they cannot be ruled out.
 - The west bank cap coring results from the winter investigation indicate that limited, localized, discrete intervals of NAPL are present at the apparent interface between the base of the cap and the underlying soil. However, no continuous pathway of NAPL from the cribbing to the canal was observed.
5. Gas bubble-induced transport from the cap surface and/or from below the cap
- Gas bubble-induced transport from the cap surface and gas bubble-induced transport from below the cap are NAPL migration pathways to the canal. The data indicate that gas bubbles are carrying NAPL through the cap and picking up NAPL on the cap surface. If ebullition is occurring in the cap or organic silt/sediment, the ebullition rate may be affected by temperature. If gas bubble generation is occurring in the peat or silt layers, the rate of bubble generation is not controlled by temperature.

Conclusion

Our overall conclusion is that NAPL may have migrated from the NAPL-rich peat layer to the organic silt/sediment layer and the base of the sand cap in the past as a result of consolidation and is continuing to migrate due to the effect of vertical hydraulic gradients. From the organic silt/sediment layer, gas bubbles carry the NAPL through the cap and into the canal. The effect is most pronounced where the cap is thinnest. This migration pathway appears to be the most significant of the potential ongoing NAPL migration pathways and is the primary pathway that the NAPL controls must address.

For the west bank and the majority of the east bank in the area of seepage (T9 to T12+50), which was the focus of this investigation, there is no indication that there are significant NAPL pools or that NAPL is migrating into the canal from the banks. However, there is potentially mobile NAPL within the former slip along the east bank. The NAPL controls must address the primary and secondary migration mechanisms and the impact of potentially mobile NAPL in the former slip on the cap and its ability to prevent NAPL releases.

Based on a multi-faceted analysis, the contiguous area of cap requiring NAPL control is approximately 14,000 ft², or one-third of an acre (Figure 5-3). The exact dimensions of the NAPL controls on the cap, and the need for NAPL controls on the banks, will be determined as part of the evaluation and analysis presented in the NAPL Controls Report.

7. References

- Adams, D.D., N.J. Fendinger, and D.E. Glotfelty. 1990. Biogenic gas production and mobilization of in-place sediment contaminants by gas ebullition. *Sediments: Chemistry and Toxicity of In-place Pollutants*. R. Baudo, J.P. Giesy, and H. Muntau, eds. Lewis Publishers, Inc.
- Amos, R.T., and K.U. Mayer. 2006. Investigating ebullition in a sand column using dissolved gas analysis and reactive transport modeling. *Environmental Science and Technology*, 40(17), 5361-5367.
- BBL and Hart Crowser. 2006a. Action Plan, Pine Street Canal Superfund Site, Burlington, Vermont. April 7.
- BBL and Hart Crowser. 2006b. Work Plan, Pine Street Canal Superfund Site, Burlington, Vermont. April 7.
- Brady, N.C., 1974. *The Nature and Properties of Soils*. 8th Edition, Macmillan Publishing, New York.
- C Tech. 2006. *Mining Visualization System User Manual*. Huntington Beach: C Tech Development Corporation, February 2, 2006.
- Chatzis, I., N.R. Morrow, and H.T. Lim. 1983. Magnitude and detailed structure of residual oil saturation. *Society of Petroleum Engineers Journal*. April.
- Chau, Y.K., W.J. Snodgrass, and P.T.S. Wong. 1977. A sampler for collecting evolved gases from sediment. *Water Research*, Vol 11, 807-809.
- Cohen, R.M., and J.W. Mercer. 1993. DNAPL Site Evaluation. C. K. Smoley, Boca Raton, Florida.
- de maximis*. 2005. Email from Thor Helgason of DeMaximis to Michael Smith of ANR and Karen Lumino of USEPA Regarding: Pine St. Site Insp. Summary Report. September 23.
- Electric Power Research Institute (EPRI). 2004. Residual Saturation of Coal Tar in Porous Media. Report 1009426. April 2004.
- Fendinger, N.J. 1981. Distributions and Related Fluxes of Dissolved Pore Water Gases (CH₄, N₂ and ΣCO₂) in the Sediments of Lake Erie and Two Polluted Harbors. M.S. Thesis, Fredonia State University.
- Heslein, R.H. 1976. The Fluxes of Methane, Sigma (Carbon-Dioxide), and Ammonia-Nitrogen from Sediments and Their Consequent Distribution in a Small Lake. Ph.D. Dissertation, Columbia University.
- Howard, D.L., J.I. Frea, and R.M Pfister. 1971. The potential for methane-carbon cycling in Lake Erie. Proceedings Fourteenth Conf. Great Lakes Res., 236-240.
- Huling, S.G., and J.W. Weaver. 1991. Ground Water Issue – Dense Nonaqueous Phase Liquids. EPA/540/4-91-002. March.
- Johnson, B.D., B.P. Boudreau, B.S. Gardiner, and R. Maass. 2002. Mechanical response of sediments to bubble growth. *Marine Geology*, 187, 347-363.

Kelly, C.A., and D.P. Chynoweth. 1981. The contributions of temperature and of the input of organic matter in controlling rates of sediment methanogenesis. *Limnology and Oceanography*, 26(5), 891-897.

Kipphut, G.W., and C.S. Martens. 1982. Biogeochemical cycling in an organic-rich coastal marine basin 3. Dissolved gas transport in methane-saturated sediments. *Geochimica et Cosmochimica Acta*, Vol 46, 2049-2060.

Kueper, B. 2007a. Personal communication between Bernard H. Kueper, Ph.D., P.Eng, Queen's University, Ontario, Canada, and Michael Gefell, ARCADIS BBL.

Kueper, B. 2007b. Personal communication between Bernard H. Kueper, Ph.D., P.Eng, Queen's University, Ontario, Canada, and Barry Kellems, ARCADIS BBL.

Martens, C.S., and J.V. Klump. 1984. Biogeochemical cycling in an organic-rich coastal marine basin 4. An organic carbon budget for sediments dominated by sulfate reduction and methanogenesis. *Geochimica et Cosmochimica Acta*, Vol. 48, 1987-2004.

Mercer, J.W., and R.M. Cohen. 1990. A review of immiscible fluids in the subsurface: Properties, models, characterization and remediation. *Jour. of Contaminant Hydrology*, Vol. 6, pp. 107-163.

Metcalf and Eddy. 1992. Supplemental Remedial Investigation Final Report: Pine Street Canal Superfund Site. Prepared under USEPA contract number 68-W9-0036. March.

Oregon Department of Environmental Quality (ODEQ). 2003. Technical Memorandum: NAPL Flux Assessment of Beach Seeps in Willamette Cove, McCormick and Baxter Creosoting Company, Portland, Oregon. January 17.

PEER. 1990. Draft Remedial Investigation Report for Pine Street Canal Site. Report prepared for the U.S. Environmental Protection Agency as cited in Metcalf and Eddy 1992.

Perkins-Jordan. 1984. Burlington Southern Connector, Pine Street Canal Site, Vermont Agency of Environmental Conservation, Permit Application for Remedial Action and Highway Construction, Volume I Design Report and Volume II Technical Appendices. January.

Pinder, George F., and Joseph F. Guarnaccia. 1993. Numerical Analysis of Contaminant Flow and Transport Processes at the Pine Street Barge Canal Site. May 24.

Reible, D. 2005. In-situ sediment remediation through capping: Status and research needs. <http://www.hrsc-ssw.org/pdf/cap-bkgd.pdf>. February 2005. Retrieved February 24, 2005.

Reible, D.D., and T.H. Illangasekare. 1989. Subsurface processes of nonaqueous phase contaminants. *Intermedia Pollutant Transport: Modeling and Field Measurements*. D. T. Allen, ed. Plenum Press.

The Johnson Company, Inc. 1997. Additional Remedial Investigation, Pine Street Canal Superfund Site, Burlington, Vermont. July 3.

----- . 2003. Proposed NAPL Response Strategy Between Transects T9 and T14, Pine Street Superfund Site, Burlington, Vermont. Revision 0. September 12.

----- . 2004a. Remedial Action Construction Completion Report, Pine Street Canal Superfund Site, Burlington, Vermont. September 7.

----- . 2004b. Technical Memo: Physical Property Testing of Coal Tar DNAPL. March.

----- . 2005a. Compliance Monitoring Report Fall 2004, Pine Street Canal Superfund Site, Burlington, Vermont. Revision 0. January 27.

----- . 2005b. Email from Don Maynard of The Johnson Company, Inc. to Thor Helgason of DeMaximis Re: Pine St. - Report of Inspection on October 21, 2005. October 24.

----- . 2005c. Compliance Monitoring Report Fall 2005, Pine Street Canal Superfund Site, Burlington, Vermont. Revision 0. December.

----- . 2006a. Email from Don Maynard of The Johnson Company to Thor Helgason of DeMaximis Re: Pine St. - Report of Inspection on January 24, 2006.

----- . 2006b. Email from Don Maynard of The Johnson Company to Thor Helgason of DeMaximis Re: Pine St. - Report of Inspection on March 1, 2006.

----- . 2006c. Email from Don Maynard of The Johnson Company to Thor Helgason of DeMaximis Re: Pine St. - Report of Inspection on June 8, 2006.

----- . 2006d. Email from Don Maynard of The Johnson Company to Thor Helgason of DeMaximis Re: Pine St. - Report of Inspection on June 21, 2006.

----- . 2006e. Compliance Monitoring Report Spring 2006, Pine Street Canal Superfund Site, Burlington, Vermont. Revision 0. July.

----- . 2006f. Email from Don Maynard of The Johnson Company to Thor Helgason of DeMaximis Regarding: Re: Pine St. - Report of Inspection on July 19, 2006.

----- . 2006g. Email from Don Maynard of The Johnson Company to Thor Helgason of DeMaximis Re: Pine Street - Report of Inspection on August 25, 2006.

----- . 2006h. Email from Don Maynard of The Johnson Company to Thor Helgason of DeMaximis Re: Pine Street - Report of Inspection on September 17, 2006.

U.S. Environmental Protection Agency (USEPA). 1990. Laboratory Investigation of Residual Liquid Organics from Spills, Leaks, and the Disposal of Hazardous Wastes in Groundwater. EPA/600/6-90/004. April.

----- . 2005. Email from Karen Lumino of USEPA to Thor Helgason of DeMaximis Regarding: Pine Street Canal – June 1, 2005. June 2.

Ward, T.E., and J.I. Frea. 1979. Estimate of microbial activities in lake sediments by measurement of sediment gas evolution. *Methodology for Biomass Determinations and Microbial Activities in Sediments*, ASTM STP 673. C.D. Litchfield and P.L. Seyfried, eds. pp. 156-166.

**TABLE 2-1
SUMMARY OF SPRING, SUMMER, AND WINTER INVESTIGATION SAMPLING LOCATIONS**

**NAPL INVESTIGATION REPORT
PINE STREET CANAL SUPERFUND SITE
BURLINGTON, VERMONT**

Location	Cap Swab	Water Column	Cap Probe	Cap Sample Depth ¹	TarGOST ID	Conf. Boring	Environmental Sample Depth ¹	Geotech Composite Samples ²		Shelby Tube Depth ¹	Piezo.
								C-1 Depth ¹	C-2 Depth ¹		
Spring Investigation											
T09+30E30			CP01	0.0-0.32, 0.32-0.64, 0.64-0.80	LIF01						
T09+48E20			CP02	0.0-0.32, 0.32-0.50	LIF02	CB02	7-9, 10-12, 15-17, 25-27	6-8, 10-12, 15-17	25-27	12-14, 17-19, 27-29	
T09+75E15			CP03	0.0-0.32, 0.32-0.64, 0.64-0.96, 0.96-1.28	LIF03	CB03	7-9, 14-16				
T09+92E15			CP04	0.0-0.32, 0.32-0.64	LIF04						
T10+37E20			CP05	0.0-0.32, 0.32-0.64	LIF05						
T10+50E20		SW01	CP06	0.0-0.32, 0.32-0.64, 0.64-0.90	LIF06	CB06	6-8, 13-15, 16-18			0.0-2, 4-6, 8-10	PZ05
T10+50E35											PZ06
T10+67E20	CS01/CS07/CS08	SW04	CP07	0.0-0.32	LIF07						
T10+76E20	CS02/CS09	SW02	CP08	0.0-0.32, 0.32-0.64, 0.64-0.85	LIF08	CB08	14-16, 17-19			4-6, 8-10, 12-14	PZ07
T10+76E32											PZ08
T11+03E25			CP09	0.0-0.32, 0.32-0.64	LIF09						
T10+96E30	CS03		CP10	0.0-0.32, 0.32-0.64, 0.64-0.96, 0.96-1.28	LIF10						
T10+76E60			CP11	0.0-0.32, 0.32-0.64, 0.64-0.96	LIF11						
T10+98E40	CS05										
T11+04E20	CS04/CS06		CP12	0.0-0.32, 0.32-0.64	LIF12						
T11+45E25			CP13	0.0-0.32, 0.32-0.64, 0.64-0.96	LIF13						
T11+70E30			CP14	0.0-0.32, 0.32-0.64, 0.64-0.96	LIF14						
T10+76E40		SW03	CP16	0.0-0.32, 0.32-0.64	LIF16						
T09+00E60					TG01						
T09+00E60					TG01B						
T09+00E60					TG01Conf		11.5-13.5				
T09+50E60					TG02						
T10+00E60					TG03						
T10+50E60					TG04						
T11+00E60					TG05						
T11+50E60					TG06						
T12+00E60					TG07						
T12+00E60					TG07B						
T12+00E60					TG07C	CB07	10-12, 16-18	16-18	21.5-23.5	4-6, 8-10, 14-16	PZ03
T11+90E60											PZ04
T12+50E60					TG08						
T10+50E40					TG09						
T12+00E40					TG10	CB10	6-8, 10-12, 14-15			4-6, 8-10	PZ01
T11+90E40											PZ02
T10+75E80					TG11						
Turning Basin					LIFTB2						

TABLE 2-1
SUMMARY OF SPRING, SUMMER, AND WINTER INVESTIGATION SAMPLING LOCATIONS

NAPL INVESTIGATION REPORT
PINE STREET CANAL SUPERFUND SITE
BURLINGTON, VERMONT

Location	Cap Swab	Water Column	Cap Probe	Cap Sample Depth ¹	TarGOST ID	Conf. Boring	Environmental Sample Depth ¹	Geotech Composite Samples ²		Shelby Tube Depth ¹	Piezo.
								C-1 Depth ¹	C-2 Depth ¹		
Summer Investigation											
T09+55E20	CS31	SW05	CP26	0.0-0.33, 0.33-0.66							
T09+75E20	CS32	SW06	CP25	0.0-0.33, 0.33-0.50							
T10+50E20		SW15	CP27	0.0-0.33, 0.33-0.66, 0.66-0.85							
T10+65E20	CS33	SW07									
T10+70E20		SW14	CP22	0.0-0.33							
T10+74E20			CP23	0.0-0.33, 0.33-0.55							
T10+75E30		SW19									
T10+75E35		SW17									
T10+75E70	CS37	SW16	CP24	0.0-0.33, 0.33-0.66, 0.66-0.80							
T11+00E40	CS34/CS35	SW08/SW09	CP20	0.0-0.33, 0.33-0.64							
T11+05E20	CS38	SW13	CP21	0.0-0.33, 0.33-0.66, 0.66-0.99							
T11+10E20		SW10	CP19	No sample, zero recovery							
T11+20E20		SW12	CP18	0.0-0.33, 0.33-0.60							
T11+20E30		SW18									
T11+25E50	CS36	SW11	CP17	0.0-0.33, 0.33-0.66, 0.66-0.80							
T09+00E20	CS10										
T09+00E40	CS11										
T09+00E60	CS12										
T09+50E20	CS13										
T09+50E40	CS14										
T09+50E60	CS15										
T10+00E20	CS16										
T10+00E40	CS17										
T10+00E60	CS18										
T10+50E40	CS19										
T10+50E60	CS20										
T11+00E60	CS21										
T11+50E20	CS22										
T11+50E40	CS23										
T11+50E60	CS24										
T12+00E20	CS25										
T12+00E40	CS26										
T12+00E60	CS27										
T12+50E20	CS28										
T12+50E40	CS29										
T12+50E60	CS30										

**TABLE 2-1
SUMMARY OF SPRING, SUMMER, AND WINTER INVESTIGATION SAMPLING LOCATIONS**

**NAPL INVESTIGATION REPORT
PINE STREET CANAL SUPERFUND SITE
BURLINGTON, VERMONT**

Location	Cap Swab	Water Column	Cap Probe	Cap Sample Depth ¹	TarGOST ID	Conf. Boring	Environmental Sample Depth ¹	Geotech Composite Samples ²		Shelby Tube Depth ¹	Piezo.
								C-1 Depth ¹	C-2 Depth ¹		
Winter Investigation											
WB05-T08+25					TG115						
WB05-T08+75					TG114						
WB05-T09+25					TG113						
WB05-T09+50					TG116						
WB05-T09+75					TG101	CB101	10.5-11, 14.5-15, 18.3-18.8, 21.3-21.8, 4.4-4.9, 16.5-17	10.5-11, 14.5-15, 18.3-18.8, 21.3-21.8		6-8, 22-24	
WB15-T09+75					TG117						
WB05-T10+00			CP100 CP101 CP102	CP100 (0.0-0.5, 0.5-1, 1.5-2.0) CP101 (0.0-0.5, 1-1.5, 1.5-2) CP102 (0.0-0.5, 1.5-2, 2.5-3)	TG102B						
WB05-T10+25					TG103						
WB06-T10+50			CP103 CP104 CP105	CP103 (0.5-1, 1.5-1.8, 1.8-2) CP104 (0.0-0.5, 1-1.5, 1.5-2, 2-2.5, 2.5-3) CP105 (2-2.5, 2.5-2.7, 2.7-3)	TG104	CB104	2.6-3.1, 12.9-13.4, 17.3-17.8, 22.5-23, 10-10.5, 15-15.5, 18.4-18.9, 20.8-21.3	2.6-3.1, 12.9-13.4, 17.3-17.8, 22.5-23			PZ100, PZ101
WB05-T10+75					TG105						
WB05-T11+00			CP106 CP107 CP108	CP106 (0.0-0.5, 0.5-1, 1.5-2) CP107 (2-2.2, 2.2-2.5, 2.5-3) CP108 (1.5-2, 2-2.5, 2.5-3)	TG106						
WB24-T11+03					TG123						
WB05-T11+25					TG107						
WB05-T11+50					TG108						
WB04-T11+75					TG100	CB100	7.5-8, 10-10.5, 16.3-16.8, 20.3-20.8, 8.4-8.9, 13-13.5, 18.7-19.2	7.5-8, 10-10.5, 16.3-16.8, 20.3-20.8		14-16	
WB15-T11+75					TG118						
WB05-T12+25					TG119						
WB05-T12+75					TG120	CB120	6-6.5, 12-12.4, 14.9-15.4, 18.6-19.1, 4.4-4.9	6-6.5, 12-12.4, 14.9-15.4, 18.6-19.1			
WB05-T13+25					TG121						
WB05-T13+75					TG122						
WB05-T14+05					TG109						
WB00-T14+27					TG110B						
WB00-T14+50					TG111						
WB00-T14+75					TG112						
EB17-T10+00					TG127						
EB11-T10+25					TG128						
EB05-T11+00					TG130	CB130	18-18.5, 21.5-22, 22.7-23.2	18-18.5, 21.5-22, 22.7-23.2		2-4, 26-28	PZ102, PZ103, PZ104
EB05-T11+75					TG126						
EB20-T11+95					TG125	CB125	14-14.5, 16.6-17.1, 20.3-20.8, 24-24.5	14-14.5, 16.6-17.1, 20.3-20.8, 24-24.5			
EB05-T12+25					TG131						
EB05-T12+50						CB131	15.5-16, 16.7-17.2, 19.5-20, 24.9-25.4	15.5-16, 16.7-17.2, 19.5-20, 24.9-25.4		2-4	
EB05-T13+18					TG132						
EB05-T14+25					TG124						

Notes:

Conf. = Confirmation

Piezo. = Piezometers

1. All depths are measured in feet below sediment surface (top of cap).

2. Winter geotech samples were not composites.

**TABLE 2-2
MONITORING WELL COORDINATES**

**NAPL INVESTIGATION REPORT
PINE STREET CANAL SUPERFUND SITE
BURLINGTON, VERMONT**

Location ID	Northing ¹	Easting ¹	Elevation (ft) ²
MW11A	717,415	1,453,099	104.55
MW11B	717,391	1,453,091	101.98
MW17	717,872	1,452,842	101.13
MW23B	717,860	1,452,803	103.19
MW103B	717,599	1,453,114	101.35
MW110	717,747	1,453,066	101.38
RW9+80	717,584	1,452,956	101.69
RW10+25	717,544	1,452,954	102.23
RW11	717,480	1,452,956	101.96
RW14	717,165	1,452,972	102.04

Notes:

1. Horizontal datum is Vermont State Plane, North American Datum 83.
2. Vertical datum is 1988 North American Vertical Datum (NAVD88).
Elevation is at top of inner casing.

**TABLE 2-3
PIEZOMETER COORDINATES AND SCREEN DEPTHS**

**NAPL INVESTIGATION REPORT
PINE STREET CANAL SUPERFUND SITE
BURLINGTON, VERMONT**

Location ID	Northing ¹	Easting ¹	Top of Casing Elevation (ft) ²	Screen Interval Elevation (ft) ²
PZ03	717,387	1,453,031	99.21	71.51 to 70.51
PZ05	717,528	1,452,984	100.25	80.03 to 79.03
PZ06	717,529	1,453,000	100.17	88.97 to 87.97
PZ07	717,507	1,452,988	100.08	72.88 to 71.88
PZ08	717,507	1,453,000	100.71	87.49 to 86.49
PZ100	717,520	1,452,953	101.36	72.43 to 71.78
PZ101	717,517	1,452,957	101.39	86.30 to 85.65
PZ102	717,470	1,453,051	100.44	71.29 to 70.64
PZ103	717,464	1,453,051	100.23	81.20 to 80.55
PZ104	717,467	1,453,056	101.36	91.44 to 90.79

Notes:

1. Horizontal datum is Vermont State Plane, North American Datum 83.
2. Vertical datum is 1988 North American Vertical Datum (NAVD88).

**TABLE 3-1
SEDIMENT CLASSIFICATION RESULTS**

**NAPL INVESTIGATION REPORT
PINE STREET CANAL SUPERFUND SITE
BURLINGTON, VERMONT**

Table 3-1a Sediment Classification Results from the Spring Investigation								
Boring and Sample Number	Depth Interval in Feet	Soil Description	Water Content ¹ (%)	Bulk (wet) Density ² (pcf)	Dry Density ³ (pcf)	Liquid Limit (LL)	Plastic Limit (PL)	Organic Content (%)
CB-02 S-4	12 to 14	Peat	253	66.1	18.7	NV	NP	26
CB-02 S-6	17 to 19	Silt with organic material	56	102.5	65.7	26	27	--
CB-02 S-8	27 to 29	Clayey Silt	32	133.9	101.4	20	18	--
CB-06 S-1	0 to 2	Silty fine Sand	18	126.1	106.9	NV	NP	--
CB-06 S-2	4 to 6	Sandy, clayey, Organic Silt	156	75.6	29.5	132	71	--
CB-06 S-6	10 to 12	Peat	346	61.3	13.7	NV	NP	64
CB-07 S-2	4 to 6	Organic Silt	161	58	22.2	NV	NP	26
CB-07 S-3	8 to 10	Peat	557	71.6	10.9	NV	NP	92
CB-07 S-5	14 to 16	Sandy, clayey Silt with organic material	63	103.9	63.7	41	31	--
CB-08 S-1	4 to 6	Organic Silt	259	60.1	16.7	NV	NP	57
Composite 1 ⁴	25 to 27, 21.5 to 23.5	Clayey Silt and silty Clay	28	126	98.4	20	20	--
Composite 2 ⁵	15 to 17, 16 to 18, 13 to 15	Clayey Silt to silty Clay with lenses or interbedding silty fine sand	29	113.5	88.0	NV	NP	5

**TABLE 3-1
SEDIMENT CLASSIFICATION RESULTS**

**NAPL INVESTIGATION REPORT
PINE STREET CANAL SUPERFUND SITE
BURLINGTON, VERMONT**

Table 3-1b Sediment Classification Results from the Winter Investigation								
Boring and Sample Number	Depth Interval in Feet	Soil Description	Water Content ¹ (%)	Bulk (wet) Density ² (pcf)	Dry Density ³ (pcf)	Liquid Limit (LL)	Plastic Limit (PL)	Organic Content in Percent
CB-101 S-4	6 to 8	Peat	--	76	--	--	--	--
CB-101 S-11	20 to 22	Slightly sandy Silt	53	--	--	33	30	--
CB-100 S-11	20 to 22	Silt	27	--	--	21	18	--
CB-104 S-2	2 to 4	Slightly gravelly, silty Sand	32	--	--	NV	NP	--
CB-104 S-12	22 to 24	Silty, medium to fine Sand	20	--	--	NV	NP	--
CB-120 S-8	14 to 16	Sandy Silt	20	--	--	16	NP	--
CB-120 S-10	18 to 20	Clayey Silt	28	--	--	22	18	--
CB-125 S-9	16 to 18	Very sandy Silt	41	--	--	28	24	--
CB-125 S-11	20 to 22	Clayey, very sandy Silt	26	--	--	NV	NP	--
CB-125 S-13	24 to 26	Silt	32	--	--	22	20	--
CB-130 S-12	22 to 24	Very sandy Silt	35	--	--	NV	NP	--
CB-130 S-14	26 to 28	Clayey Silt	22	100.2	82.1	18	13	--
CB-131 S-2	2 to 4	Clay-Silt (Bank Soil)	25	137.8	110.2	28	21	--
CB-131 S-10	18 to 20	Silty fine Sand	31	--	--	NV	NP	--
CB-131 S-13	26 to 28	Silt	27	--	--	22	19	--

**TABLE 3-1
SEDIMENT CLASSIFICATION RESULTS**

**NAPL INVESTIGATION REPORT
PINE STREET CANAL SUPERFUND SITE
BURLINGTON, VERMONT**

Table 3-1c Sediment Classification Summary Results								
Boring and Sample Number	Depth Interval in Feet	Soil Description	Water Content ¹ (%)	Bulk (wet) Density ² (pcf)	Dry Density ³ (pcf)	Liquid Limit (LL)	Plastic Limit (PL)	Organic Content in Percent
CB-06 S-1	0 to 2	Silty fine Sand	18	126.1	106.9	NV	NP	--
Average Values		Sand Cap	18*	126.1	106.9	--	--	--
CB-07 S-2	4 to 6	Organic Silt	161	58	22.2	NV	NP	26
CB-08 S-1	4 to 6	Organic Silt	259	60.1	16.7	NV	NP	57
CB-06 S-2	4 to 6	Sandy, clayey, Organic Silt	156	75.6	29.5	132	71	--
Average Values		Organic Silt	192	65	22.8	--	--	42
CB-02 S-4	12 to 14	Peat	253	66.1	18.7	NV	NP	26
CB-101 S-4	6 to 8	Peat	--	76	--	--	--	--
CB-06 S-6	10 to 12	Peat	346	61.3	13.7	NV	NP	64
CB-07 S-3	8 to 10	Peat	557	71.6	10.9	NV	NP	92
Average Values		Peat	385	69	14	--	--	61
CB-131 S-10	18 to 20	Silty fine Sand	31	--	--	NV	NP	--
CB-104 S-12	22 to 24	Silty, medium to fine Sand	20	--	--	NV	NP	--
CB-120 S-8	14 to 16	Sandy Silt	20	--	--	16	NP	--
CB-101 S-11	20 to 22	Slightly sandy Silt	53	--	--	33	30	--
CB-125 S-9	16 to 18	Very sandy Silt	41	--	--	28	24	--
CB-125 S-11	20 to 22	Clayey, very sandy Silt	26	--	--	NV	NP	--
CB-130 S-12	22 to 24	Very sandy Silt	35	--	--	NV	NP	--
Average Values		Stratified Silt and Sand	32	--	--	--	--	--

**TABLE 3-1
SEDIMENT CLASSIFICATION RESULTS**

**NAPL INVESTIGATION REPORT
PINE STREET CANAL SUPERFUND SITE
BURLINGTON, VERMONT**

Table 3-1c Sediment Classification Summary Results								
Boring and Sample Number	Depth Interval in Feet	Soil Description	Water Content ¹ (%)	Bulk (wet) Density ² (pcf)	Dry Density ³ (pcf)	Liquid Limit (LL)	Plastic Limit (PL)	Organic Content in Percent
CB-125 S-13	24 to 26	Silt	32	--	--	22	20	--
CB-100 S-11	20 to 22	Silt	27	--	--	21	18	--
CB-131 S-13	26 to 28	Silt	27	--	--	22	19	--
CB-02 S-6	17 to 19	Silt with organic material	56	102.5	65.7	26	27	--
Average Values		Silt	36	103	65.7	23	21	--
CB-07 S-5	14 to 16	Sandy, clayey Silt with organic material	63	103.9	63.7	41	31	--
CB-02 S-8	27 to 29	Clayey Silt	32	133.9	101.4	20	18	--
CB-120 S-10	18 to 20	Clayey Silt	28	--	--	22	18	--
CB-130 S-14	26 to 28	Clay-Silt (Clayey Silt)	22	100.2	82.1	18	13	--
Average Values		Clayey Silt	36	113	82	25	20	--
CB-131 S-2	2 to 4	Clay-Silt (Clayey Silt)	25	137.8	110.2	28	21	--
Average Values		Bank Soil	25	138	110	28	21	--

Notes:

NV= No Value.

NP= Non-Plastic.

pcf = pounds per cubic foot.

-- = not analyzed.

Average values are in bold

*Average (arithmetic) value for a single boring depth

1. The water content is as received (initial/before). The water content data is reported on the grain size distribution and hydraulic conductivity laboratory reports in Appendix G.

2. The bulk (wet) density was determined by measuring the weight of the Shelby tube alone, the weight of the tube with the soil, and the volume of the soil. The data is from the bulk density data tables (Pages G-9 and G-41 of Appendix G).

3. Dry density was calculated from the moisture content and bulk (wet) density using the following formula:

$$\text{dry density} = \text{bulk (wet) density} / (1 + \text{water content})$$

4. Composite 1 is composed of two samples (CB-02 S-7 and CB-07 S-7).

5. Composite 2 is composed of three samples (CB-02 S-5, CB-07 S-6, and CB-10 S-6).

6. The geotechnical laboratory report is included in Appendix G.

**TABLE 3-2
ESTIMATED FLUID EXPELLED FROM CAP SURFACE FROM 2003 TO 2006**

**NAPL INVESTIGATION REPORT
PINE STREET CANAL SUPERFUND SITE
BURLINGTON, VERMONT**

Station	Last Survey Date	Settlement through 2003 (ft)	Estimated Volume of Fluid Expelled per Area of Cap Surface through 2003 (ft³/ft²)	Extrapolated Settlement through October 2006 (ft)	Estimated Volume of Fluid Expelled per Area of Cap Surface through October 2006 (ft³/ft²)
T08+50 W	7/1/2003	2.6	1.7	4.0	2.8
T08+50 C	10/8/2003	2.2	1.4	3.5	2.2
T08+50 E	3/22/2003	1.1	0.7	--	--
T10+50 W	10/28/2003	2.7	1.7	4.0	2.5
T10+50 C	10/28/2003	2.4	1.5	3.4	2.2
T10+50 E	3/22/2003	1.7	1.1	--	--
T12+50 W	4/10/2003	1.0	0.6	--	--
T12+50 C	10/28/2003	1.6	1.0	2.1	1.4
T12+50 E	10/25/2003	1.2	0.8	1.5	1.0

Notes:

ft = feet

-- = not measured

**TABLE 3-3
SEDIMENT HYDRAULIC CONDUCTIVITY TESTING RESULTS**

**NAPL INVESTIGATION REPORT
PINE STREET CANAL SUPERFUND SITE
BURLINGTON, VERMONT**

Table 3-3a Sediment Hydraulic Conductivity Testing Results from Under the Canal				
Boring and Sample Number	Depth Interval (ft)	Soil Description	Permeability, K (cm/s)	Permeability, K (ft/day)
CB-02 S-4	12 to 14	Peat	3.12E-06	8.84E-03
CB-02 S-6	17 to 19	Silt with organic material	2.49E-06	7.06E-03
CB-02 S-8	27 to 29	Clayey Silt	2.70E-07	7.65E-04
CB-06 S-1	0 to 2	Silty fine Sand	2.15E-03	6.09E+00
CB-06 S-2	4 to 6	Sandy, clayey, Organic Silt	6.20E-07	1.76E-03
CB-06 S-6	10 to 12	Peat	1.20E-05	3.40E-02
CB-07 S-2	4 to 6	Organic Silt	8.10E-05	2.30E-01
CB-07 S-3	8 to 10	Peat	6.81E-06	1.93E-02
CB-07 S-5	14 to 16	Sandy, clayey Silt with organic material	1.64E-06	4.65E-03
CB-08 S-1	4 to 6	Organic Silt	9.20E-04	2.61E+00

Table 3-3b Sediment Hydraulic Conductivity Testing Results from the Canal Banks				
Boring and Sample Number	Depth Interval (ft)	Soil Description	Permeability, K (cm/s)	Permeability, K (ft/day)
CB-131 S-2	2 to 4	Clayey Silt	3.20E-06	9.06E-03
CB-101 S-4	6 to 8	Peat	1.53E-04	4.33E-01
CB-130 S-14	26 to 28	Clayey Silt	1.60E-07	4.53E-04

**TABLE 3-3
SEDIMENT HYDRAULIC CONDUCTIVITY TESTING RESULTS**

**NAPL INVESTIGATION REPORT
PINE STREET CANAL SUPERFUND SITE
BURLINGTON, VERMONT**

Table 3-3c Summary of Sediment Hydraulic Conductivity Testing Results				
Boring and Sample Number	Depth Interval (ft)	Soil Description	Permeability, K (cm/s)	Permeability, K (ft/day)
CB-06 S-1	0 to 2	Silty fine Sand	2.15E-03	6.09E+00
Average Values		Sand Cap	Arithmetic mean	6.09*
CB-08 S-1	4 to 6	Organic Silt	9.20E-04	2.61E+00
CB-06 S-2	4 to 6	Sandy, clayey, Organic Silt	6.20E-07	1.76E-03
CB-07 S-2	4 to 6	Organic Silt	8.10E-05	2.30E-01
Average Values		Organic Silt	Arithmetic mean	9.47E-01
			Geometric mean	1.02E-01
CB-02 S-4	12 to 14	Peat	3.12E-06	8.84E-03
CB-06 S-6	10 to 12	Peat	1.20E-05	3.40E-02
CB-07 S-3	8 to 10	Peat	6.81E-06	1.93E-02
CB-101 S-4	6 to 8	Peat	1.53E-04	4.33E-01
Average Values		Peat	Arithmetic mean	1.24E-01
			Geometric mean	3.98E-02

**TABLE 3-3
SEDIMENT HYDRAULIC CONDUCTIVITY TESTING RESULTS**

**NAPL INVESTIGATION REPORT
PINE STREET CANAL SUPERFUND SITE
BURLINGTON, VERMONT**

Table 3-3c Summary of Sediment Hydraulic Conductivity Testing Results				
Boring and Sample Number	Depth Interval (ft)	Soil Description	Permeability, K (cm/s)	Permeability, K (ft/day)
CB-02 S-6	17 to 19	Silt with organic material	2.49E-06	7.06E-03
CB-07 S-5	14 to 16	Sandy, clayey Silt with organic material	1.64E-06	4.65E-03
Average Values		Stratified Silt and Sand	Arithmetic mean	5.86E-03
			Geometric mean	5.73E-03
CB-02 S-8	27 to 29	Clayey Silt	2.70E-07	7.65E-04
CB-130 S-14	26 to 28	Clayey Silt	1.60E-07	4.53E-04
Average Values		Clayey Silt	Arithmetic mean	6.09E-04
			Geometric mean	5.89E-04
CB-131 S-2	2 to 4	Clay-Silt (Bank Soil)	3.20E-06	9.06E-03
Average Values		Bank Soil	Arithmetic mean	9.06E-03*

Notes:

K = permeability

cm/s = centimeters per second

ft/day = feet per day

*Average (arithmetic) value for a single boring depth

**TABLE 3-4
HYDRAULIC PARAMETERS FROM PREVIOUS INVESTIGATIONS**

**NAPL INVESTIGATION REPORT
PINE STREET CANAL SUPERFUND SITE
BURLINGTON, VERMONT**

Stratigraphic Unit	Average In-Situ Hydraulic Conductivity (ft/day)¹	Average Laboratory Hydraulic Conductivity (ft/day)¹	Vertical Hydraulic Gradient Direction	Horizontal Hydraulic Gradient (ft/ft)	General Horizontal Hydraulic Gradient Direction
Bank Soil	0.65	--	--	0.0067-0.0360	west
Bank Soil/Peat	0.2	0.002	variable	0.007-0.01	west
Peat	0.3	--	variable	--	--
Upper Silt/Clay	0.24	0.13	upward	0.008-0.016	northwest
Lower Silt/Clay	0.32	--	upward	0.004	north

Notes:

ft = foot

-- = not evaluated for this unit

1. Averages of hydraulic conductivities from Metcalf and Eddy (1992) and Perkins-Jordan (1984).

**TABLE 3-5
CAP SETTLEMENT PLATE RESULTS**

**NAPL INVESTIGATION REPORT
PINE STREET CANAL SUPERFUND SITE
BURLINGTON, VERMONT**

Date	Elevation in Feet ¹												
	SP-01	SP-02	SP-03	SP-04	SP-05	SP-06	SP-07	SP-08	SP-09	SP-10	SP-11	SP-12	SP-13
5/22/2006	10.50	9.78	9.04	10.06	7.15	10.91	9.51	10.31	8.81	8.51	10.52	9.12	9.38
5/23/2006	10.52	9.79	9.06	10.08	7.17	10.92	9.53	10.32	8.82	8.52	10.53	9.12	9.39
5/24/2006	10.50	9.76	9.03	10.06	7.15	10.90	9.50	10.31	8.80	8.51	10.52	9.11	9.37
5/25/2006	10.50	9.78	9.04	10.07	7.16	10.90	9.51	10.31	8.80	8.50	10.51	9.10	9.37
5/31/2006	10.50	9.76	9.03	10.07	7.15	10.90	9.51	10.31	8.80	8.50	10.52	9.10	9.37
6/8/2006	10.49	9.75	9.02	10.06	7.13	10.89	9.50	10.30	8.79	8.49	10.51	9.10	9.36
6/21/2006	10.48	9.75	9.02	10.07	7.13	10.89	9.50	10.30	8.78	8.47	10.51	9.09	9.35
8/5/2006	10.49	9.75	9.04	10.07	7.13	10.91	9.52	10.30	8.78	8.48	10.51	9.10	9.37
8/25/2006	10.51	9.77	8.94	10.06	7.14	10.94	9.53	10.31	8.80	8.51	10.53	9.13	9.40
9/17/2006	10.47	9.78	9.07	10.06	7.15	10.95	9.54	10.30	8.79	8.50	10.52	9.12	9.39
10/25/2006	10.48	9.76	9.05	10.05	7.12	10.93	9.52	10.30	8.79	8.49	10.52	9.11	9.38

Notes:

1. Elevations are for a given point on the riser pipe of the settlement plate.

**TABLE 3-6
CAP THICKNESS MEASUREMENTS**

**NAPL INVESTIGATION REPORT
PINE STREET CANAL SUPERFUND SITE
BURLINGTON, VERMONT**

Location	Sample ID	Water Depth (ft)	Cap Thickness (ft)
Spring Investigation			
T09+30E30	CP01	4.2	--
T09+48E20	CP02	4.0	1.4
T09+75E15	CP03	4.7	2.7
T09+92E15	CP04	4.7	2.2
T10+37E20	CP05	3.9	2.7
T10+50E20	CP06	2.9	1.2
T10+67E20	CP07	2.4	0.7
T10+76E20	CP08	3.0	1.0
T11+03E25	CP09	3.0	1.9
T10+96E30	CP10	4.9	3.5
T10+76E60	CP11	3.9	2.1
T11+04E20	CP12	3.6	2.1
T11+45E25	CP13	5.1	3.0
T11+70E30	CP14	4.8	2.6
T10+76E40	CP16	3.7	1.7
T09+00E60	TG01	4.3	3.3
T09+00E60	TG01B	4.3	3.3
T09+50E60	TG02	5.0	2.3
T10+00E60	TG03	4.1	2.3
T10+50E60	TG04	4.0	2.1
T11+00E60	TG05	3.4	2.6
T11+50E60	TG06	3.4	2.6
T12+00E60	TG07	3.6	3.5
T12+00E60	TG07B	3.6	3.0
T12+00E60	TG07C	3.6	2.1
T12+50E60	TG08	2.4	2.1
T10+50E40	TG09	3.2	1.7
T12+00E40	TG10	3.8	1.8
T10+75E80	TG11	2.5	2.3
T11+90E40	PZ02	4.3	2.5
T11+90E60	PZ04	4.2	5.5
T10+50E35	PZ06	5.8	2.2
T10+76E32	PZ08	4.3	2.0
Turning Basin	LIFTB2	5.8	5.5
Summer Investigation			
T11+25E50	CP17	5.5	1.1
T11+20E20	CP18	4.5	--
T11+10E15	CP19	4.5	2.8
T11+00E40	CP20	4.2	1.4
T11+05E20	CP21	3.5	1.8
T10+70E20	CP22	2.9	0.8
T10+74E20	CP23	2.8	0.8
T10+75E70	CP24	4.4	1.9
T09+75E20	CP25	3.8	0.9
T09+55E20	CP26	4.2	1.5
T10+50E20	CP27	3.0	0.9

Notes:

-- = Data were not collected

**TABLE 3-7
MONITORING WELL GAUGING DATA**

**NAPL INVESTIGATION REPORT
PINE STREET CANAL SUPERFUND SITE
BURLINGTON, VERMONT**

Location ID	Well Elevation (ft) ¹	Depth to Bottom of Well (ft BTOC) ²	Gauging Time	PID Reading (ppm)	Depth to Water (ft BTOC) ²	Water Elevation ¹ (ft)	Measurable LNAPL detected	Measurable DNAPL detected
MW11A	104.55	12.65	5/2/06 11:00	0.0	7.54	97.01	No	No
			8/14/06 9:40	3.6	7.20	97.35	No	No
			2/2/07 7:35	0.0	7.61	96.94	No	No
MW11B	101.98	23.18	5/2/06 11:05	3.8	5.13	96.85	No	Yes, approx. 11 feet of DNAPL
			8/14/06 9:44	51.7	4.80	97.18	No	Yes, approx. 10 feet of DNAPL
			2/2/07 7:40	2.8	5.14	96.84	No	Yes, 9.4 feet of DNAPL
MW11D					N/A			
MW17	101.33	27.43	5/2/06 12:06	10.7	4.42	96.91	No (sheen present)	No, some DNAPL droplets
			8/14/06 10:57	5.5	3.98	97.35	No, some LNAPL droplets	No, some DNAPL droplets
			2/2/07 8:15	1.7	4.49	96.84	No, some NAPL on tip of probe	No, some NAPL on tip of probe
MW23B	103.19	30.65	5/2/06 11:56	8.0	6.54	96.65	No	No, some DNAPL droplets
			8/14/06 10:48	3.3	6.10	97.09	No	No, some DNAPL droplets
			2/6/07 13:42 ⁽³⁾	1.1	6.81	96.38	No	Yes, 0.1 inches of DNAPL
MW103B	101.35	22.05	5/2/06 10:51	0.0	4.14	97.18	No	No
			8/14/06 9:30	0.0	5.11	96.24	No	No
			2/2/07 7:55	0.0	4.54	96.81	No	No
MW110	102.68	25.78	5/2/06 10:39	0.0	5.87	96.81	No	No
			8/14/06 9:17	2.2	5.36	97.32	No	No
			2/2/07 8:05	0.0	5.86	96.82	No	No
RW9+80	101.69	6.83	5/2/06 13:54	0.0	5.05	96.64	No (sheen present)	No
			8/14/06 10:05	55.7	4.65	97.04	No	No
			2/2/07 8:30	0.0 ⁴	4.92	96.77	No, trace sheen on ice	No
RW10+25	102.23	7.40	5/2/06 14:13	0.0	5.26	96.97	No	No
			8/14/06 10:10	0.0	5.22	97.01	No (film present)	No, trace amount
			2/2/07 8:40	0.0 ⁵	--	--	No, trace sheen on ice	--
RW11	101.96	6.81	5/2/06 14:04	0.4	5.07	96.89	No (sheen present)	No
			8/14/06 10:19	0.0	5.06	96.90	No (sheen present)	No
			2/2/07 8:50	0.0 ⁶	--	--	No	--
RW14	102.04	7.73	5/2/06 14:21	0.7	5.33	96.71	No	Yes, approx. 8 inches of DNAPL
			8/14/06 10:25	0.0	4.96	97.08	No (film present)	Yes, 6 inches on probe
			2/2/07 9:00	3.0	5.40	96.64	No (sheen present)	Yes, 1.0 feet of DNAPL

Notes:

PID = photoionization detector

ppm = parts per million

ft = foot

LNAPL = light nonaqueous-phase liquid

DNAPL = dense nonaqueous-phase liquid

N/A = MW11D not gauged because it had been previously sampled by the Johnson Company and never had detectable PAHs in groundwater samples

-- = data not available

1. Elevations determined from well survey information. Vertical datum is 1988 North American Vertical Datum (NAVD88).

Elevations for wells MW103A, MW110, MW11A, MW17, MW23B, and MW11B are from top of the inner PVC casing.

Elevations for wells RW14, RW11, RW10, and RW9 are from top of casing.

2. BTOC = below top of casing. Field measurements were taken below top of outer casing.

3. Due to deep snow, MW-23B had to be located with a metal detector and was not gauged until 2/6/07.

4. Water in top of well RW9+80 was frozen and field personnel broke through 3 inches of ice to take measurements. Trace sheen was observed on ice.

5. Water in well RW10+25 frozen at 5.2 feet below top of casing.

6. Water in well RW11 frozen at 4.75 feet below top of casing.

**TABLE 3-8
GROUNDWATER VERTICAL GRADIENTS**

**NAPL INVESTIGATION REPORT
PINE STREET CANAL SUPERFUND SITE
BURLINGTON, VERMONT**

Shallower Stratigraphic Unit	Deeper Stratigraphic Unit	Vertical Hydraulic Gradient Direction	Minimum Vertical Hydraulic Gradient (ft/ft)¹	Maximum Vertical Hydraulic Gradient (ft/ft)¹	Average Vertical Hydraulic Gradient (ft/ft)¹
Shallow organic silt/sediment (PZ6)	Deep organic silt/sediment (PZ8)	variable	-0.28	0.26	0.00031
Deep organic silt/sediment (PZ8)	Clayey silt (PZ7)	upward	-0.18	-0.035	-0.052

Notes:

ft = foot

1. Negative vertical hydraulic gradient values indicate upward groundwater flow, positive hydraulic gradient values indicated downward groundwater flow

**TABLE 3-9
NAPL CHEMISTRY RESULTS**

**NAPL INVESTIGATION REPORT
PINE STREET CANAL SUPERFUND SITE
BURLINGTON, VERMONT**

BBL Sample ID: MW-11B Lab Sample ID: WW2124-1 Sampling Date: 5/02/2006	RW14 WW2124-2 5/02/2006	
PAHs in mg/kg		
2-Methylnaphthalene	36,000	31,000
Acenaphthene	12,000	14,000
Acenaphthylene	1,500 J	3,300
Anthracene	6,100 J	7,500 J
Benzo(a)anthracene	2,500	3,500
Benzo(a)pyrene	1,700 J	2,600
Benzo(b)fluoranthene	1,600 J	2,200
Benzo(k)fluoranthene	2,000 U	2,000 U
Benzo(g,h,i)perylene	2,000 U	2,000 U
Chrysene	2,400	3,300
Dibenzo(a,h)anthracene	2,000 U	2,000 U
Fluoranthene	4,000	6,000
Fluorene	6,400	8,200
Indeno(1,2,3-cd)pyrene	2,000 U	2,000 U
Naphthalene	39,000	38,000
Phenanthrene	16,000 J	18,000 J
Pyrene	6,300	9,400
Total PAHs ^{1,2}	135,500	147,000
Volatiles in µg/kg		
Benzene	460,000 J	890,000 J
Toluene	1,000,000 J	2,300,000
Ethylbenzene	2,500,000	3,900,000
m-,p-Xylene	2,500,000 J	3,000,000
o-Xylene	1,100,000 J	1,500,000
Xylenes (Total)	3,600,000 J	4,600,000

Notes:

U = Compound was not detected. Value is the detection limit.

J = Estimated value.

mg/kg = milligrams per kilogram.

µg/kg = micrograms per kilogram.

PAH = polycyclic aromatic hydrocarbon.

1. Total concentrations are calculated using the detected concentrations of individual constituents.

Non-detects are treated as zeros. If all the individual constituents are non-detect the total concentration is reported as non-detect using the highest detection limit.

2. The total PAHs is the sum of all the PAHs listed in the table.

**TABLE 3-10
NAPL PHYSICAL PROPERTIES**

**NAPL INVESTIGATION REPORT
PINE STREET CANAL SUPERFUND SITE
BURLINGTON, VERMONT**

	MW-11B 10°C	MW-11B 20°C	RW14 10°C	RW14 20°C
Density in grams/milliliter	1.0549	1.0532	1.0676	1.0649
Viscosity in centiStokes	120.13	60.30	104.38	69.10
Viscosity in centiPoise	126.72	63.47	111.43	73.59
Interfacial Tension in milliNewton/meter	23.12	23.46	22.75	22.87

**TABLE 3-11
SURFACE WATER OBSERVATION DATA FROM THE SPRING INVESTIGATION**

**NAPL INVESTIGATION REPORT
PINE STREET CANAL SUPERFUND SITE
BURLINGTON, VERMONT**

Transect	Time	Approximate Distance from West Bank (ft)	Number of Seeps	Rate of NAPL Seep (droplets/ 30 sec)	Diameter of Sheen (in)
T09+30	1350	20	3	NA	NA
T10+00	1359	10	1	NA	NA
T10+50	1404	20	1	NA	NA
T10+70	1406	20	1	4	12
T10+65	1408	15	1	1	12
T11+00	1411	20	3	6 and 2	12
T11+50	1421	15	2	1	12
T12+00	1426	3 and 30	2	NA	NA
T13+00	1435	3	1	NA	NA
T13+50	1438	5	5	NA	NA
T14+00	1445	5	6	NA	NA
T14+20	1514	50	1	NA	NA

Notes:

ft = feet

in = inches

sec = seconds

NA = not applicable because gas bubbles with no associated NAPL were observed.

TABLE 3-12
SURFACE WATER OBSERVATION DATA FROM THE SUMMER INVESTIGATION

NAPL INVESTIGATION REPORT
PINE STREET CANAL SUPERFUND SITE
BURLINGTON, VERMONT

Location	Time	Bubbling Rate (bubbles/min)	NAPL Droplets			Consistency ³		Seep Sampling			Qualitative Description of Seep ¹
			Present? (Y/N) ¹	Rate (droplets/min)	Diameter of droplet (in) ²	Active Time	Dormant Time	Sampled? (Y/N) ⁴	Number of Droplets	Sample Time (sec) ⁵	
T09+40E20	1305	215	N	--	--	--	--	N	--	--	No associated sheen
T09+50E20	1257	290	N	--	--	--	--	N	--	--	No associated sheen
T09+55E20	1315	185	Y	3	1/8 in	intermittent		Y - SW05	20	10	NAPL and sheen on some bubbles
T09+75E20	1320	230	N	--	--	intermittent		Y - SW06	20	10	Sheen on surface
T10+50E20	1420	270	Y	--	--	continuous		Y - SW15	20	--	Each bubble gives off NAPL sheen
T10+65E20	1327	80	Y	40	1/8 in	40 sec	20 sec	Y - SW07	20	30	
T10+70E20	1330	80	Y	9	3/16 in	8-15 sec	10-20 sec	Y - SW14	20	--	Sheen on bubbles, 1-2 / 10 bubbles with NAPL - others only gas
T10+75E30	1544	55	Y	11		intermittent		Y - SW19	20	20	All gas bubbles had sheen, brown droplets at rate of 11/min
T10+75E35	1508	195	Y	17	1/8 in	intermittent		Y - SW17	20	60	Brown NAPL blobs
T10+75E70	1435	5	Y	5	1/8 in	--	--	Y - SW16	20	180	Brown NAPL
T11+00E40	1337	14	Y	14	1/16 in	intermittent		Y - SW08	20	10	
T11+00E40	1346	75	Y	75	1/16 in	intermittent		Y - SW09	20	300	Part of sample time spent positioning boat
T11+05E20	1230	22	Y	22	<1/4 in	20 sec	20 sec	Y - SW13	8	60	Non-dispersive brown droplets on water surface
T11+10E40	1355	91	Y	91	1/8 in	intermittent		Y - SW10	20	180	
T11+20E20	1030	27	Y	27	3/16 in	continuous		Y - SW12	20	60	Dark bubbles hit surface - delay in dispersal for few seconds
T11+20E30	1545	45	Y	25	<1/8 in	--	--	Y - SW18	20	20	NAPL droplets smaller than 1/8 in, clear bubbles bigger
T11+25E50	1405	70	Y	10	1/4 in	intermittent		Y - SW11	20	60	

Notes:

in = inches

min = minutes

sec = seconds

1. All NAPL droplets were light (LNAPL). "Light" means NAPL droplets rise to water surface. "Dense" means NAPL droplets sink to top of cap.
2. Diameter of NAPL droplet as it rises through water column (if it's possible to observe this) or the diameter of droplet at the surface of the water.
3. Describes whether seep and/or gas bubbling is consistent during a couple of minutes of observation or if it is intermittent.
4. Seep samples collected at or near water surface because of limited visibility.
5. Time it takes to collect seep sample (i.e., droplets).

**TABLE 3-13
CAP SWAB DETAILS**

**NAPL INVESTIGATION REPORT
PINE STREET CANAL SUPERFUND SITE
BURLINGTON, VERMONT**

Sample ID	Area	Qualitative Amount of NAPL	Sample Notes ¹
Spring Investigation			
PSC-T10+67E20-CS01	1 square meter	Visible NAPL - Saturated	
PSC-T10+76E20-CS02	1 square meter	Visible NAPL - Saturated	
PSC-T10+96E30-CS03	1 square meter	Visible NAPL - Saturated	
PSC-T11+04E20-CS04	1 square meter	Visible NAPL - Saturated	
PSC-T10+98E40-CS05	1 square meter	Visible NAPL - Saturated	
PSC-T11+04E20-CS06	Vegetation on top of cap	Visible NAPL - Saturated	
PSC-T10+67E20-CS07	1/9 square meter	Visible NAPL - Unsaturated	
PSC-T10+67E20-CS08	1/3 square meter	Visible NAPL - Unsaturated	
PSC-T10+76E20-CS09	1/9 square meter	Visible NAPL - Unsaturated	
Summer Investigation			
PSC-T09+00E20-CS10	1 square meter	Appeared clean	HOLD
PSC-T09+00E40-CS11	1 square meter	Appeared clean	HOLD
PSC-T09+00E60-CS12	1 square meter	Appeared clean	
PSC-T09+50E20-CS13	1 square meter	Appeared clean	
PSC-T09+50E40-CS14	1 square meter	Appeared clean	HOLD
PSC-T09+50E60-CS15	1 square meter	Appeared clean	
PSC-T10+00E20-CS16	1 square meter	Visible NAPL - Unsaturated	
PSC-T10+00E40-CS17	1 square meter	Visible NAPL - Unsaturated	
PSC-T10+00E60-CS18	1 square meter	Appeared clean	
PSC-T10+50E40-CS19	1 square meter	Visible NAPL - Unsaturated	
PSC-T10+50E60-CS20	1 square meter	Visible NAPL - Unsaturated	
PSC-T11+00E60-CS21	1 square meter	Visible NAPL - Unsaturated	
PSC-T11+50E20-CS22	1 square meter	Appeared clean	HOLD
PSC-T11+50E40-CS23	1 square meter	Appeared clean	
PSC-T11+50E60-CS24	1 square meter	Appeared clean	HOLD
PSC-T12+00E20-CS25	1 square meter	Appeared clean	
PSC-T12+00E40-CS26	1 square meter	Visible NAPL - Unsaturated	
PSC-T12+00E60-CS27	1 square meter	Visible NAPL - Unsaturated	
PSC-T12+50E20-CS28	1 square meter	Appeared clean	HOLD
PSC-T12+50E40-CS29	1 square meter	Appeared clean	HOLD
PSC-T12+50E60-CS30	1 square meter	Appeared clean	HOLD
PSC-T09+55E20-CS31	1 square meter	Visible NAPL - Unsaturated	
PSC-T09+75E20-CS32	1 square meter	Visible NAPL - Unsaturated	
PSC-T10+65E20-CS33	1 square meter	Visible NAPL - Saturated	
PSC-T11+00E40-CS34	1 square meter	Visible NAPL - Saturated	
PSC-T11+00E40-CS35	1 square meter	Visible NAPL - Saturated	
PSC-T11+25E50-CS36	1 square meter	Visible NAPL - Unsaturated	
PSC-T10+75E70-CS37	1 square meter	Visible NAPL - Unsaturated	
PSC-T11+05E20-CS38	1 square meter	Visible NAPL - Unsaturated	

Notes:

1. HOLD = Selected samples that appeared clean were archived at Katahdin Analytical Services of Scarborough, Maine.

**TABLE 3-14
CAP SWAB CHEMISTRY RESULTS**

**NAPL INVESTIGATION REPORT
PINE STREET CANAL SUPERFUND SITE
BURLINGTON, VERMONT**

BBL Sample ID:	T10+67E20 CS01	T10+76E20 CS02	T10+96E30 CS03	T11+04E20 CS04	T10+98E40 CS05	T11+04E20 CS06	T10+67E20 CS07	T10+67E20 CS08
Lab Sample ID:	WW2167-1	WW2167-2	WW2167-3	WW2167-4	WW2167-5	WW2167-6	WW2167-7	WW2167-8
Sampling Date:	5/03/2006	5/03/2006	5/03/2006	5/03/2006	5/03/2006	5/03/2006	5/04/2006	5/04/2006
PAHs in µg/wipe								
2-Methylnaphthalene	130,000	140,000	300,000	270,000	270,000	4,500	12,000	17,000
Acenaphthene	44,000	35,000	93,000	73,000	51,000	1,300	3,600	5,300
Acenaphthylene	9,600 J	14,000 J	17,000 J	26,000	29,000	480 J	1,800	2,100
Anthracene	34,000 J	39,000 J	56,000 J	48,000 J	44,000 J	1,100 J	3,800 J	6,100 J
Benzo(a)anthracene	15,000	16,000 J	23,000	19,000	18,000	500 J	1,600	2,500
Benzo(a)pyrene	11,000	11,000 J	15,000 J	13,000 J	13,000 J	330 J	1,200	1,900 J
Benzo(b)fluoranthene	9,600 J	11,000 J	16,000 J	11,000 J	11,000 J	330 J	1,000	1,600 J
Benzo(k)fluoranthene	10,000 U	20,000 U	20,000 U	15,000 U	15,000 U	500 U	1,000 U	2,000 U
Benzo(g,h,i)perylene	10,000 U	20,000 U	20,000 U	15,000 U	15,000 U	500 U	1,000 U	2,000 U
Chrysene	14,000	15,000 J	23,000	18,000	16,000	490 J	1,600	2,300
Dibenzo(a,h)anthracene	10,000 U	20,000 U	20,000 U	15,000 U	15,000 U	500 U	1,000 U	2,000 U
Fluoranthene	27,000	29,000	42,000	32,000	31,000	810	3,100	4,500
Fluorene	34,000	35,000	60,000	52,000	49,000	1,000	3,900	5,600
Indeno(1,2,3-cd)pyrene	10,000 U	20,000 U	20,000 U	15,000 U	15,000 U	500 U	1,000 U	2,000 U
Naphthalene	55,000	68,000	250,000	290,000	200,000	3,300	4,100	5,200
Phenanthrene	98,000 J	120,000 J	160,000 J	130,000 J	130,000 J	3,100 J	11,000 J	17,000 J
Pyrene	42,000	47,000	63,000	56,000	54,000	1,200	5,200	8,100
Total PAHs ^{1,2}	523,200	580,000	1,118,000	1,038,000	916,000	18,440	53,900	79,200
TPH in µg/wipe	2,700,000	180,000	5,800,000	4,000,000	3,600,000	100,000	300,000	500,000

**TABLE 3-14
CAP SWAB CHEMISTRY RESULTS**

**NAPL INVESTIGATION REPORT
PINE STREET CANAL SUPERFUND SITE
BURLINGTON, VERMONT**

BBL Sample ID:	T10+76E20 CS09	T09+00E60 CS12	T09+50E20 CS13	T09+50E60 CS15	T10+00E20 CS16	T10+00E40 CS17	T10+00E60 CS18	T10+50E40 CS19
Lab Sample ID:	WW2167-9	WW4274-1	WW4274-2	WW4274-3	WW4274-4	WW4274-5	WW4274-6	WW4274-7
Sampling Date:	5/04/2006	8/15/2006						
PAHs in µg/wipe								
2-Methylnaphthalene	42,000	4 J	17	10 U	37,000	2,500	10 U	690
Acenaphthene	16,000	62	83	8 J	15,000	960	10 U	830
Acenaphthylene	1,800 J	11	19	7 J	1,500 J	270	10 U	300
Anthracene	8,700 J	63 J	73 J	41 J	8,300 J	780 J	7 J	750 J
Benzo(a)anthracene	3,600	51	62	40	3,800	360	8 J	480 J
Benzo(a)pyrene	2,800	41	51	34	2,700	300	7 J	370 J
Benzo(b)fluoranthene	2,200 J	36	45	31	2,300	210 J	7 J	290 J
Benzo(k)fluoranthene	2,500 U	15 J	19 J	14 J	1,200 J	250 U	10 U	140 J
Benzo(g,h,i)perylene	2,500 U	20	18	15	2,000 U	250 U	10 U	140 J
Chrysene	3,600	49	60	40	3,100	310	7 J	380 J
Dibenzo(a,h)anthracene	2,500 U	10 U	10 U	10 U	2,000 U	250 U	10 U	100 UJ
Fluoranthene	6,600	96 J	110 J	73 J	7,200	640	14 J	1,000
Fluorene	9,100	49	80	14	8,400	610	10 U	1,000
Indeno(1,2,3-cd)pyrene	2,500 U	24	26	19	1,700 J	190 J	10 U	180 J
Naphthalene	37,000	4 J	4 J	10 U	26,000	1,300	4 J	57 J
Phenanthrene	24,000 J	140 J	140 J	94 J	21,000 J	2,200 J	22 J	1,900 J
Pyrene	11,000	120 J	130 J	98 J	10,000 J	860 J	22 J	1,400 J
Total PAHs ^{1,2}	168,400	785	937	528	149,200	11,490	98	9,907
TPH in µg/wipe	850,000	11,000	15,000	8,300	1,300,000	140,000	1,500	150,000

**TABLE 3-14
CAP SWAB CHEMISTRY RESULTS**

**NAPL INVESTIGATION REPORT
PINE STREET CANAL SUPERFUND SITE
BURLINGTON, VERMONT**

BBL Sample ID:	T10+50E60 CS20	T11+00E60 CS21	T11+50E40 CS23	T12+00E20 CS25	T12+00E40 CS26	T12+00E60 CS27	T09+55E20 CS31	T09+75E20 CS32
Lab Sample ID:	WW4274-8	WW4274-9	WW4274-10	WW4274-11	WW4274-12	WW4274-13	WW4274-16	WW4274-17
Sampling Date:	8/15/2006							
PAHs in µg/wipe								
2-Methylnaphthalene	740	64,000	40	10 U	1,800	6,200	7,000	31,000
Acenaphthene	590	16,000	110	48	1,300	1,800	2,900	13,000
Acenaphthylene	48 J	4,100 J	25	11	160 J	850	180 J	1,700 J
Anthracene	400 J	12,000 J	140 J	65 J	1,100 J	1,800 J	1,800 J	7,600 J
Benzo(a)anthracene	210	5,200	100 J	56 J	590	720 J	850	3,400
Benzo(a)pyrene	170	3,600 J	74 J	44 J	480	540 J	600	2,200
Benzo(b)fluoranthene	140	3,200 J	65 J	39 J	420	390 J	480	2,000
Benzo(k)fluoranthene	63 J	5,000 U	31 J	18 J	180 J	800 U	270 J	1,200 J
Benzo(g,h,i)perylene	100 U	5,000 U	28 J	18 J	200 U	800 U	400 U	2,000 U
Chrysene	160	3,700 J	83 J	53 J	500	560 J	680	2,800
Dibenzo(a,h)anthracene	100 U	5,000 U	20 UJ	10 UJ	200 U	800 U	400 U	2,000 U
Fluoranthene	400	9,300	200	100 J	1,300	1,200	1,700 J	6,200
Fluorene	350	11,000	120	57	980	1,500	1,600	7,400
Indeno(1,2,3-cd)pyrene	95 J	5,000 U	39 J	21 J	230	800 U	350 J	2,000 U
Naphthalene	57 J	55,000	7 J	4 J	440	4,100	3,500	22,000
Phenanthrene	1,000 J	34,000 J	310 J	140 J	2,700 J	5,400 J	4,400 J	20,000 J
Pyrene	540 J	14,000 J	250 J	120 J	1,300 J	2,200 J	2,000 J	9,300 J
Total PAHs ^{1,2}	4,963	235,100	1,622	794	13,480	27,260	28,310	129,800
TPH in µg/wipe	63,000	2,000,000	26,000	12,000	160,000	270,000	260,000	1,400,000

**TABLE 3-14
CAP SWAB CHEMISTRY RESULTS**

**NAPL INVESTIGATION REPORT
PINE STREET CANAL SUPERFUND SITE
BURLINGTON, VERMONT**

BBL Sample ID:	T10+65E20 CS33	T11+00E40 CS34	T11+00E40 CS35	T11+25E50 CS36	T10+75E70 CS37	T11+05E20 CS38
Lab Sample ID:	WW4274-19	WW4275-1	WW4275-3	WW4275-6	WW4275-12	WW4275-13
Sampling Date:	8/15/2006	8/15/2006	8/15/2006	8/15/2006	8/17/2006	8/17/2006
PAHs in µg/wipe						
2-Methylnaphthalene	85,000	64,000	280,000	80,000	91	30,000
Acenaphthene	28,000	19,000	68,000	21,000	170	9,700
Acenaphthylene	3,300 J	2,900 J	18,000 J	5,700	26 J	1,800 J
Anthracene	16,000 J	12,000 J	50,000 J	14,000 J	180 J	6,600 J
Benzo(a)anthracene	7,300	5,400	21,000	5,700	100	2,800
Benzo(a)pyrene	5,700	4,000 J	16,000 J	4,100	88	2,200
Benzo(b)fluoranthene	4,100 J	3,200 J	12,000 J	3,600 J	70	1,900 J
Benzo(k)fluoranthene	2,400 J	4,000 U	20,000 U	1,900 J	32 J	2,000 U
Benzo(g,h,i)perylene	5,000 U	4,000 U	20,000 U	4,000 U	50 U	2,000 U
Chrysene	5,600	3,800 J	16,000 J	4,100	84	2,100
Dibenzo(a,h)anthracene	5,000 U	4,000 U	20,000 U	4,000 U	50 U	2,000 U
Fluoranthene	15,000	10,000	43,000	10,000	220	5,200
Fluorene	16,000	12,000	46,000	14,000	140	6,700
Indeno(1,2,3-cd)pyrene	4,000 J	4,000 U	20,000 U	4,000 U	48 J	2,000 U
Naphthalene	69,000	50,000	210,000	66,000	18 J	21,000
Phenanthrene	47,000 J	34,000 J	140,000 J	38,000 J	460 J	18,000 J
Pyrene	17,000 J	13,000 J	51,000 J	18,000 J	240 J	8,600 J
Total PAHs ^{1,2}	325,400	233,300	971,000	286,100	1,967	116,600
TPH in µg/wipe	3,200,000	2,400,000	11,000,000	2,400,000	25,000	1,600,000

Notes:
 U = Compound was not detected.
 Value is the detection limit.
 J = Estimated value.
 µg/wipe = micrograms per wipe
 TPH = total petroleum hydrocarbons
 PAH = polycyclic aromatic hydrocarbons
 1. Total concentrations are calculated using the detected concentrations of individual constituents. Non-detects are treated as zeros. If all the individual constituents are non-detect the total concentration is reported as non-detect using the highest detection limit.
 2. The total PAHs is the sum of all the PAHs listed in the table.

**TABLE 3-15
WATER COLUMN NAPL SEEP CHEMISTRY RESULTS**

**NAPL INVESTIGATION REPORT
PINE STREET CANAL SUPERFUND SITE
BURLINGTON, VERMONT**

BBL Sample ID:	T10+50E20	T10+76E20	T10+76E40	T10+67E20	T09+95E20	T09+75E20	T10+65E20	T11+00E40
Lab Sample ID:	SW01	SW02	SW03	SW04	SW05	SW06	SW07	SW08
Sampling Date:	WW2167-10	WW2167-11	WW2167-12	WW2167-13	WW4274-14	WW4274-15	WW4274-18	WW4274-20
	5/03/2006	5/04/2006	5/04/2006	5/04/2006	8/15/2006	8/15/2006	8/15/2006	8/15/2006
PAHs in µg/wipe								
2-Methylnaphthalene	560	720	1,800	4,800	8 J	82	990	13
Acenaphthene	220	310	440	1,300	27	130	470	21
Acenaphthylene	72	53 J	270	330 J	5 J	14 J	59 J	9 J
Anthracene	150 J	180 J	400 J	940 J	25 J	100 J	290 J	28 J
Benzo(a)anthracene	69	80 J	160	360 J	23	86	130	19
Benzo(a)pyrene	46	62 J	120	200 J	17	72	98 J	15
Benzo(b)fluoranthene	49	55 J	110	190 J	20	70	87 J	14
Benzo(k)fluoranthene	35 J	33 J	64 J	500 U	8 J	28 J	49 J	6 J
Benzo(g,h,i)perylene	40 U	100 UJ	100 U	500 U	10 U	29	100 U	10 U
Chrysene	70	83 J	150	350 J	22	90	110	15
Dibenzo(a,h)anthracene	40 U	100 UJ	100 U	500 U	10 U	20 U	100 U	10 U
Fluoranthene	130	140	310	620	52	220	260	38 J
Fluorene	170	200	440	950	20	110	310	18
Indeno(1,2,3-cd)pyrene	40 U	100 U	100 U	500 U	12	41	100 U	9 J
Naphthalene	250	430	930	4,000	4 J	22	700	7 J
Phenanthrene	410 J	630 J	1,100 J	3,000 J	90 J	330 J	850 J	78 J
Pyrene	180	230	460	1,100	63 J	210 J	370 J	47 J
Total PAHs ^{1,2}	2,411	3,206	6,754	18,140	396	1,634	4,773	337
TPH in µg/wipe	20,000	26,000	45,000	100,000	5,000	20,000	42,000	4,000

**TABLE 3-15
WATER COLUMN NAPL SEEP CHEMISTRY RESULTS**

**NAPL INVESTIGATION REPORT
PINE STREET CANAL SUPERFUND SITE
BURLINGTON, VERMONT**

BBL Sample ID:	T11+00E40	T11+10E20	T11+25E50	T11+20E20	T11+05E20	T10+70E20	T10+50E20	T10+75E70
Lab Sample ID:	SW09	SW10	SW11	SW12	SW13	SW14	SW15	SW16
Sampling Date:	WW4275-2	WW4275-4	WW4275-5	WW4275-9	WW4275-10	WW4275-11	WW4275-7	WW4275-8
	8/15/2006	8/15/2006	8/15/2006	8/16/2006	8/16/2006	8/16/2006	8/16/2006	8/16/2006
PAHs in µg/wipe								
2-Methylnaphthalene	780	51	1,400	10 U	28	10 U	9 J	670
Acenaphthene	300	93	300	10 U	35	10 U	16	390
Acenaphthylene	99	22	400	3 J	11	10 U	4 J	29 J
Anthracene	220 J	57 J	360 J	7 J	36 J	10 U	19 J	210 J
Benzo(a)anthracene	100	37	170	13	21	10 U	12	120
Benzo(a)pyrene	82	28	130	12	16	10 U	9 J	98
Benzo(b)fluoranthene	66	22	95 J	11	14	10 U	8 J	84
Benzo(k)fluoranthene	33 J	11 J	60 J	5 J	6 J	10 U	10 U	42 J
Benzo(g,h,i)perylene	42 J	12	100 U	10 U	10 U	10 U	10 U	50 U
Chrysene	90	31	130	13	17	10 U	10 J	100
Dibenzo(a,h)anthracene	50 U	10 U	100 U	10 U	10 U	10 U	10 U	50 U
Fluoranthene	200	75	300	27	44	10 U	20	260
Fluorene	250	64	390	3 J	24	10 U	11	210
Indeno(1,2,3-cd)pyrene	50	16	100 U	8 J	11	10 U	10 U	52
Naphthalene	360	14	740	4 J	12	10 U	4 J	300
Phenanthrene	570 J	140 J	1,000 J	36 J	99 J	10 U	60 J	550 J
Pyrene	310 J	77 J	510 J	36 J	48 J	10 U	35 J	280 J
Total PAHs ^{1,2}	3,552	750	5,985	178	422	10 U	217	3,395
TPH in µg/wipe	34,000	9,100	53,000	2,600	5,100	570	3,400	43,000

**TABLE 3-15
WATER COLUMN NAPL SEEP CHEMISTRY RESULTS**

**NAPL INVESTIGATION REPORT
PINE STREET CANAL SUPERFUND SITE
BURLINGTON, VERMONT**

BBL Sample ID:	T10+75E35 SW17	T11+20E30 SW18	T10+75E30 SW19
Lab Sample ID:	WW4275-14	WW4275-15	WW4275-16
Sampling Date:	8/17/2006	8/17/2006	8/17/2006
PAHs in µg/wipe			
2-Methylnaphthalene	5 J	130	16
Acenaphthene	7 J	95	32
Acenaphthylene	4 J	25	5 J
Anthracene	14 J	74 J	27 J
Benzo(a)anthracene	10 J	35	17
Benzo(a)pyrene	8 J	25	13
Benzo(b)fluoranthene	8 J	22	12
Benzo(k)fluoranthene	10 U	12 J	5 J
Benzo(g,h,i)perylene	10 U	20 U	10 U
Chrysene	9 J	27	15
Dibenzo(a,h)anthracene	10 U	20 U	10 U
Fluoranthene	21	64	38
Fluorene	6 J	68	21
Indeno(1,2,3-cd)pyrene	10 U	20 U	10
Naphthalene	4 J	66	6 J
Phenanthrene	48 J	190 J	85 J
Pyrene	28 J	110 J	40 J
Total PAHs ^{1,2}	172	943	342
TPH in µg/wipe	2,500	10,000	4,600

Notes:

U = Compound was not detected. Value is the detection limit.

J = Estimated value.

µg/wipe = micrograms per wipe

TPH = total petroleum hydrocarbons

PAH = polycyclic aromatic hydrocarbons

1. Total concentrations are calculated using the detected concentrations of individual constituents. Non-detects are treated as zeros. If all the individual constituents are non-detect the total concentration is reported as non-detect using the highest detection limit.

2. The total PAHs is the sum of all the PAHs listed in the table.

**TABLE 3-16
CAP CORE CHEMISTRY RESULTS FROM THE SPRING INVESTIGATION**

**NAPL INVESTIGATION REPORT
PINE STREET CANAL SUPERFUND SITE
BURLINGTON, VERMONT**

BBL Sample ID:	T09+30E30	T09+30E30	T09+30E30	T09+48E20	T09+48E20	T09+75E15	T09+75E15
Lab Sample ID:	CP01-0.0-0.32	CP01-0.32-0.64	CP01-0.64-0.8	CP02-0.0-0.32	CP02-0.32-0.5	CP03-0.0-0.32	CP03-0.32-0.64
Sampling Date:	WW2273-17	WW2273-18	WW2273-19	WW2273-7	WW2273-8	WW2273-9	WW2273-10
	5/06/2006	5/06/2006	5/06/2006	5/06/2006	5/06/2006	5/06/2006	5/06/2006
Total Organic Carbon in mg/kg	3,400	1,400	2,000	1,200	1,600	3,300	1,400
Total Solids in %	84.1	82.4	84.7	80.8	80.8	80.9	81.2
PAHs in µg/kg							
2-Methylnaphthalene	250 J	400 U	310 J	2,000	1,200	590,000	12,000
Acenaphthene	320 J	400 U	390 U	2,100	1,700	200,000	7,800
Acenaphthylene	200 J	400 U	390 U	830	620	34,000 J	510
Anthracene	560	400 U	140 J	2,300	1,800	88,000	3,700
Benzo(a)anthracene	1,200	350 J	400	2,400	1,600	42,000	1,700
Benzo(a)pyrene	670	230 J	260 J	1,800	1,300	30,000 J	1,000
Benzo(b)fluoranthene	900	240 J	270 J	2,100	1,400	24,000 J	1,000
Benzo(k)fluoranthene	290 J	400 U	390 U	720	600	10,000 J	400 J
Benzo(g,h,i)perylene	390 U	400 U	390 U	840	400 J	6,600 J	410 U
Chrysene	1,000	310 J	330 J	2,300	1,700	37,000 J	1,200
Dibenzo(a,h)anthracene	390 U	400 U	390 U	240 J	410 U	1,700 J	410 U
Fluoranthene	2,000 J	470 J	460 J	4,400	3,500	89,000	2,600
Fluorene	440	230 J	250 J	2,100	1,700	120,000	4,200
Indeno(1,2,3-cd)pyrene	390 U	400 U	390 U	900	570	7,000 J	410 U
Naphthalene	390 U	400 U	390 U	430	200 J	570,000	8,000
Phenanthrene	3,800	1,400	1,600	8,000	6,500	290,000	14,000
Pyrene	3,900	1,100	1,300	7,600	5,700	140,000	6,300
Total PAHs ^{1,2}	15,530	4,330	5,320	41,060	30,490	2,279,300	64,410
TPH in mg/kg	340	350	80	200	320	3,500	1700

**TABLE 3-16
CAP CORE CHEMISTRY RESULTS FROM THE SPRING INVESTIGATION**

**NAPL INVESTIGATION REPORT
PINE STREET CANAL SUPERFUND SITE
BURLINGTON, VERMONT**

BBL Sample ID:	T09+75E15	T09+75E15	T09+92E15	T09+92E15	T10+37E20	T10+37E20	T10+50E20
Lab Sample ID:	CP03-0.64-0.96	CP03-0.96-1.23	CP04-0.0-0.32	CP04-0.32-0.64	CP05-0.0-0.32	CP05-0.32-0.64	CP06-0-0.32
Sampling Date:	5/06/2006	5/06/2006	5/06/2006	5/06/2006	5/06/2006	5/06/2006	5/07/2006
Total Organic Carbon in mg/kg	1,500	820	1,600	690	1,800	500	790
Total Solids in %	84.1	84.7	83.5	85.0	83.2	84.5	80.2
PAHs in µg/kg							
2-Methylnaphthalene	13,000	250 J	1,200	390 U	400 U	390 U	280 J
Acenaphthene	7,900	340 J	830	390 U	400 U	390 U	170 J
Acenaphthylene	570	390 U	400 U	390 U	400 U	390 U	410 U
Anthracene	3,600	530	410	390 U	740	390 U	230 J
Benzo(a)anthracene	1,600	1,200	510	390 U	770	180 J	280 J
Benzo(a)pyrene	980	740	400	390 U	510	390 U	210 J
Benzo(b)fluoranthene	1,000	970	480	390 U	480	390 U	220 J
Benzo(k)fluoranthene	340 J	340 J	210 J	390 U	210 J	390 U	410 U
Benzo(g,h,i)perylene	390 U	390 U	400 U	390 U	400 U	390 U	410 U
Chrysene	1,200	1,100	520	390 U	660	140 J	300 J
Dibenzo(a,h)anthracene	390 U	390 U	400 U	390 U	400 U	390 U	410 U
Fluoranthene	2,600	1,500	540	390 U	870	390 U	580
Fluorene	4,400	410	460	390 U	320 J	390 U	220 J
Indeno(1,2,3-cd)pyrene	390 U	330 J	400 U	390 U	400 U	390 U	410 U
Naphthalene	9,700	390 U	740	390 U	400 U	390 U	410 U
Phenanthrene	13,000	3,900	2,900	390 U	3,000	420	760
Pyrene	5,600	4,200	2,200	280 J	3,100	400	850
Total PAHs ^{1,2}	65,490	15,810	11,400	280	10,660	1,140	4,100
TPH in mg/kg	370	880	590	46	100	52	97

**TABLE 3-16
CAP CORE CHEMISTRY RESULTS FROM THE SPRING INVESTIGATION**

**NAPL INVESTIGATION REPORT
PINE STREET CANAL SUPERFUND SITE
BURLINGTON, VERMONT**

BBL Sample ID:	T10+50E20	T10+50E20	T10+67E20	T10+76E20	T10+76E20	T10+76E20	T11+03E25
Lab Sample ID:	CP06-0.32-0.64	CP06-0.64-0.90	CP07-0.0-0.32	CP08-0.0-0.32	CP08-0.32-0.64	CP08-0.64-0.85	CP09-0-0.32
Sampling Date:	WW2272-19	WW2272-20	WW2273-1	WW2273-2	WW2273-3	WW2273-4	WW2272-13
	5/07/2006	5/07/2006	5/07/2006	5/07/2006	5/07/2006	5/07/2006	5/08/2006
Total Organic Carbon in mg/kg	620	890	1,600	2,500	2,800	2,100	11,000
Total Solids in %	82.7	84.4	83.7	82.7	85.0	85.3	82.5
PAHs in µg/kg							
2-Methylnaphthalene	400 U	660	12,000	29,000	66,000	59,000	260,000
Acenaphthene	400 U	540	6,400	10,000	21,000	19,000	60,000
Acenaphthylene	400 U	370 J	2,600	4,000	7,200	6,500	35,000
Anthracene	400 U	850	4,500	5,400	12,000	10,000	39,000
Benzo(a)anthracene	400 U	670	3,000	3,200	5,300	4,900	21,000
Benzo(a)pyrene	400 U	440	2,200	2,400	3,900 J	3,700 J	14,000 J
Benzo(b)fluoranthene	400 U	410	2,100	2,300	3,500 J	3,400 J	13,000 J
Benzo(k)fluoranthene	400 U	190 J	930	980	1,700 J	1,400 J	3,900
Benzo(g,h,i)perylene	400 U	390 U	850	860	1,300 J	1,300 J	3,100
Chrysene	400 U	600	2,600	2,800	4,300	3,900	17,000 J
Dibenzo(a,h)anthracene	400 U	390 U	270 J	240 J	400 J	290 J	920
Fluoranthene	400 U	1,400	5,600	6,300	13,000	12,000	44,000
Fluorene	400 U	700	5,600	7,100	17,000	14,000	54,000
Indeno(1,2,3-cd)pyrene	400 U	390 U	950	1,000	1,600	1,400	3,700
Naphthalene	400 U	270 J	4,400	17,000	48,000	41,000	210,000
Phenanthrene	400 U	2,600	14,000	21,000	39,000	34,000	130,000
Pyrene	400 U	2,000	10,000	11,000	18,000	16,000	64,000
Total PAHs ^{1,2}	400 U	11,700	78,000	124,580	263,200	231,790	972,620
TPH in mg/kg	12	86	1,200	1,400	2,600	1,100	7,000

**TABLE 3-16
CAP CORE CHEMISTRY RESULTS FROM THE SPRING INVESTIGATION**

**NAPL INVESTIGATION REPORT
PINE STREET CANAL SUPERFUND SITE
BURLINGTON, VERMONT**

BBL Sample ID:	T11+03E25	T10+96E30	T10+96E30	T10+96E30	T10+96E30	T10+96E30	T10+76E60	T10+76E60
Lab Sample ID:	CP09-0.32-0.64	CP10-0-0.32	CP10-0.32-0.64	CP10-0.64-0.96	CP10-0.96-1.28	CP11-0-0.32	CP11-0.32-0.64	CP11-0.32-0.64
Sampling Date:	WW2272-14	WW2272-7	WW2272-8	WW2272-9	WW2272-10	WW2272-4	WW2272-5	WW2272-5
Sampling Date:	5/08/2006	5/08/2006	5/08/2006	5/08/2006	5/08/2006	5/08/2006	5/08/2006	5/08/2006
Total Organic Carbon in mg/kg	13,000	7,400	1,400	610	830	3,900	2,500	
Total Solids in %	84.6	81.6	83.1	84.4	81.7	82.2	83.2	
PAHs in µg/kg								
2-Methylnaphthalene	540,000	130,000	400 UJ	390 U	400 U	430	400 U	400 U
Acenaphthene	110,000	50,000	400 UJ	390 U	400 U	330 J	400 U	400 U
Acenaphthylene	92,000	18,000	400 UJ	390 U	400 U	180 J	400 U	400 U
Anthracene	75,000	26,000	400 UJ	390 U	400 U	390 J	400 U	400 U
Benzo(a)anthracene	37,000 J	14,000	250 J	390 U	400 U	420	120 J	400 U
Benzo(a)pyrene	26,000 J	11,000	180 J	390 U	400 U	370 J	400 U	400 U
Benzo(b)fluoranthene	21,000 J	9,300	170 J	390 U	400 U	420	400 U	400 U
Benzo(k)fluoranthene	39,000 U	4,200	400 UJ	390 U	400 U	170 J	400 U	400 U
Benzo(g,h,i)perylene	39,000 U	3,500 J	400 U	390 U	400 U	240 J	400 U	400 U
Chrysene	31,000 J	13,000	220 J	390 U	400 U	420	400 U	400 U
Dibenzo(a,h)anthracene	39,000 U	4,000 U	400 U	390 U	400 U	400 U	400 U	400 U
Fluoranthene	78,000	26,000	490 J	390 U	400 U	860	400 U	400 U
Fluorene	110,000	35,000	400 UJ	390 U	400 U	340 J	400 U	400 U
Indeno(1,2,3-cd)pyrene	39,000 U	3,900 J	400 UJ	390 U	400 U	400 U	400 U	400 U
Naphthalene	500,000	120,000	400 UJ	390 U	400 U	400 U	400 U	400 U
Phenanthrene	250,000	76,000	180 J	390 U	200 J	1,200	290 J	400 U
Pyrene	120,000	47,000	950 J	390 U	400 U	1,300	340 J	400 U
Total PAHs ^{1,2}	1,990,000	586,900	2,440	390 U	200	7,070	750	400 U
TPH in mg/kg	9,300	4,500	68	11	11	260	100	

**TABLE 3-16
CAP CORE CHEMISTRY RESULTS FROM THE SPRING INVESTIGATION**

**NAPL INVESTIGATION REPORT
PINE STREET CANAL SUPERFUND SITE
BURLINGTON, VERMONT**

BBL Sample ID:	T10+76E60	T11+04E20	T11+04E20	T11+45E25	T11+45E25	T11+45E25	T11+70E30
Lab Sample ID:	CP11-0.64-0.96	CP12-0-0.32	CP12-0.32-0.64	CP13-0-0.32	CP13-0.32-0.64	CP13-0.64-0.96	CP14-0-0.32
Sampling Date:	5/08/2006	5/08/2006	5/08/2006	5/08/2006	5/08/2006	5/08/2006	5/09/2006
Total Organic Carbon in mg/kg	2,900	550	850	2,400	480 U	480 U	2,000
Total Solids in %	84.3	82.8	84.2	84.0	83.7	83.6	82.7
PAHs in µg/kg							
2-Methylnaphthalene	390 U	400 U	390 U	3,300	390 U	390 U	560
Acenaphthene	390 U	140 J	390 U	1,800	140 J	390 U	290 J
Acenaphthylene	390 U	400 U	390 U	360 J	390 U	390 U	400 U
Anthracene	390 U	230 J	390 U	1,100	140 J	390 U	220 J
Benzo(a)anthracene	390 U	350 J	390 U	820	390 U	390 U	310 J
Benzo(a)pyrene	390 U	290 J	390 U	610	390 U	390 U	350 J
Benzo(b)fluoranthene	390 U	290 J	390 U	670	390 U	390 U	580
Benzo(k)fluoranthene	390 U	400 U	390 U	250 J	390 U	390 U	240 J
Benzo(g,h,i)perylene	390 U	400 U	390 U	240 J	390 U	390 U	400 U
Chrysene	390 U	360 J	390 U	860	390 U	390 U	580
Dibenzo(a,h)anthracene	390 U	400 U	390 U	390 U	390 U	390 U	400 U
Fluoranthene	390 U	750	390 U	1,600	390 U	390 U	950
Fluorene	390 U	160 J	390 U	1,200	390 U	390 U	280 J
Indeno(1,2,3-cd)pyrene	390 U	400 U	390 U	390 U	390 U	390 U	400 U
Naphthalene	390 U	400 U	390 U	1,800	390 U	390 U	300 J
Phenanthrene	100 J	820	390 U	3,600	500	390 U	1,100
Pyrene	390 U	1,000	390 U	2,400	290 J	390 U	1,200
Total PAHs ^{1,2}	100	4,390	390 U	20,610	1,070	390 U	6,960
TPH in mg/kg	66	68	30	300	32	4.9 J	270

**TABLE 3-16
CAP CORE CHEMISTRY RESULTS FROM THE SPRING INVESTIGATION**

**NAPL INVESTIGATION REPORT
PINE STREET CANAL SUPERFUND SITE
BURLINGTON, VERMONT**

BBL Sample ID:	T11+70E30	T11+70E30	T10+76E40	T10+76E40
Lab Sample ID:	CP14-0.32-0.64	CP14-0.64-0.96	CP16-0.0-0.32	CP16-0.32-0.64
Sampling Date:	5/09/2006	5/09/2006	5/07/2006	5/07/2006
Total Organic Carbon in mg/kg	470 U	1,000	670	830
Total Solids in %	84.3	82.9	80.6	85.2
PAHs in µg/kg				
2-Methylnaphthalene	390 U	400 U	410 U	390 U
Acenaphthene	390 U	400 U	410 U	390 U
Acenaphthylene	390 U	400 U	410 U	390 U
Anthracene	390 U	400 U	130 J	390 U
Benzo(a)anthracene	390 U	400 U	120 J	390 U
Benzo(a)pyrene	390 U	400 U	410 U	390 U
Benzo(b)fluoranthene	390 U	400 U	410 U	390 U
Benzo(k)fluoranthene	390 U	400 U	410 U	390 U
Benzo(g,h,i)perylene	390 U	400 U	410 U	390 U
Chrysene	390 U	400 U	410 U	390 U
Dibenzo(a,h)anthracene	390 U	400 U	410 U	390 U
Fluoranthene	390 U	400 U	280 J	390 U
Fluorene	390 U	400 U	410 U	390 U
Indeno(1,2,3-cd)pyrene	390 U	400 U	410 U	390 U
Naphthalene	390 U	400 U	410 U	390 U
Phenanthrene	390 U	400 U	350 J	160 J
Pyrene	390 U	400 U	370 J	390 U
Total PAHs ^{1,2}	390 U	400 U	1,250	160
TPH in mg/kg	4.6 J	5.5 J	51	28

Notes:
 U = Compound was not detected. Value is the detection limit.
 J = Estimated value.
 mg/kg = milligrams per kilogram
 µg/kg = micrograms per kilogram
 TPH = total petroleum hydrocarbons
 PAH = polycyclic aromatic hydrocarbons
 1. Total concentrations are calculated using the detected concentrations of individual constituents. Non-detects are treated as zeros. If all the individual constituents are non-detect the total concentration is reported as non-detect using the highest detection limit.
 2. The total PAHs is the sum of all the PAHs listed in the table.

**TABLE 3-17
CAP CORE CHEMISTRY RESULTS FROM THE SUMMER INVESTIGATION**

**NAPL INVESTIGATION REPORT
PINE STREET CANAL SUPERFUND SITE
BURLINGTON, VERMONT**

BBL Sample ID:	T11+25E50 CP17-0.0-0.33	T11+25E50 CP17-0.33-0.66	T11+25E50 CP17-0.66-0.80	T11+20E20 CP18-0.0-0.33	T11+20E20 CP18-0.33-0.60	T11+00E40 CP20-0.0-0.33	T11+00E40 CP20-0.33-0.64
Lab Sample ID:	WW4280-8	WW4280-9	WW4280-10	WW4280-11	WW4280-12	WW4280-14	WW4280-15
Sampling Date:	8/16/2006	8/16/2006	8/16/2006	8/16/2006	8/16/2006	8/16/2006	8/16/2006
Total Organic Carbon in mg/kg	1,800	470 U	1,100	14,000	17,000	850	11,000
Total Solids in %	83	85	85	86	86	84	82
PAHs in µg/kg							
2-Methylnaphthalene	33,000	610	64,000	680,000	760,000	5,600	4,500
Acenaphthene	11,000	220 J	7,400 J	160,000	190,000	2,800	1,800
Acenaphthylene	2,100 J	300 J	13,000	48,000 J	54,000 J	800	820
Anthracene	7,000 J	480 J	12,000 J	120,000 J	140,000 J	1,700	1,700 J
Benzo(a)anthracene	2,800 J	200 J	4,900 J	49,000 J	62,000 J	960	800
Benzo(a)pyrene	2,000 J	150 J	3,500 J	37,000 J	42,000 J	680	610
Benzo(b)fluoranthene	1,900 J	390 U	7,800 U	77,000 U	32,000 J	620	470
Benzo(k)fluoranthene	3,200 U	390 U	7,800 U	77,000 U	77,000 U	180 J	220 J
Benzo(g,h,i)perylene	3,200 U	390 U	7,800 U	77,000 U	77,000 U	350 J	400 U
Chrysene	2,200 J	150 J	3,300 J	37,000 J	43,000 J	850	480
Dibenzo(a,h)anthracene	3,200 U	390 U	7,800 U	77,000 U	77,000 U	390 U	400 U
Fluoranthene	5,900	380 J	9,400	96,000	110,000	2,000 J	1,400
Fluorene	6,500	350 J	10,000	94,000	120,000	2,400	1,800
Indeno(1,2,3-cd)pyrene	3,200 U	390 U	7,800 U	77,000 U	77,000 U	430	400 U
Naphthalene	26,000	210 J	71,000	790,000	970,000	2,300	1,900
Phenanthrene	20,000 J	1,400 J	40,000 J	380,000 J	420,000 J	7,000	4,200 J
Pyrene	8,900 J	500 J	14,000 J	120,000 J	130,000 J	2,800	2,000 J
Total PAHs ^{1,2}	129,300	4,950	252,500	2,611,000	3,073,000	31,470	22,700
TPH in mg/kg	410	45	1000	14000	14000	330	70

**TABLE 3-17
CAP CORE CHEMISTRY RESULTS FROM THE SUMMER INVESTIGATION**

**NAPL INVESTIGATION REPORT
PINE STREET CANAL SUPERFUND SITE
BURLINGTON, VERMONT**

BBL Sample ID:	T11+05E20 CP21-0.0-0.33	T11+05E20 CP21-0.33-0.66	PSC-DUP1	T11+05E20 CP21-0.66-0.99	T10+70E20 CP22-0.0-0.33	T10+74E20 CP23-0.0-0.33	T10+74E20 CP23-0.33-0.55
Lab Sample ID:	WW4280-16	WW4280-13	WW4281-8	WW4281-1	WW4281-2	WW4281-3	WW4281-4
Sampling Date:	8/16/2006	8/16/2006	8/16/2006 Dup of T11+05E20 CP21-0.33-0.66	8/16/2006	8/16/2006	8/16/2006	8/16/2006
Total Organic Carbon in mg/kg	11,000	11,000	11,000	18,000	1,000	11,000	3,600
Total Solids in %	83	85	85	86	84	84	84
PAHs in µg/kg							
2-Methylnaphthalene	450,000	590,000	520,000	850,000	4,800	120,000	120,000
Acenaphthene	64,000	74,000 J	76,000	120,000	3,600	37,000	31,000
Acenaphthylene	86,000	95,000	100,000	150,000	270 J	7,400 J	7,500 J
Anthracene	55,000	100,000 J	64,000	110,000	1,900 J	16,000	22,000 J
Benzo(a)anthracene	31,000 J	40,000 J	38,000 J	58,000 J	1,100 J	9,700	8,600 J
Benzo(a)pyrene	21,000 J	28,000 J	23,000 J	39,000 J	980 J	7,400 J	6,000 J
Benzo(b)fluoranthene	20,000 J	77,000 U	27,000 J	96,000 U	820 J	6,200 J	4,700 J
Benzo(k)fluoranthene	40,000 U	77,000 U	39,000 U	96,000 U	410 J	7,800 U	12,000 U
Benzo(g,h,i)perylene	40,000 U	77,000 U	39,000 U	96,000 U	410 J	7,800 U	12,000 U
Chrysene	26,000 J	77,000 U	33,000 J	50,000 J	1,000 J	8,600	6,600 J
Dibenzo(a,h)anthracene	40,000 U	77,000 U	39,000 U	96,000 U	390 UJ	7,800 U	12,000 U
Fluoranthene	77,000 J	77,000 J	92,000 J	140,000 J	2,100	22,000 J	16,000
Fluorene	85,000	78,000	100,000	150,000	2,300	26,000	20,000
Indeno(1,2,3-cd)pyrene	40,000 U	77,000 U	39,000 U	96,000 U	510 J	7,800 U	12,000 U
Naphthalene	500,000	820,000	550,000	1,000,000	1,800	97,000	120,000
Phenanthrene	220,000	340,000 J	250,000	410,000	4,700 J	68,000	66,000 J
Pyrene	97,000	110,000 J	120,000	170,000	3,700 J	30,000	27,000 J
Total PAHs ^{1,2}	1,732,000	2,352,000	1,993,000	3,247,000	30,400	455,300	455,400
TPH in mg/kg	11000	33000	17000	26000	380	5700	3400

**TABLE 3-17
CAP CORE CHEMISTRY RESULTS FROM THE SUMMER INVESTIGATION**

**NAPL INVESTIGATION REPORT
PINE STREET CANAL SUPERFUND SITE
BURLINGTON, VERMONT**

BBL Sample ID:	T10+75E70 CP24-0.0-0.33	T10+75E70 CP24-0.33-0.66	T10+75E70 CP24-0.66-0.80	T09+75E20 CP25-0.0-0.33	T09+75E20 CP25-0.33-0.5	T09+55E20 CP26-0.0-0.33	T09+55E20 CP26-0.33-0.66
Lab Sample ID:	WW4281-5	WW4281-6	WW4281-7	WW4281-9	WW4281-10	WW4281-11	WW4281-12 ³
Sampling Date:	8/16/2006	8/16/2006	8/16/2006	8/17/2006	8/17/2006	8/17/2006	8/17/2006
Total Organic Carbon in mg/kg	3,600	2,700	6,000	19,000	480 U	4,000	470 U
Total Solids in %	86	84	85	84	84	82	85
PAHs in µg/kg							
2-Methylnaphthalene	200,000	77,000	120,000	140,000	490	26,000	40
Acenaphthene	72,000	31,000	49,000	62,000	700	14,000	110
Acenaphthylene	6,300 J	7,900 U	3,800 J	6,500 J	390 U	980 J	20 J
Anthracene	29,000	18,000 J	18,000	27,000	590 J	6,700	65
Benzo(a)anthracene	19,000 J	7,100 J	11,000	15,000	270 J	5,700	70
Benzo(a)pyrene	14,000 J	4,200 J	7,800 J	12,000	170 J	4,800	42
Benzo(b)fluoranthene	11,000 J	4,800 J	6,800 J	11,000	390 U	5,000	43
Benzo(k)fluoranthene	19,000 U	7,900 U	9,700 U	7,800 U	390 U	1,600 J	11 J
Benzo(g,h,i)perylene	19,000 U	7,900 U	9,700 U	7,800 U	390 U	1,600 J	16 UJ
Chrysene	17,000 J	5,100 J	11,000	16,000	210 J	6,300	43
Dibenzo(a,h)anthracene	19,000 U	7,900 U	9,700 U	7,800 U	390 U	2,400 U	23 U
Fluoranthene	44,000 J	13,000	26,000 J	36,000 J	400	12,000 J	120
Fluorene	41,000	14,000	27,000	38,000	410	8,000	81
Indeno(1,2,3-cd)pyrene	19,000 U	7,900 U	9,700 U	7,800 U	390 U	2,000 J	32 UJ
Naphthalene	180,000	71,000	100,000	110,000	210 J	20,000	16 J
Phenanthrene	110,000	52,000 J	73,000	120,000	1,700 J	30,000	190
Pyrene	53,000	22,000 J	40,000	44,000	910 J	18,000	130
Total PAHs ^{1,2}	796,300	319,200	493,400	637,500	6,060	162,680	981
TPH in mg/kg	11000	4600	6700	7300	140	2000	14

**TABLE 3-17
CAP CORE CHEMISTRY RESULTS FROM THE SUMMER INVESTIGATION**

**NAPL INVESTIGATION REPORT
PINE STREET CANAL SUPERFUND SITE
BURLINGTON, VERMONT**

BBL Sample ID:	T10+50E20 CP27-0.0-0.33	T10+50E20 CP27-0.33-0.66	T10+50E20 CP27-0.66-0.85
Lab Sample ID:	WW4281-13	WW4281-14	WW4281-15
Sampling Date:	8/17/2006	8/17/2006	8/17/2006
Total Organic Carbon in mg/kg	1,400	2,000	1,200
Total Solids in %	81	85	86
PAHs in µg/kg			
2-Methylnaphthalene	7,900	4,800	1,900
Acenaphthene	4,800	2,700	1,600
Acenaphthylene	620 J	560	180 J
Anthracene	3,200 J	1,600 J	1,000 J
Benzo(a)anthracene	1,800	770	440
Benzo(a)pyrene	1,400	520	280 J
Benzo(b)fluoranthene	1,400	450	280 J
Benzo(k)fluoranthene	660 J	220 J	400 U
Benzo(g,h,i)perylene	460 J	270 J	400 U
Chrysene	1,600	610	320 J
Dibenzo(a,h)anthracene	770 U	390 U	400 U
Fluoranthene	4,000	1,400	860
Fluorene	3,500	1,900	1,000
Indeno(1,2,3-cd)pyrene	700 J	390 J	400 U
Naphthalene	2,500	2,000	610
Phenanthrene	7,600 J	3,700 J	2,600 J
Pyrene	4,500 J	2,000 J	1,100 J
Total PAHs ^{1,2}	46,640	23,890	12,170
TPH in mg/kg	2400	210	99

Notes:

U = Compound was not detected. Value is the detection limit.

J = Estimated value.

mg/kg = milligrams per kilogram

µg/kg = micrograms per kilogram

TPH = total petroleum hydrocarbons

PAH = polycyclic aromatic hydrocarbons

1. Total concentrations are calculated using the detected concentrations of individual constituents. Non-detects are treated as zeros. If all the individual constituents are non-detect the total concentration is reported as non-detect using the highest detection limit.

2. The total PAHs is the sum of all the PAHs listed in the table.

3. PAH data from Lab Sample ID WW4281-21 because of sample dilution.

**TABLE 3-18
CAP CORE CHEMISTRY RESULTS FROM THE WINTER INVESTIGATION**

**NAPL INVESTIGATION REPORT
PINE STREET CANAL SUPERFUND SITE
BURLINGTON, VERMONT**

BBL Sample ID:	WB-T10+00	WB-T10+00	WB-T10+00	WB-T10+00	WB-T10+00	WB-T10+00	WB-T10+00
Lab Sample ID:	CP100-0.0-0.5	CP100-DUP	CP100-0.5-1	CP100-1.5-2	CP101-0.0-0.5	CP101-1-1.5	CP101-1.5-2
Sampling Date:	SA0750-8 2/20/2007	SA0750-30 2/20/2007 Dup of WB-T10+00 CP100-0-0.5	SA0750-9 2/20/2007	SA0750-10 2/20/2007	SA0750-21RA 2/19/2007	SA0750-22 2/19/2007	SA0750-23 2/19/2007
Total Solids in %	54	58	76	84	70	77	79
PAHs in µg/kg							
2-Methylnaphthalene	180 J	84 J	20 J	24 U	12 J	26 U	25 U
Acenaphthene	57	26 J	15 J	30	29 U	26 U	25 U
Acenaphthylene	34 J	18 J	8 J	6 J	23 J	3 J	25 U
Anthracene	39 J	20 J	14 J	6 J	15 J	26 U	25 U
Benzo(a)anthracene	84 J	37 J	11 J	24 U	88	4 J	25 U
Benzo(a)pyrene	95 J	53 J	7 J	24 U	78	26 U	25 U
Benzo(b)fluoranthene	160 J	78 J	8 J	24 U	110	26 U	25 U
Benzo(k)fluoranthene	67	40	26 U	24 U	39 J	26 U	25 U
Benzo(g,h,i)perylene	46	34 J	26 U	24 U	46	26 U	25 U
Chrysene	110 J	53 J	10 J	24 U	98	26 U	25 U
Dibenzo(a,h)anthracene	18 J	34 U	26 U	24 U	12 J	26 U	25 U
Fluoranthene	140 J	72 J	19 J	24 U	110	6 J	25 U
Fluorene	43 J	23 J	15 J	4 J	12 J	26 U	25 U
Indeno(1,2,3-cd)pyrene	100 J	58 J	26 U	24 U	66 J	26 U	25 U
Naphthalene	130 J	68 J	6 J	20 J	4 J	5 J	7 J
Phenanthrene	140 J	76 J	56	46	50	8 J	25 U
Pyrene	140 J	78 J	28	5 J	120 J	7 J	25 U
Total PAHs ^{1,2}	1,583	818	217	117	883	33	7
TPH in mg/kg	160	130	9.2 U	7 U	43	7 U	6.3 U

**TABLE 3-18
CAP CORE CHEMISTRY RESULTS FROM THE WINTER INVESTIGATION**

**NAPL INVESTIGATION REPORT
PINE STREET CANAL SUPERFUND SITE
BURLINGTON, VERMONT**

BBL Sample ID:	WB-T10+00	WB-T10+00	WB-T10+00	WB-T10+50	WB-T10+50	WB-T10+50	WB-T10+50
Lab Sample ID:	CP102-0.0-0.5	CP102-1.5-2	CP102-2.5-3	CP103-0.5-1	CP103-1.5-1.8	CP103-1.8-2	CP104-0.0-0.5
Sampling Date:	SA0750-18 2/19/2007	SA0750-19 2/19/2007	SA0750-20 2/19/2007	SA0750-11 2/20/2007	SA0750-27 2/20/2007	SA0750-28 2/20/2007	SA0750-24 2/19/2007
Total Solids in %	77	76	78	82.0	78	76	51
PAHs in µg/kg							
2-Methylnaphthalene	26 U	26 U	25 U	12 J	3,500	540,000 D	350 J
Acenaphthene	26 U	26 U	25 U	12 J	1,100	120,000 D	280 J
Acenaphthylene	26 U	26 U	6 J	24 U	1,000	130,000 D	480 J
Anthracene	26 U	26 U	25 U	9 J	960	85,000 D	420 J
Benzo(a)anthracene	5 J	26 U	25 U	24 U	390 J	35,000 J	670
Benzo(a)pyrene	5 J	26 U	25 U	24 U	270 J	24,000 J	610 J
Benzo(b)fluoranthene	7 J	26 U	25 U	24 U	200 J	20,000 J	660
Benzo(k)fluoranthene	26 U	26 U	25 U	24 U	420 U	7,800 J	650 U
Benzo(g,h,i)perylene	26 U	26 U	25 U	24 U	420 U	7,200 J	290 J
Chrysene	6 J	26 U	25 U	24 U	350 J	25,000 J	800
Dibenzo(a,h)anthracene	26 U	26 U	25 U	24 U	340 J	3,900 J	580 J
Fluoranthene	8 J	26 U	25 U	8 J	1,000	95,000 D	1,400
Fluorene	26 U	26 U	25 U	10 J	1,000	100,000 D	460 J
Indeno(1,2,3-cd)pyrene	26 U	26 U	25 U	24 U	420 U	11,000 J	650 U
Naphthalene	26 U	5 J	46	12 J	2,200	590,000 D	280 J
Phenanthrene	6 J	26 U	5 J	43	2,800	270,000 D	1,600
Pyrene	10 J	26 U	25 U	10 J	1,100	120,000 D	1,900
Total PAHs ^{1,2}	47	5	58	115	16,210	2,183,900	10,780
TPH in mg/kg	6.5 U	6.6 U	6.4 U	6.5 U	83	19000	410

**TABLE 3-18
CAP CORE CHEMISTRY RESULTS FROM THE WINTER INVESTIGATION**

**NAPL INVESTIGATION REPORT
PINE STREET CANAL SUPERFUND SITE
BURLINGTON, VERMONT**

BBL Sample ID:	WB-T10+50	WB-T10+50	WB-T10+50	WB-T10+50	WB-T10+50	WB-T10+50	WB-T10+50
Lab Sample ID:	CP104-1-1.5	CP104-1.5-2	CP104-2-2.5 ³	CP104-2.5-3 ³	CP105-2-2.5	CP105-2.5-2.7	CP105-2.7-3
Sampling Date:	SA0750-25 2/19/2007	SA0750-26 2/19/2007	SA1999-1 2/19/2007	SA1999-2 2/19/2007	SA0750-12 2/20/2007	SA0750-13 2/20/2007	SA0750-14 2/20/2007
Total Solids in %	78	80	85	84	80	80	76.0
PAHs in µg/kg							
2-Methylnaphthalene	21 J	15 J	NA	NA	25 U	100,000 D	440 U
Acenaphthene	17 J	15 J	NA	NA	15 J	43,000 D	440 U
Acenaphthylene	8 J	7 J	NA	NA	10 J	18,000 D	440 U
Anthracene	5 J	25 U	NA	NA	15 J	28,000 D	440 U
Benzo(a)anthracene	9 J	25 U	NA	NA	12 J	14,000 D	440 U
Benzo(a)pyrene	7 J	25 U	NA	NA	9 J	10,000 D	440 U
Benzo(b)fluoranthene	8 J	25 U	NA	NA	10 J	8,900 EJ	440 U
Benzo(k)fluoranthene	26 U	25 U	NA	NA	4 J	3,200	440 U
Benzo(g,h,i)perylene	26 U	25 U	NA	NA	25 U	2,700	440 U
Chrysene	8 J	25 U	NA	NA	11 J	15,000 D	440 U
Dibenzo(a,h)anthracene	26 U	25 U	NA	NA	25 U	1,200	440 U
Fluoranthene	16 J	25 U	NA	NA	18 J	37,000 D	440 U
Fluorene	6 J	6 J	NA	NA	10 J	32,000 D	440 U
Indeno(1,2,3-cd)pyrene	26 U	25 U	NA	NA	6 J	3,800	360 J
Naphthalene	120	42	NA	NA	20 J	66,000 D	440 U
Phenanthrene	24 J	15 J	NA	NA	66	88,000 D	510
Pyrene	20 J	25 U	NA	NA	33	44,000 D	230 J
Total PAHs ^{1,2}	269	100	NA	NA	239	514,800	1,100
TPH in mg/kg	6.4 U	6.2 U	5.3 JB	6.5 B	7 U	4,600	34

**TABLE 3-18
CAP CORE CHEMISTRY RESULTS FROM THE WINTER INVESTIGATION**

**NAPL INVESTIGATION REPORT
PINE STREET CANAL SUPERFUND SITE
BURLINGTON, VERMONT**

BBL Sample ID:	WB-T11+00	WB-T11+00	WB-T11+00	WB-T11+00	WB-T11+00	WB-T11+00	WB-T11+00
Lab Sample ID:	CP106-0.0-0.5	CP106-0.5-1	CP106-DUP	CP106-1.5-2	CP107-2-2.2	CP107-2.2-2.5	CP107-2.5-3
Sampling Date:	SA0750-5 2/20/2007	SA0750-6 2/20/2007	SA0750-29 2/20/2007 Dup of WB-T10+00 CP106-0.5-1	SA0750-7 2/20/2007	SA0750-15 2/20/2007	SA0750-16 2/20/2007	SA0750-17 2/20/2007
Total Solids in %	49	76	77	84	83	79	80
PAHs in µg/kg							
2-Methylnaphthalene	44	26 U	26 U	68	8,300 D	130,000 D	80
Acenaphthene	36 J	26 U	26 U	28	4,900	70,000 D	210 D
Acenaphthylene	60	7 J	4 J	22 J	1,100	13,000 D	70
Anthracene	58	26 U	26 U	24 U	3,500 D	41,000 D	120 D
Benzo(a)anthracene	220	5 J	4 J	24 U	2,300	24,000 D	98 D
Benzo(a)pyrene	210	5 J	4 J	24 U	1,600	17,000	61
Benzo(b)fluoranthene	320	5 J	6 J	24 U	1,500	13,000	61
Benzo(k)fluoranthene	120	26 U	26 U	24 U	830 D	6,900	25 J
Benzo(g,h,i)perylene	110	26 U	26 U	24 U	530	5,600	20 J
Chrysene	260 D	5 J	5 J	24 U	2,300 D	22,000 D	93 D
Dibenzo(a,h)anthracene	38 J	26 U	26 U	24 U	460	4,800	7 J
Fluoranthene	350 D	6 J	8 J	24 U	5,500 D	56,000 D	190 D
Fluorene	48	26 U	26 U	10 J	4,200	56,000	120 D
Indeno(1,2,3-cd)pyrene	210	26 U	26 U	24 U	1,000 D	9,200 D	36
Naphthalene	57	50	32	58	5,400 D	78,000 D	260 D
Phenanthrene	240	10 J	10 J	7 J	12,000 D	130,000 D	480 D
Pyrene	370 D	8 J	8 J	5 J	7,100 D	70,000 D	240 D
Total PAHs ^{1,2}	2,751	101	82	198	62,520	746,500	2,171
TPH in mg/kg	370	9 U	19 U	7 U	220	5600	53

**TABLE 3-18
CAP CORE CHEMISTRY RESULTS FROM THE WINTER INVESTIGATION**

**NAPL INVESTIGATION REPORT
PINE STREET CANAL SUPERFUND SITE
BURLINGTON, VERMONT**

BBL Sample ID:	WB-T11+00	WB-T11+00	WB-T11+00	WB-T11+00
Lab Sample ID:	CP108-0.5-1	CP108-1.5-2	CP108-2-2.5	CP108-2.5-3
Sampling Date:	SA0750-1 2/20/2007	SA0750-2 2/20/2007	SA0750-3 2/20/2007	SA0750-4 2/20/2007
Total Solids in %	80	84	83	84
PAHs in µg/kg				
2-Methylnaphthalene	25 U	24 U	1,700	24 U
Acenaphthene	25 U	14 J	2,300	29
Acenaphthylene	5 J	6 J	620	15 J
Anthracene	5 J	14 J	2,100	41
Benzo(a)anthracene	14 J	11 J	1,300	29
Benzo(a)pyrene	10 J	7 J	920	19 J
Benzo(b)fluoranthene	10 J	9 J	800	20 J
Benzo(k)fluoranthene	4 J	24 U	390 J	8 J
Benzo(g,h,i)perylene	4 J	24 U	300 J	7 J
Chrysene	13 J	12 J	1,200	26
Dibenzo(a,h)anthracene	25 U	24 U	410	24 U
Fluoranthene	16 J	28	2,500	59
Fluorene	25 U	9 J	1,700	28
Indeno(1,2,3-cd)pyrene	6 J	24 U	520	11 J
Naphthalene	25 U	4 J	2,900	81
Phenanthrene	16 J	62	5,300	140
Pyrene	24 J	38	3,400	68
Total PAHs ^{1,2}	127	214	28,360	580
TPH in mg/kg	6.2 UJ	7.2 U	180	7.7 U

Notes:

- U = Compound was not detected. Value is the detection limit.
- J = Estimated value.
- D = Result was obtained from the analysis of a diluted sample
- E = Analyte exceeded calibration range.
- B = Analyte was detected in laboratory method blank.
- NA = not analyzed
- mg/kg = milligrams per kilogram
- µg/kg = micrograms per kilogram
- TPH = total petroleum hydrocarbons
- PAH = polycyclic aromatic hydrocarbons
- 1. Total concentrations are calculated using the detected concentrations of individual constituents. Non-detects are treated as zeros. If all the individual constituents are non-detect the total concentration is reported as non-detect using the highest detection limit.
- 2. The total PAHs is the sum of all the PAHs listed in the table.
- 3. Draft data that are not validated. Date may change based on validation.

**TABLE 3-19
CONFIRMATION SAMPLE CHEMISTRY RESULTS FROM THE SPRING INVESTIGATION**

**NAPL INVESTIGATION REPORT
PINE STREET CANAL SUPERFUND SITE
BURLINGTON, VERMONT**

BBL Sample ID:	T09+48E20 CB02-7-9	T09+48E20 CB02-10-12	PSC-DUP2	T09+48E20 CB02-15-17	T09+48E20 CB02-25-27	T09+75E15 CB03-7-9
Lab Sample ID:	WW2336-5	WW2336-3	WW2336-1	WW2336-4	WW2336-2	WW2336-7
Sampling Date:	5/12/2006	5/12/2006	5/12/2006 Dup of T9+48E20 CB02-10-12	5/12/2006	5/12/2006	5/11/2006
Total Organic Carbon in mg/kg	400,000	790,000	740,000	70,000	--	400,000
Total Solids in %	36.3	17.3	16.2	71.7	--	34.4
PAHs in µg/kg						
2-Methylnaphthalene	15,000,000	28,000,000	22,000,000	10,000,000	37,000	12,000,000
Acenaphthene	3,800,000	6,000,000	5,100,000	2,000,000	5,500	3,200,000
Acenaphthylene	1,200,000	3,600,000	3,800,000	2,400,000	14,000	1,800,000
Anthracene	1,300,000	2,600,000	2,700,000	1,500,000	7,200	1,900,000
Benzo(a)anthracene	710,000	1,400,000	1,400,000	540,000	3,400 J	900,000
Benzo(a)pyrene	480,000	1,100,000	1,100,000	380,000 J	2,500 J	640,000
Benzo(b)fluoranthene	450,000	910,000	870,000	360,000 J	2,000 J	510,000
Benzo(k)fluoranthene	160,000	190,000 U	410,000	110,000 J	4,300 U	240,000 J
Benzo(g,h,i)perylene	160,000	300,000	330,000	160,000 J	4,300 U	480,000 U
Chrysene	490,000	1,200,000	1,200,000	400,000	2,900 J	750,000
Dibenzo(a,h)anthracene	49,000 J	190,000 U	200,000 U	31,000 J	4,300 U	480,000 U
Fluoranthene	1,300,000	2,500,000	2,500,000	1,400,000	6,400	1,900,000
Fluorene	1,800,000	3,600,000	3,900,000	2,100,000	10,000	2,600,000
Indeno(1,2,3-cd)pyrene	210,000	340,000	380,000	190,000	4,300 U	480,000 U
Naphthalene	13,000,000	30,000,000	25,000,000	12,000,000	28,000	12,000,000
Phenanthrene	6,700,000	13,000,000	10,000,000	4,800,000	25,000	6,000,000
Pyrene	1,800,000	6,100,000	5,000,000	2,200,000	14,000	3,200,000
Total PAH ^{1,2}	48,609,000	100,650,000	85,690,000	40,571,000	157,900	47,640,000
TPH in mg/kg	440,000	530,000	590,000	110,000	710	340,000

**TABLE 3-19
CONFIRMATION SAMPLE CHEMISTRY RESULTS FROM THE SPRING INVESTIGATION**

**NAPL INVESTIGATION REPORT
PINE STREET CANAL SUPERFUND SITE
BURLINGTON, VERMONT**

BBL Sample ID:	T09+75E15 CB03-14-16	PSC-DUP1	T10+50E20 CB06-6-8	T10+50E20 CB06-13-15	T10+50E20 CB06-16-18	T12+00E60 CB07-0-0.32
Lab Sample ID:	WW2336-8	WW2336-6	WW2471-12	WW2471-13	WW2471-14	WW2471-6
Sampling Date:	5/11/2006	5/11/2006 Dup of T9+75E15 CB03-14-16	5/17/2006	5/17/2006	5/17/2006	5/16/2006
Total Organic Carbon in mg/kg	26,000	25,000	82,000	380,000	72,000	2,000
Total Solids in %	63.6	63.5	41.8	18.2	73.3	82.4
PAHs in µg/kg						
2-Methylnaphthalene	330,000	300,000	90,000	4,900,000	2,400,000	1,000 J
Acenaphthene	53,000 J	51,000	38,000	660,000	280,000	840 J
Acenaphthylene	82,000 J	78,000	3,600 J	2,000,000 J	970,000 J	630 J
Anthracene	49,000 J	45,000	20,000 J	1,200,000 J	200,000 J	1,200 J
Benzo(a)anthracene	23,000 J	21,000	10,000 J	290,000 J	140,000 J	770 J
Benzo(a)pyrene	17,000 J	15,000	9,700 J	240,000 J	120,000 J	660 J
Benzo(b)fluoranthene	15,000 J	12,000	9,400 J	210,000 J	110,000 J	760 J
Benzo(k)fluoranthene	5,700 J	5,100 J	4,200 J	110,000 J	51,000 J	400 U
Benzo(g,h,i)perylene	5,900 J	5,200	4,200 J	87,000 J	45,000 J	210 J
Chrysene	19,000 J	17,000	12,000 J	340,000 J	170,000 J	920 J
Dibenzo(a,h)anthracene	5,200 U	5,200 U	4,000 UJ	16,000 J	13,000 J	400 U
Fluoranthene	44,000 J	39,000	19,000	780,000	380,000	1,400 J
Fluorene	69,000 J	64,000	20,000	1,200,000	560,000	960 J
Indeno(1,2,3-cd)pyrene	6,600 J	6,700	4,300 J	85,000 J	45,000 J	400 U
Naphthalene	330,000	310,000	63,000	5,500,000	2,600,000	400 U
Phenanthrene	170,000	160,000	48,000 J	2,800,000 J	1,300,000 J	2,900 J
Pyrene	74,000 J	69,000	41,000 J	1,400,000	580,000	3,000 J
Total PAH ^{1,2}	1,293,200	1,198,000	396,400	21,818,000	9,964,000	15,250
TPH in mg/kg	3,800	4,800	5,200	100,000	55,000	240

**TABLE 3-19
CONFIRMATION SAMPLE CHEMISTRY RESULTS FROM THE SPRING INVESTIGATION**

**NAPL INVESTIGATION REPORT
PINE STREET CANAL SUPERFUND SITE
BURLINGTON, VERMONT**

BBL Sample ID:	T12+00E60 CB07-10-12	T12+00E60 CB07-16-18	T10+76E20 CB08-14-16	T10+76E20 CB08-17-19	PSC-DUP3 WW2471-11 5/17/2006 Dup of T10+76E20 CB08-17-19	T12+00E40 CB10-0.0-0.32 WW2471-1 5/15/2006
Lab Sample ID:	WW2471-7	WW2471-8	WW2471-9	WW2471-10	WW2471-11	WW2471-1
Sampling Date:	5/16/2006	5/16/2006	5/17/2006	5/17/2006	5/17/2006	5/15/2006
Total Organic Carbon in mg/kg	220,000	70,000	15,000	67,000	65,000	1,800
Total Solids in %	37.5	82.6	63.0	83.3	83.5	79.0
PAHs in µg/kg						
2-Methylnaphthalene	2,800,000	1,400,000	9,800	2,800,000	2,800,000	1,400
Acenaphthene	820,000	480,000	4,000	320,000	310,000	970 J
Acenaphthylene	290,000 J	800,000 J	1,400 J	1,100,000 J	1,200,000 J	540 J
Anthracene	580,000 J	300,000 J	1,600 J	680,000 J	650,000 J	1,200
Benzo(a)anthracene	180,000 J	210,000 J	280 J	170,000 J	160,000 J	900
Benzo(a)pyrene	140,000 J	170,000 J	190 J	150,000 J	140,000 J	730
Benzo(b)fluoranthene	130,000 J	140,000 J	520 U	130,000 J	120,000 J	820
Benzo(k)fluoranthene	49,000 J	67,000 J	520 U	73,000 J	65,000 J	190 J
Benzo(g,h,i)perylene	57,000 J	60,000 J	520 U	58,000 J	61,000 J	280 J
Chrysene	210,000 J	240,000 J	520 U	300,000 U	200,000 J	1,000
Dibenzo(a,h)anthracene	22,000 UJ	20,000 UJ	520 U	13,000 J	11,000 J	420 U
Fluoranthene	320,000	330,000	630	420,000	420,000	1,700
Fluorene	650,000	810,000	1,900	660,000	640,000	840
Indeno(1,2,3-cd)pyrene	57,000 J	60,000 J	520 U	56,000 J	55,000 J	380 J
Naphthalene	2,800,000	1,500,000	19,000	3,000,000	3,000,000	700
Phenanthrene	1,400,000 J	1,100,000 J	4,300 J	1,500,000 J	1,500,000 J	2,900 J
Pyrene	660,000	750,000	1,400	700,000	700,000	3,100
Total PAH ^{1,2}	11,143,000	8,417,000	44,500	11,830,000	12,032,000	17,650
TPH in mg/kg	78,000	92,000	510	86,000	75,000	270

**TABLE 3-19
CONFIRMATION SAMPLE CHEMISTRY RESULTS FROM THE SPRING INVESTIGATION**

**NAPL INVESTIGATION REPORT
PINE STREET CANAL SUPERFUND SITE
BURLINGTON, VERMONT**

BBL Sample ID:	T12+00E40 CB10-6-8	T12+00E40 CB10-10-12	T12+00E40 CB10-14-15	T09+00E60 TGCONF-11.5-13
Lab Sample ID:	WW2471-2	WW2471-3	WW2471-4	WW2336-9
Sampling Date:	5/15/2006	5/15/2006	5/15/2006	5/10/2006
Total Organic Carbon in mg/kg	440,000	720,000	24,000	54,000
Total Solids in %	27.9	19.6	73.7	85.9
PAHs in µg/kg				
2-Methylnaphthalene	7,500,000	21,000,000	370,000	2,700,000
Acenaphthene	2,300,000	5,000,000	50,000 J	680,000
Acenaphthylene	680,000 J	4,200,000 J	130,000 J	540,000
Anthracene	910,000 J	3,100,000 J	39,000 J	450,000
Benzo(a)anthracene	430,000 J	1,500,000	22,000 J	220,000
Benzo(a)pyrene	300,000 J	1,100,000	17,000 J	160,000
Benzo(b)fluoranthene	280,000 J	1,000,000	15,000 J	140,000
Benzo(k)fluoranthene	67,000 J	230,000 J	7,200 J	57,000
Benzo(g,h,i)perylene	81,000 J	270,000 J	6,900 J	61,000
Chrysene	480,000 J	1,500,000	25,000 J	180,000
Dibenzo(a,h)anthracene	120,000 UJ	420,000 U	1,400 J	38,000 U
Fluoranthene	780,000	2,500,000 J	41,000 J	430,000
Fluorene	1,700,000	5,600,000	67,000	610,000
Indeno(1,2,3-cd)pyrene	110,000 J	350,000 J	6,800 J	80,000
Naphthalene	7,800,000	23,000,000	450,000	2,600,000
Phenanthrene	1,900,000 J	6,600,000	220,000 J	1,400,000
Pyrene	1,800,000 J	6,300,000	62,000	680,000
Total PAH ^{1,2}	27,118,000	83,250,000	1,530,300	10,988,000
TPH in mg/kg	270,000	650,000	7,200	90,000

Notes:

-- = compound not analyzed
 U = Compound was not detected.
 Value is the detection limit.
 J = Estimated value.
 mg/kg = milligrams per kilogram
 µg/kg = micrograms per kilogram
 TPH = total petroleum hydrocarbons
 PAH = polycyclic aromatic hydrocarbons

1. Total concentrations are calculated using the detected concentrations of individual constituents. Non-detects are treated as zeros. If all the individual constituents are non-detect the total concentration is reported as non-detect using the highest detection limit.

2. The total PAHs is the sum of all the PAHs listed in the table.

**TABLE 3-20
CONFIRMATION SAMPLE CHEMISTRY RESULTS FROM THE WINTER INVESTIGATION**

**NAPL INVESTIGATION REPORT
PINE STREET CANAL SUPERFUND SITE
BURLINGTON, VERMONT**

BBL Sample ID:	EB5-T11+00	EB5-T11+00	EB5-T11+00	EB5-T11+00	EB5-T12+50	EB5-T12+50
Lab Sample ID:	CB130-18-18.5	CB130-DUP	CB130-21.5-22	CB130-22.7-23.2	CB131-15.5-16	CB131-16.7-17.2
Sampling Date:	SA0797-1 2/20/2007	SA0797-12 2/20/2007 Dup of EB5-T11+00 CB130-18-18.5	SA0797-2 2/20/2007	SA0797-3 2/20/2007	SA0797-8 2/22/2007	SA0797-9 2/22/2007
Total Organic Carbon in mg/kg	810,000	690,000	31,000 J	23,000	840,000	990,000
Total Solids in %	19.0	18.0	58.0	68.0	20	23.0
PAHs in µg/kg						
2-Methylnaphthalene	9,900,000 D	9,900,000 D	6,500	240,000 D	13,000,000 D	26,000,000 D
Acenaphthene	3,500,000 D	3,200,000 D	2,000	71,000 D	4,000,000 D	8,600,000 D
Acenaphthylene	1,400,000 D	890,000	580	38,000 D	2,200,000 D	5,000,000 D
Anthracene	1,900,000 D	1,400,000 D	1,100	39,000 D	2,200,000 D	4,900,000 D
Benzo(a)anthracene	780,000 J	660,000	450 J	17,000	890,000 D	2,100,000 D
Benzo(a)pyrene	560,000 J	460,000	490 J	12,000	570,000 J	1,300,000
Benzo(b)fluoranthene	470,000 J	350,000	340 J	10,000	480,000 J	1,100,000
Benzo(k)fluoranthene	230,000 J	180,000	570 U	4,600	200,000 J	410,000
Benzo(g,h,i)perylene	170,000 J	160,000	570 U	3,400	170,000 J	430,000
Chrysene	700,000 D	580,000	420 J	16,000 D	840,000 D	1,900,000 D
Dibenzo(a,h)anthracene	120,000 J	110,000	490 J	2,600	88,000 J	240,000
Fluoranthene	2,100,000 D	1,600,000 D	1,200	46,000 D	2,200,000 D	5,200,000 D
Fluorene	2,100,000 D	1,700,000 D	1,100	49,000 D	2,600,000 D	5,900,000 D
Indeno(1,2,3-cd)pyrene	280,000 J	210,000	570 U	5,500	230,000 J	570,000
Naphthalene	8,700,000 D	9,600,000 D	7,900	240,000 D	13,000,000 D	26,000,000 D
Phenanthrene	5,000,000 D	4,600,000 D	3,100	120,000 D	6,300,000 D	14,000,000 D
Pyrene	2,400,000 D	2,000,000 D	1,500	56,000 D	2,700,000 D	6,200,000 D
Total PAH ^{1,2}	40,310,000	37,600,000	27,170	970,100	51,668,000	109,850,000
TPH in mg/kg	260,000	270,000	330	3,900	520,000	830,000

**TABLE 3-20
CONFIRMATION SAMPLE CHEMISTRY RESULTS FROM THE WINTER INVESTIGATION**

**NAPL INVESTIGATION REPORT
PINE STREET CANAL SUPERFUND SITE
BURLINGTON, VERMONT**

BBL Sample ID:	EB5-T12+50	EB5-T12+50	EB18-T11+95	EB18-T11+95	EB18-T11+95	EB18-T11+95
Lab Sample ID:	CB131-19.5-20	CB131-24.9-25.4	CB125-14-14.5	CB125-16.6-17.1	CB125-20.3-20.8	CB125-24-24.5
Sampling Date:	SA0797-10 2/22/2007	SA0797-11 2/22/2007	SA0797-4 2/21/2007	SA0797-5 2/21/2007	SA0797-6 2/22/2007	SA0797-7 2/22/2007
Total Organic Carbon in mg/kg	13,000	2,600	450,000	17,000	4,900	4,000
Total Solids in %	78.0	77.0	24.0	68.0	80.0	76.0
PAHs in µg/kg						
2-Methylnaphthalene	87,000 EDJ	570 D	8,600,000 D	25,000 D	79,000 D	12,000 D
Acenaphthene	32,000 D	180 D	1,500,000 D	10,000 D	24,000 D	2,700 D
Acenaphthylene	23,000 D	94	2,200,000 D	2,200 D	21,000 D	4,500 D
Anthracene	20,000 D	120	1,200,000 D	4,500 D	16,000 D	2,900 D
Benzo(a)anthracene	8,400 D	78	500,000 J	2,100 D	7,200 D	1,600
Benzo(a)pyrene	5,800 D	44	340,000 J	1,400	4,900 D	1,100
Benzo(b)fluoranthene	3,900 J	39	270,000 J	1,100	3,800	840
Benzo(k)fluoranthene	1,200 J	14 J	120,000 J	390 J	1,200	440
Benzo(g,h,i)perylene	1,900 J	17 J	100,000 J	440 J	1,300	330 J
Chrysene	7,900 D	64	370,000 J	1,800 D	6,900 D	1,300
Dibenzo(a,h)anthracene	690 J	26 U	62,000 J	480 J	680	440
Fluoranthene	21,000 D	160 D	1,400,000 D	5,100 D	19,000 D	3,500 D
Fluorene	27,000 D	170 D	1,500,000 D	5,800 D	21,000 D	4,300
Indeno(1,2,3-cd)pyrene	1,600 J	20 J	160,000 J	540	1,500	590
Naphthalene	84,000 D	320 D	9,300,000 D	27,000 D	79,000 D	10,000 D
Phenanthrene	54,000 D	540 D	4,100,000 D	13,000 D	46,000 D	8,200 D
Pyrene	24,000 D	210 D	1,700,000 D	6,000 D	22,000 D	4,400 D
Total PAH ^{1,2}	403,390	2,640	33,422,000	106,850	354,480	59,140
TPH in mg/kg	2,400	22	180,000	620	22,000	410

**TABLE 3-20
CONFIRMATION SAMPLE CHEMISTRY RESULTS FROM THE WINTER INVESTIGATION**

**NAPL INVESTIGATION REPORT
PINE STREET CANAL SUPERFUND SITE
BURLINGTON, VERMONT**

BBL Sample ID:	WB5-T9+75 CB101-4.4-4.9	WB5-T9+75 CB101-10.5-11	WB5-T9+75 CB101-14.5-15	WB5-T9+75 CB101-16.5-17	WB5-T9+75 CB101-18.3-18.8	WB5-T9+75 CB101-DUP SA0661-17 2/11/2007 Dup of WB5-T9+75 CB101-18.3-18.8
Lab Sample ID:	SA0661-22	SA0661-9	SA0661-10	SA0661-23	SA0661-11	
Sampling Date:	2/11/2007	2/11/2007	2/11/2007	2/11/2007	2/11/2007	
Total Organic Carbon in mg/kg	170,000	360,000	630,000	730,000	730,000	500,000
Total Solids in %	35.0	19.0	14.0	14.0	16.0	17.0
PAHs in µg/kg						
2-Methylnaphthalene	780,000 D	36,000	6,800,000 D	10,000,000 D	14,000,000 D	13,000,000 D
Acenaphthene	210,000 D	13,000	2,200,000 D	2,900,000 D	3,100,000 D	2,600,000 D
Acenaphthylene	130,000 D	5,700	730,000 D	1,600,000 D	3,500,000 D	2,800,000 D
Anthracene	120,000 D	6,900	1,100,000 D	1,700,000 D	2,500,000 D	2,000,000 D
Benzo(a)anthracene	46,000 DJ	3,800	520,000	760,000	1,100,000	840,000 D
Benzo(a)pyrene	29,000	2,400	380,000	510,000	760,000	620,000
Benzo(b)fluoranthene	26,000	1,900	300,000	440,000	610,000	550,000
Benzo(k)fluoranthene	10,000	1,000 J	150,000	210,000	310,000	220,000
Benzo(g,h,i)perylene	8,600	780 J	120,000	160,000	190,000	170,000
Chrysene	34,000	3,200	430,000	580,000	880,000 D	840,000 D
Dibenzo(a,h)anthracene	3,400	1,600 J	75,000	73,000	190,000	94,000 J
Fluoranthene	130,000 D	8,100	1,200,000 D	1,700,000 D	2,400,000 D	2,300,000 D
Fluorene	140,000 D	8,700	1,200,000 D	1,800,000 D	2,700,000 D	2,200,000 D
Indeno(1,2,3-cd)pyrene	12,000	1,800 U	180,000	250,000	360,000	270,000
Naphthalene	940,000 D	35,000	7,200,000 D	11,000,000 D	14,000,000 D	14,000,000 D
Phenanthrene	400,000 D	20,000	3,400,000 D	5,100,000 D	7,300,000 D	6,100,000 D
Pyrene	140,000 D	9,800	1,400,000 D	2,100,000 D	3,200,000 D	2,600,000 D
Total PAH^{1,2}	3,159,000	157,880	27,385,000	40,883,000	57,100,000	51,204,000
TPH in mg/kg	15,000	860	180,000	510,000	310,000	210,000

**TABLE 3-20
CONFIRMATION SAMPLE CHEMISTRY RESULTS FROM THE WINTER INVESTIGATION**

**NAPL INVESTIGATION REPORT
PINE STREET CANAL SUPERFUND SITE
BURLINGTON, VERMONT**

BBL Sample ID:	WB5-T9+75	WB5-T10+50	WB5-T10+50	WB5-T10+50	WB5-T10+50	WB5-T10+50
Lab Sample ID:	CB101-21.3-21.8	CB104-2.6-3.1	CB104-10-10.5	CB104-12.9-13.4	CB104-15-15.5	CB104-17.3-17.8
Sampling Date:	SA0661-12 2/11/2007	SA0661-13 2/11/2007	SA0661-24 2/11/2007	SA0661-14 2/11/2007	SA0661-25 2/11/2007	SA0661-15 2/11/2007
Total Organic Carbon in mg/kg	19,000	22,000	230,000	490,000	670,000	750,000
Total Solids in %	65.0	76.0	23.0	15.0	15.0	17.0
PAHs in µg/kg						
2-Methylnaphthalene	4,400	5,800 J	10,000	2,000 J	9,400,000 D	13,000,000 D
Acenaphthene	1,000	6,100	3,300	2,200 U	3,000,000 D	3,300,000 D
Acenaphthylene	210 J	990	1,100 J	2,200 U	710,000	2,500,000 D
Anthracene	480 J	3,100	1,700	2,200 U	1,500,000 D	2,200,000 D
Benzo(a)anthracene	260 J	1,900	790 J	2,200 U	650,000	900,000 D
Benzo(a)pyrene	510 U	1,400	530 J	2,200 U	460,000	580,000
Benzo(b)fluoranthene	510 U	1,300	1,400 U	2,200 U	380,000	500,000
Benzo(k)fluoranthene	510 U	730	1,400 U	2,200 U	180,000	220,000
Benzo(g,h,i)perylene	510 U	500	1,400 U	2,200 U	140,000	170,000
Chrysene	210 J	1,700	730 J	2,200 U	570,000	810,000 D
Dibenzo(a,h)anthracene	410 J	500	1,200 J	2,200 U	65,000	96,000
Fluoranthene	570	4,000	2,000	2,200 U	1,800,000 D	2,200,000 D
Fluorene	630	4,400 J	2,000	1,100 J	1,600,000 D	2,400,000 D
Indeno(1,2,3-cd)pyrene	510 U	950	1,400 U	2,200 U	210,000	250,000
Naphthalene	6,400	4,300 J	11,000	5,200	10,000,000 D	14,000,000 D
Phenanthrene	1,900	8,300 J	6,000	980 J	4,700,000 D	6,400,000 D
Pyrene	800	4,600	2,400	2,200 U	1,800,000 D	2,600,000 D
Total PAH ^{1,2}	17,270	50,570	42,750	9,280	37,165,000	52,126,000
TPH in mg/kg	430	520	1,100	960	520,000	270,000

**TABLE 3-20
CONFIRMATION SAMPLE CHEMISTRY RESULTS FROM THE WINTER INVESTIGATION**

**NAPL INVESTIGATION REPORT
PINE STREET CANAL SUPERFUND SITE
BURLINGTON, VERMONT**

BBL Sample ID:	WB5-T10+50	WB5-T10+50	WB5-T10+50	WB5-T11+75	WB5-T11+75	WB5-T11+75
Lab Sample ID:	CB104-18.4-18.9	CB104-20.8-21.3	CB104-22.5-23	CB100-7.5-8	CB100-8.4-8.9	CB100-10-10.5
Sampling Date:	SA0661-26 2/12/2007	SA0661-27 2/12/2007	SA0661-16 2/12/2007	SA0661-5 2/9/2007	SA0661-19 2/9/2007	SA0661-6 2/10/2007
Total Organic Carbon in mg/kg	740,000	21,000	38,000	95,000	76,000	120,000
Total Solids in %	16.0	64.0	84.0	82.0	85.0	85.0
PAHs in µg/kg						
2-Methylnaphthalene	11,000,000 D	48,000 D	1,600,000 D	3,100,000 D	2,900,000 D	4,800,000 D
Acenaphthene	2,400,000 D	15,000 D	400,000 D	1,300,000 D	1,100,000 D	1,700,000 D
Acenaphthylene	2,200,000 D	9,400 D	350,000 D	280,000 D	260,000 D	480,000 D
Anthracene	1,800,000 D	8,500 D	280,000 D	640,000 D	560,000 D	550,000
Benzo(a)anthracene	700,000	4,200	120,000	290,000 D	260,000 D	390,000 D
Benzo(a)pyrene	460,000	2,800	88,000 D	210,000	180,000	270,000
Benzo(b)fluoranthene	420,000	2,200	64,000	180,000	150,000	230,000
Benzo(k)fluoranthene	160,000	1,000	29,000	68,000	58,000	110,000
Benzo(g,h,i)perylene	130,000	930 J	25,000	66,000	61,000	74,000
Chrysene	540,000	3,600 D	110,000 D	250,000 D	230,000 D	300,000
Dibenzo(a,h)anthracene	76,000	1,000 J	14,000	30,000	26,000	52,000
Fluoranthene	2,000,000 D	9,800 D	290,000 D	640,000 D	550,000 D	910,000 D
Fluorene	1,900,000 D	12,000	360,000 D	730,000 D	620,000 D	920,000 D
Indeno(1,2,3-cd)pyrene	190,000	1,200	37,000	82,000	71,000	130,000
Naphthalene	11,000,000 D	49,000 D	1,600,000 D	2,800,000 D	2,600,000 D	4,700,000 D
Phenanthrene	5,500,000 D	26,000 D	800,000 D	1,800,000 D	1,600,000 D	2,500,000 D
Pyrene	2,100,000 D	12,000 D	390,000 D	820,000 D	750,000 D	1,200,000 D
Total PAH^{1,2}	42,576,000	206,630	6,557,000	13,286,000	11,976,000	19,316,000
TPH in mg/kg	500,000	29,000	37,000	100,000	80,000	99,000

**TABLE 3-20
CONFIRMATION SAMPLE CHEMISTRY RESULTS FROM THE WINTER INVESTIGATION**

**NAPL INVESTIGATION REPORT
PINE STREET CANAL SUPERFUND SITE
BURLINGTON, VERMONT**

BBL Sample ID:	WB5-T11+75	WB5-T11+75	WB5-T11+75	WB5-T11+75	WB5-T12+75	WB5-T12+75
Lab Sample ID:	CB100-13-13.5	CB100-16.3-16.8	CB100-18.7-19.2	CB100-20.3-20.8	CB120-4.4-4.9	CB120-12-12.4
Sampling Date:	SA0661-20	SA0661-7	SA0661-21	SA0661-8	SA0661-18	SA0661-2
	2/10/2007	2/10/2007	2/10/2007	2/10/2007	2/9/2007	2/9/2007
Total Organic Carbon in mg/kg	120,000	320,000	4,000	2,800	350,000	210,000
Total Solids in %	78.0	38.0	82.0	80.0	26.0	31.0
PAHs in µg/kg						
2-Methylnaphthalene	4,200,000 D	6,400,000 D	37,000 D	2,000	64 J	540,000 D
Acenaphthene	1,400,000 D	2,700,000 D	16,000 D	910	29 J	260,000 D
Acenaphthylene	560,000 D	490,000 D	3,500 D	190 J	78 U	20,000 J
Anthracene	710,000 D	1,300,000 D	7,300 D	400 J	16 J	100,000 D
Benzo(a)anthracene	310,000	570,000 D	3,400 D	200 J	27 J	58,000 D
Benzo(a)pyrene	230,000	390,000	2,000	410 U	78 U	32,000 J
Benzo(b)fluoranthene	200,000	300,000	1,700	410 U	78 U	29,000 J
Benzo(k)fluoranthene	96,000	160,000	900	410 U	25 J	11,000 J
Benzo(g,h,i)perylene	64,000	110,000	580 J	410 U	78 U	8,200 J
Chrysene	250,000	460,000	3,100 D	160 J	30 J	49,000 D
Dibenzo(a,h)anthracene	39,000	92,000	760 J	340 J	78 U	4,000 J
Fluoranthene	770,000 D	1,300,000 D	8,400 D	490	45 J	110,000 D
Fluorene	820,000 D	1,500,000 D	9,500	520	22 J	120,000 D
Indeno(1,2,3-cd)pyrene	110,000	190,000	1,000	410 U	78 U	12,000 J
Naphthalene	4,300,000 D	5,900,000 D	28,000 D	1,400	150	450,000 D
Phenanthrene	2,200,000 D	3,600,000 D	23,000 D	1,500	65 J	340,000 D
Pyrene	950,000 D	1,700,000 D	9,400 D	580	49 J	140,000 D
Total PAH ^{1,2}	17,209,000	27,162,000	155,540	8,690	522	2,283,200
TPH in mg/kg	96,000	140,000	22,000	100	1,000	15,000

**TABLE 3-20
CONFIRMATION SAMPLE CHEMISTRY RESULTS FROM THE WINTER INVESTIGATION**

**NAPL INVESTIGATION REPORT
PINE STREET CANAL SUPERFUND SITE
BURLINGTON, VERMONT**

BBL Sample ID:	WB5-T12+75 CB120-14.9-15.4	WB5-T12+75 CB120-18.6-19.1
Lab Sample ID:	SA0661-3	SA0661-4
Sampling Date:	2/9/2007	2/9/2007
Total Organic Carbon in mg/kg	3,400	4,800
Total Solids in %	82.0	79.0
PAHs in µg/kg		
2-Methylnaphthalene	15,000 D	570
Acenaphthene	8,200 D	270 J
Acenaphthylene	NA	420 U
Anthracene	3,700 D	420 U
Benzo(a)anthracene	1,800 D	420 U
Benzo(a)pyrene	1,200 D	420 U
Benzo(b)fluoranthene	940 D	420 U
Benzo(k)fluoranthene	420	420 U
Benzo(g,h,i)perylene	370 J	420 U
Chrysene	1,600 D	420 U
Dibenzo(a,h)anthracene	360 J	420 U
Fluoranthene	3,800 D	420 U
Fluorene	5,100	240 J
Indeno(1,2,3-cd)pyrene	490	420 U
Naphthalene	12,000 D	500
Phenanthrene	11,000 D	320 J
Pyrene	4,800 D	420 U
Total PAH ^{1,2}	70,780	1,900
TPH in mg/kg	560	18

Notes:

U = Compound was not detected.

Value is the detection limit.

J = Estimated value.

D = Result was obtained from the analysis of a diluted sample.

E = Analyte exceeded calibration range.

mg/kg = milligrams per kilogram

µg/kg = micrograms per kilogram

TPH = total petroleum hydrocarbons

PAH = polycyclic aromatic hydrocarbons

1. Total concentrations are calculated using the detected concentrations of individual constituents. Non-detects are treated as zeros. If all the individual constituents are non-detect the total concentration is reported as non-detect using the highest detection limit.

2. The total PAHs is the sum of all the PAHs listed in the table.

**TABLE 4-1
NAPL MASS CALCULATION RESULTS**

**NAPL INVESTIGATION REPORT
PINE STREET CANAL SUPERFUND SITE
BURLINGTON, VERMONT**

Cell	Mass of Potentially Mobile NAPL in Subsurface, M_{SS} (kg)	Mass of NAPL in Lower Cap¹, M_{CP} (kg)	Mass of NAPL in Upper Cap², M_{CP-top} (kg)	Mass of NAPL Deposition³, M_{CS} (kg)	NAPL Seepage Rate, R_{SW} (kg/yr)
9.1A	7,010	2.940	2.400	0.001	0.000
9.1B	11,100	2.940	2.400	0.001	0.000
9.1C	12,300	2.940	2.400	0.001	0.000
9.2A	8,290	2.940	2.400	0.008	0.000
9.2B	15,400	15.800	3.710	0.001	0.000
9.2C	14,900	2.940	2.400	0.001	0.000
9.3A	13,100	11.800	22.500	0.015	10.500
9.3B	17,200	2.940	2.400	0.001	0.000
9.3C	14,700	2.940	2.400	0.000	0.000
9.4A	12,100	78.900	82.100	0.081	2.640
9.4B	11,400	2.940	2.400	0.010	0.000
9.4C	11,000	2.940	2.400	0.000	0.000
10.1A	9,660	2.950	6.440	0.076	3.450
10.1B	10,700	2.940	2.400	0.008	0.000
10.1C	9,620	2.940	2.400	0.000	0.000
10.2A	13,000	4.220	1.090	0.100	0.000
10.2B	10,800	2.940	2.400	0.008	0.172
10.2C	5,330	2.940	2.400	0.002	0.000
10.3A	17,200	46.500	27.000	0.100	7.470
10.3B	14,300	2.940	2.400	0.009	5.060
10.3C	8,020	2.940	2.400	0.004	0.000
10.4A	14,600	136.000	64.100	0.444	32.000
10.4B	15,900	1.320	0.556	0.100	15.300
10.4C	11,600	271.000	124.000	0.001	1.260
11.1A	12,300	1,450.000	124.000	0.444	0.714
11.1B	15,800	2.760	49.100	0.639	2.710
11.1C	12,100	6.750	3.720	0.116	18.200
11.2A	8,140	296.000	158.000	0.100	0.228
11.2B	16,200	8.650	4.610	0.139	7.290
11.2C	11,500	6.750	3.720	0.010	0.000
11.3A	8,310	1.530	3.270	0.001	0.405
11.3B ³	13,800	0.966	3.110	0.002	3.030
11.3C	11,200	0.966	3.110	0.001	0.000
11.4A	7,070	0.966	3.110	0.001	0.000
11.4B	17,100	0.399	2.950	0.005	0.000
11.4C	12,900	0.966	3.110	0.008	0.172
12.1A	3,650	0.966	3.110	0.001	0.000
12.1B	11,100	0.966	3.110	0.009	0.000
12.1C	9,110	0.966	3.110	0.016	0.000
12.2A	6,190	0.966	3.110	0.001	0.000
12.2B	12,000	0.966	3.110	0.005	0.000
12.2C	10,500	0.966	3.110	0.008	0.000
12.3A	4,400	0.966	3.110	0.001	0.000
12.3B	12,200	0.966	3.110	0.001	0.000
12.3C	16,300	0.966	3.110	0.001	0.000
Total Mass⁴	521,000	2,400	756	2.5	111

Notes:

1. Cell 11.3B was classified as a medium relative mass of NAPL in the surface of the cap (Figure 4-15) because historical cap probing data detected NAPL droplets with gas bubbling in this cell.
2. The mass of NAPL in cells with no cap coring data from 2006 was estimated using the mass calculated in nearby cap corings. For cells in 11.1 and 11.2, the estimated mass of NAPL was calculated using the average masses in CP11 and CP17. For cells in 11.3 through 12.3 with no cap corings from 2006, the estimated mass of NAPL was calculated using the average masses in CP13 and CP14. For cells in 09.1 to 10.4, the estimated mass of NAPL was calculated using the average masses in CP04, CP05, CP06, CP11, and CP16.
3. The mass of NAPL in cells with no cap surface swab data from 2006 was estimated using the mass of NAPL in neighboring cells that were sampled. The exceptions to this are Cells 10.2A, 10.3A, 10.4B, and 11.2A, which were assumed to have 100 g of NAPL; and Cells 09.4B and 11.2C, which were assumed to have 10 g of NAPL. These nominal values were assumed based on the presence or absence of NAPL seepage in 2006 and historical cap probing data from The Johnson Company.
4. Total mass in the grid. This value is a summation of the mass in the individual cells.

**TABLE 4-2
WEST BANK CAP CORING ANALYSIS**

**NAPL INVESTIGATION REPORT
PINE STREET CANAL SUPERFUND SITE
BURLINGTON, VERMONT**

Transect Set Cap Core ID Location next to	CP 100 Cribbing	T10+00 CP 101 Midway	CP 102 Canal	CP 103 Cribbing	T10+50 CP 104 Midway	CP 105 Canal	CP 106 Cribbing	T11+00 CP 107 Midway	CP 108 Canal
Core Recovery	1.9 ft	2.3 ft	3 ft	2 ft	3 ft	3.2 ft	1.9 ft	2.9 ft	3 ft
Ground Surface Elevation¹	96.0 ft	96.0 ft	96.0 ft	96.1 ft	96.7 ft	96.1 ft	96.0 ft	96.6 ft	96.0 ft
Sample Elevations¹ (ft):									
96.5-96.0					410 mg/kg				
96.0-95.5	160 mg/kg	43 mg/kg	U	U			370 mg/kg		U
95.5-95.0	U				U		U		
95.0-94.5		U			U				U
94.5-94.0	U	U	U	83 mg/kg	U	U	U	220 mg/kg	180 mg/kg
				19000 mg/kg				5600 mg/kg	
94.0-93.5					U	U		53 mg/kg	U
93.5-93.0			U			4600 mg/kg			
						35 mg/kg			

Notes:

Chemistry values are reported as TPH in mg/kg. A 'U' indicates TPH was not detected in sample.

1. Vertical datum is 1988 North American Vertical Datum (NAVD88). Sample elevations are approximate for the 6-inch intervals. Exact sample depths are provided in Table 3-18. Split samples indicate that visible NAPL was observed in the core and subsequently preferentially sampled.

Appendix B – Photo Log

Photographs from Spring Investigation 2006:

- B-1 Diver collecting water column NAPL seep sample
- B-2 Diver removing quadrangle used to delineate cap swab area
- B-3 Diver grab sample of surface of cap near transect T11, note NAPL and organic material on surface and cap sand below
- B-4 Drilling rods with CPT and TarGOST™ cables threaded through the rods
- B-5 TarGost™ and CPT probes
- B-6 Inserting TarGost™ and CPT probe rods into boring
- B-7 ATL's drill barge piezometers in foreground
- B-8 Northern piezometer cluster: Cluster of four piezometers and one stilling well located near transect T10
- B-9 Piezometer (PZ07) and attached stilling well located in northern cluster of piezometers
- B-10 Collecting samples from the confirmation cores with ATL's drilling barge
- B-11 Bailing a piezometer in preparation for installation of a transducer
- B-12 Diver survey of cap surface
- B-13 Loading first barge section
- B-14 Sample of cap core at transect T9

Photographs from Summer Investigation 2006:

- B-15 View of canal looking south
- B-16 Divers moving vegetation from canal
- B-17 Divers moving vegetation from canal
- B-18 Diver collecting cap surface swab sample
- B-19 Diver co-locating cap coring with seep
- B-20 Collecting cap coring samples from JCO barge
- B-21 Collecting cap coring samples from JCO barge
- B-22 Cap coring sample from location CP17, description in photograph
- B-23 Close up of Photograph B-22
- B-24 Cap coring sample from location CP17, description in photograph
- B-25 Close up of Photograph B-24
- B-26 Cap coring sample from location CP17, description in photograph
- B-27 Close up of Photograph B-26
- B-28 Cap coring sample from location CP18, description in photograph
- B-29 Close up of Photograph B-28
- B-30 Cap coring sample from location CP18, description in photograph
- B-31 Close up of Photograph B-30
- B-32 Cap coring sample from location CP20, description in photograph
- B-33 Close up of Photograph B-32
- B-34 Cap coring sample from location CP21, description in photograph
- B-35 Close up of Photograph B-34
- B-36 Cap coring sample from location CP21, description in photograph
- B-37 Close up of Photograph B-36
- B-38 Cap coring sample from location CP21, description in photograph
- B-39 Close up of Photograph B-38
- B-40 Cap coring sample from location CP22, description in photograph
- B-41 Close up of Photograph B-39
- B-42 Cap coring sample from location CP23, description in photograph

-
- B-43 Close up of Photograph B-42
 - B-44 Cap coring sample from location CP24, description in photograph
 - B-45 Close up of Photograph B-44
 - B-46 Close up of Photograph B-44
 - B-47 Close up of Photograph B-44
 - B-48 Cap coring sample from location CP25, description in photograph
 - B-49 Close up of Photograph B-48
 - B-50 Cap coring sample from location CP26, description in photograph
 - B-51 Close up of Photograph B-50
 - B-52 Close up of Photograph B-50
 - B-53 Cap coring sample from location CP27, description in photograph
 - B-54 Close up of Photograph B-53
 - B-55 Close up of Photograph B-53
 - B-56 Close up of Photograph B-53

Photographs from Winter Investigation 2007:

- B-57 ATL's drill rig set up for east bank TarGOST™ probing
- B-58 ATL's drill rig set up after winter snow storm
- B-59 Clearing branches along east bank to provide access for drill rig
- B-60 Confirmation boring split spoon from CB100, description in photograph
- B-61 Confirmation boring split spoon from CB100, description in photograph
- B-62 Confirmation boring split spoon from CB100, description in photograph
- B-63 Confirmation boring split spoon from CB100, description in photograph
- B-64 Confirmation boring split spoon from CB100, description in photograph
- B-65 Confirmation boring split spoon from CB100, description in photograph
- B-66 Confirmation boring split spoon from CB100, description in photograph
- B-67 Confirmation boring split spoon from CB100, description in photograph
- B-68 Confirmation boring split spoon from CB100, description in photograph
- B-69 NAPL on outside of Shelby tube collected in confirmation boring CB100
- B-70 West bank cap coring sample from location CP105, description in photograph
- B-71 Close up of Photograph B-70
- B-72 Close up of interval with discrete NAPL from Photograph B-70



Photograph B-1 Diver collecting water column NAPL seep sample



Photograph B-2 Diver removing quadrangle used to delineate cap swab area



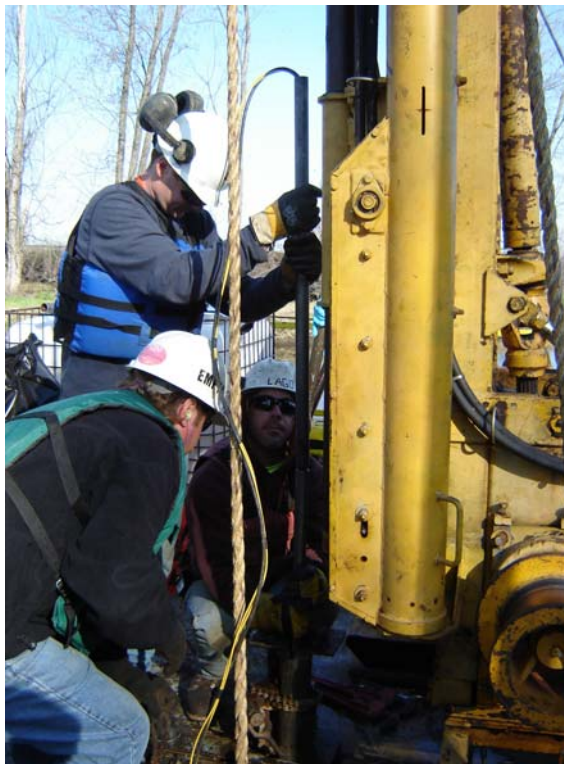
Photograph B-3 Diver grab sample of surface of cap near transect T11, note NAPL and organic material on surface and cap sand below



Photograph B-4 Drilling rods with CPT and TarGOST cables threaded through the rods



Photograph B-5 TarGost and CPT probes



Photograph B-6 Inserting TarGost and CPT probe rods into boring



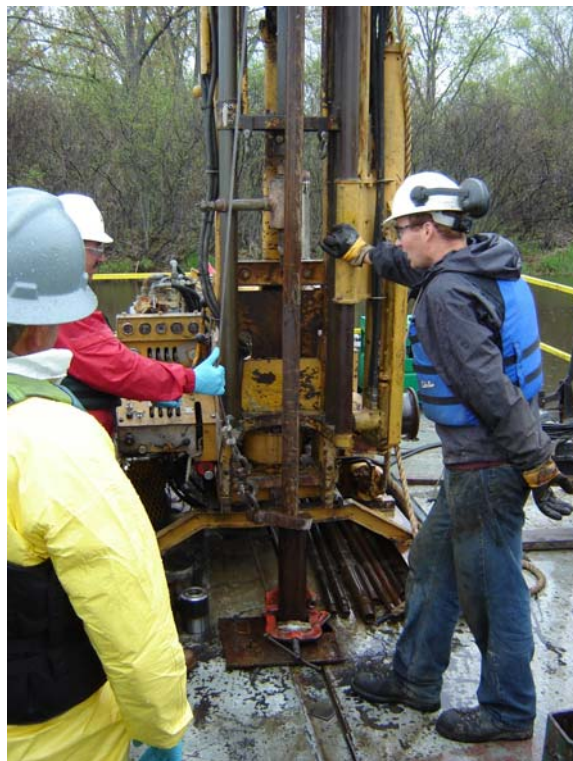
Photograph B-7 ATL's drill barge piezometers in foreground



Photograph B-8 Northern piezometer cluster: Cluster of four piezometers and one stilling well located near transect T10



Photograph B-9 Piezometer (PZ07) and attached stilling well located in northern cluster of piezometers



Photograph B-10 Collecting samples from the confirmation cores with ATL's drilling barge



Photograph B-11 Bailing a piezometer in preparation for installation of a transducer.



Photograph B-12 Diver survey of cap surface.



Photograph B-13 Loading first barge section.



Photograph B-14 Sample of cap core at transect T9.



Photograph B-15 View of canal looking south



Photograph B-16 Divers moving vegetation from canal



Photograph B-17 Divers moving vegetation from canal



Photograph B-18 Diver collecting cap surface swab sample



Photograph B-19 Diver co-locating cap coring with seep



Photograph B-20 Collecting cap coring samples from JCO barge



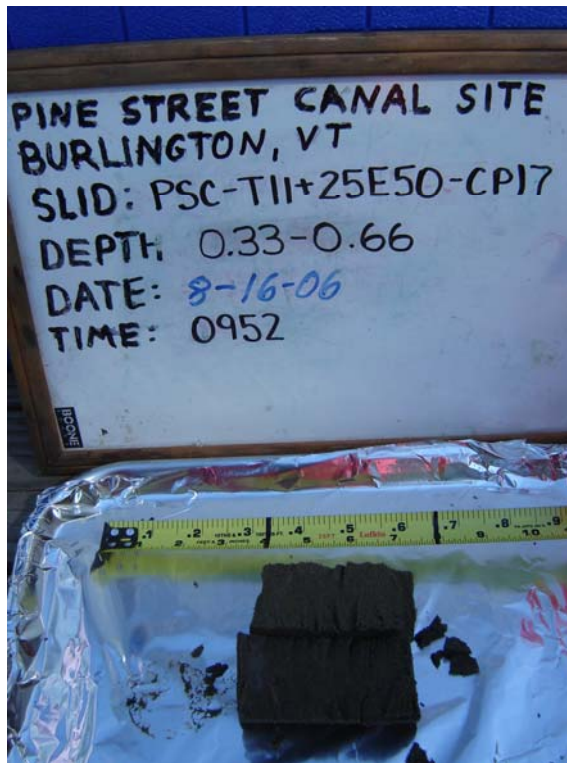
Photograph B-21 Collecting cap coring samples from JCO barge



Photograph B-22 Cap coring sample from location CP17, description in photograph



Photograph B-23 Close up of Photograph B-22



Photograph B-24 Cap coring sample from location CP17, description in photograph



Photograph B-25 Close up of Photograph B-24



Photograph B-26 Cap coring sample from location CP17, description in photograph



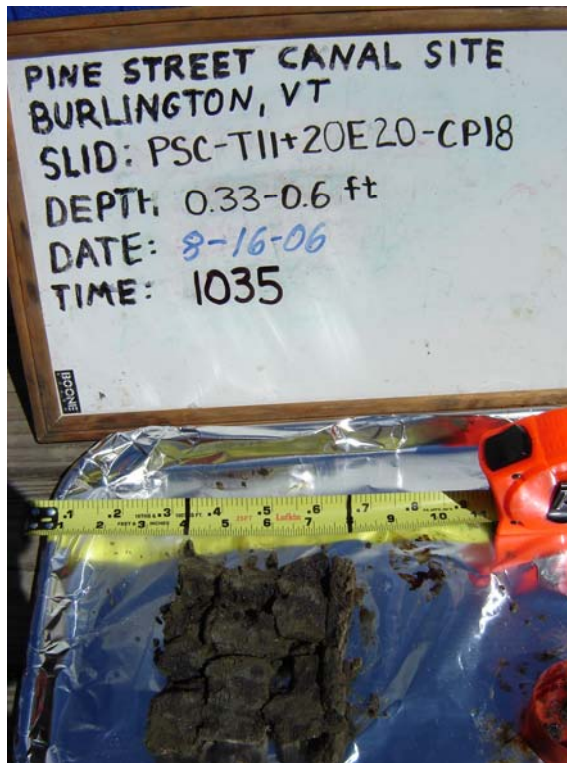
Photograph B-27 Close up of Photograph B-26



Photograph B-28 Cap coring sample from location CP18, description in photograph



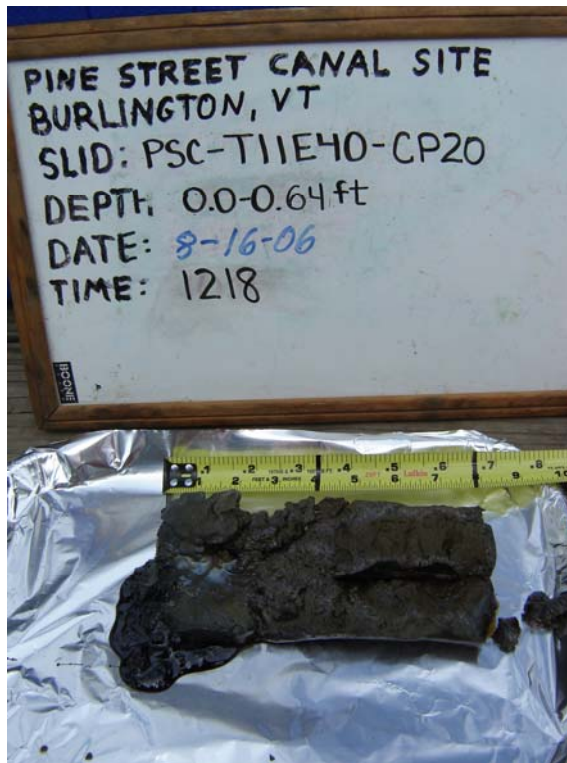
Photograph B-29 Close up of Photograph B-28



Photograph B-30 Cap coring sample from location CP18, description in photograph



Photograph B-31 Close up of Photograph B-30



Photograph B-32 Cap coring sample from location CP20, description in photograph



Photograph B-33 Close up of Photograph B-32



Photograph B-34 Cap coring sample from location CP21, description in photograph



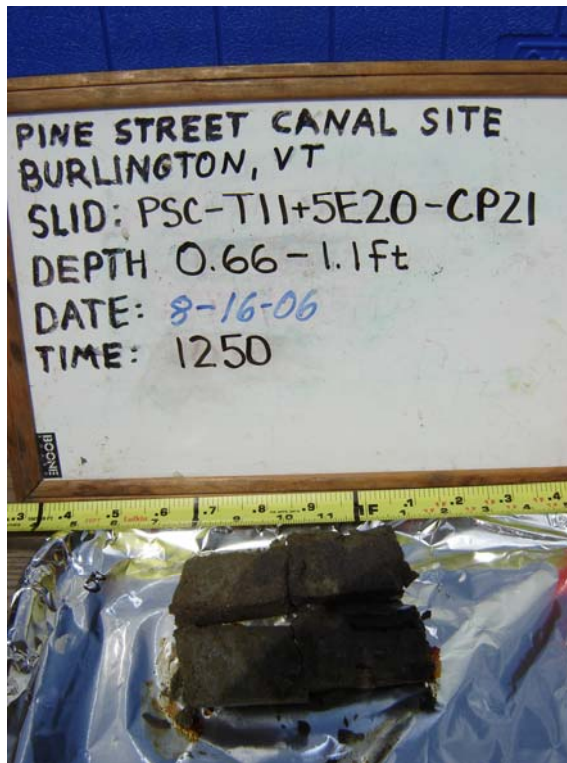
Photograph B-35 Close up of Photograph B-34



Photograph B-36 Cap coring sample from location CP21, description in photograph



Photograph B-37 Close up of Photograph B-36



Photograph B-38 Cap coring sample from location CP21, description in photograph



Photograph B-39 Close up of Photograph B-38



Photograph B-40 Cap coring sample from location CP22, description in photograph



Photograph B-41 Close up of Photograph B-40



Photograph B-42 Cap coring sample from location CP23, description in photograph



Photograph B-43 Close up of Photograph B-42



Photograph B-44 Cap coring sample from location CP24, description in photograph



Photograph B-45 Close up of Photograph B-44



Photograph B-46 Close up of Photograph B-44



Photograph B-47 Close up of Photograph B-44



Photograph B-48 Cap coring sample from location CP25, description in photograph



Photograph B-49 Close up of Photograph B-48



Photograph B-50 Cap coring sample from location CP26, description in photograph



Photograph B-51 Close up of Photograph B-50



Photograph B-52 Close up of Photograph B-50



Photograph B-53 Cap coring sample from location CP27, description in photograph



Photograph B-54 Close up of Photograph B-53



Photograph B-55 Close up of Photograph B-53



Photograph B-56 Close up of Photograph B-53



Photograph B-57 ATL's drill rig set up for east bank TarGOST™ probing



Photograph B-58 ATL's drill rig set up after winter snow storm



Photograph B-59 Clearing branches along east bank to provide access for drill rig



Photograph B-60 Confirmation boring split spoon from CB100, description in photograph



Photograph B-61 Confirmation boring split spoon from CB100, description in photograph



Photograph B-62 Confirmation boring split spoon from CB100, description in photograph



Photograph B-63 Confirmation boring split spoon from CB100, description in photograph



Photograph B-64 Confirmation boring split spoon from CB100, description in photograph



Photograph B-65 Confirmation boring split spoon from CB100, description in photograph



Photograph B-66 Confirmation boring split spoon from CB100, description in photograph



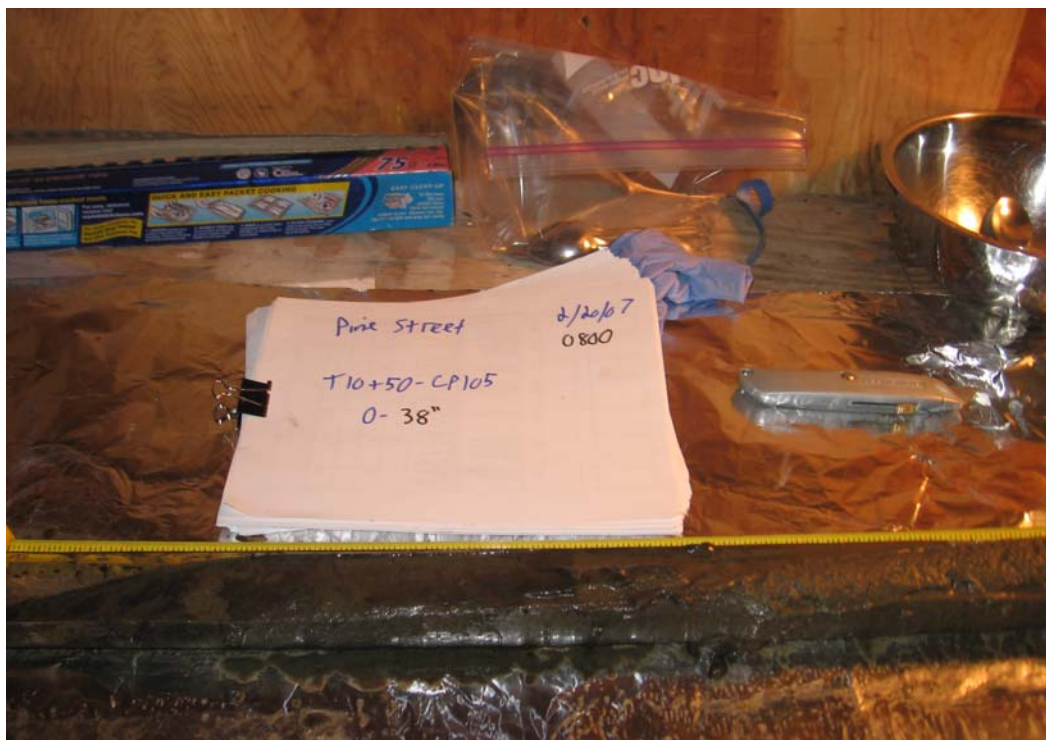
Photograph B-67 Confirmation boring split spoon from CB100, description in photograph



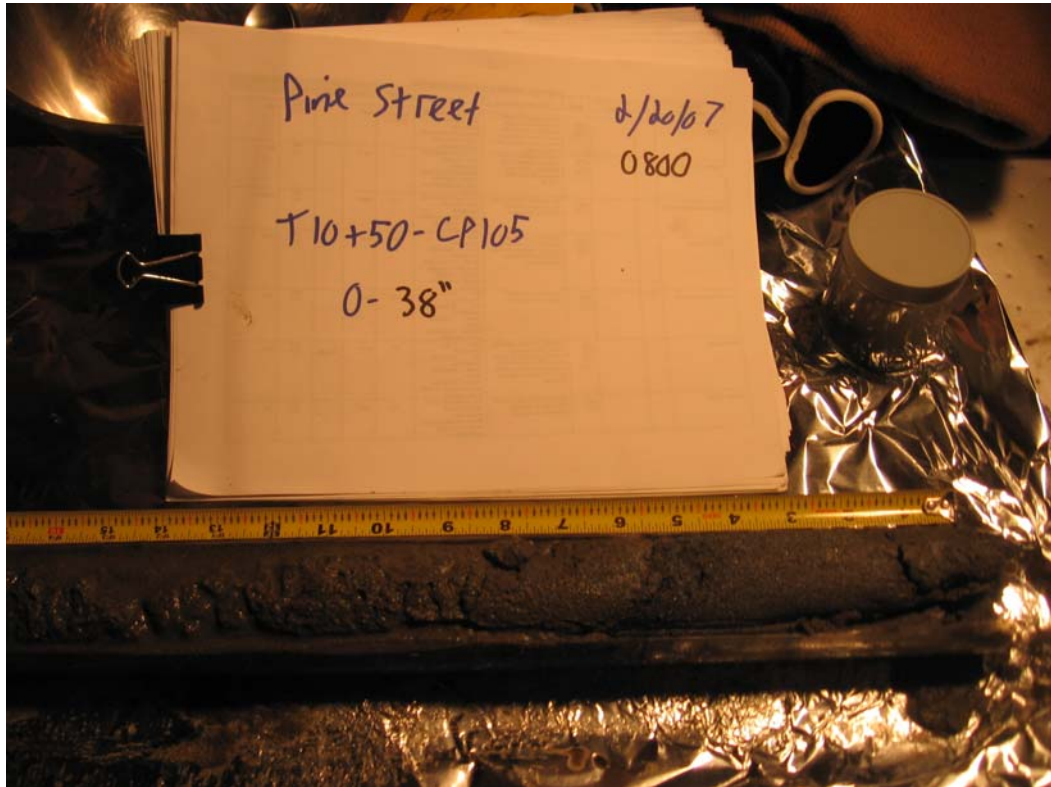
Photograph B-68 Confirmation boring split spoon from CB100, description in photograph



Photograph B-69 NAPL on outside of Shelby tube collected in confirmation boring CB100



Photograph B-70 West bank cap coring sample from location CP105, description in photograph



Photograph B-71 Close up of Photograph B-70



Photograph B-72 Close up of interval with discrete NAPL from Photograph B-70